https://doi.org/10.61092/iaea.62aw-9reb

INDC(NDS)-0678
Distr. AI+MN+NM

IAEA
International Atomic Energy Agency

INDC International Nuclear Data Committee

Prompt Fission Neutron Spectrum Evaluation Techniques

Donald L. Smith
Argonne National Laboratory, 1710 Avenida del Mundo #1506, Coronado, CA 92118, U.S.A.

Denise Neudecker
T-2 Nuclear and Particle Physics, Astrophysics and Cosmology, Theoretical Division
Los Alamos National Laboratory, Los Alamos, NM 87545, U.S.A.

Roberto Capote Noy
Nuclear Data Section, International Atomic Energy Agency

February 2015

IAEA Nuclear Data Section
Vienna International Centre, P.O. Box 100, 1400 Vienna, Austria

Selected INDC documents may be downloaded in electronic form from
http://www-nds.iaea.org/publications
or sent as an e-mail attachment.
Requests for hardcopy or e-mail transmittal should be directed to
NDS.Contact-Point@iaea.org
or to:
Nuclear Data Section
International Atomic Energy Agency
Vienna International Centre
PO Box 100
1400 Vienna
Austria

Printed by the IAEA in Austria

February 2015

INDC(NDS)-0678
LA-UR-15-20961
Distr. AI+MN+NM

Prompt Fission Neutron Spectrum Evaluation Techniques

Donald L. Smith

Argonne National Laboratory, 1710 Avenida del Mundo #1506, Coronado, CA 92118, U.S.A.

Denise Neudecker

T-2 Nuclear and Particle Physics, Astrophysics and Cosmology, Theoretical Division
Los Alamos National Laboratory, Los Alamos, NM 87545, U.S.A.

Roberto Capote Noy

Nuclear Data Section, International Atomic Energy Agency

Abstract: The authors have undertaken an investigation of techniques for evaluating prompt fission-neutron spectra (PFNS) and their covariances that began during a visit by two of them (Smith and Neudecker) to the IAEA-NDS, Vienna, Austria, in July 2013. This collaboration has continued to the present time, with on-going evolution in our understanding of various technical issues associated with PFNS data evaluation. This paper does not attempt to provide a comprehensive review of other recent studies in this field, including those having to do with neutron spectrum evaluation methods or with evaluations for specific actinides such as ^{235}U, ^{239}Pu, or ^{252}Cf. This investigation has focused on several aspects of the evaluation of PFNS shape data and corresponding covariances directly in PFNS space, with an emphasis on the issue of PFNS data scaling. Considerable attention has been given in the present work to examining techniques for preparing diverse normalized and non-normalized data from nuclear modeling and experiments, as required for their combined inclusion by either simple linear least-squares (SLS) or generalized linear least-squares (GLS) evaluation procedures. Technical issues associated with normalizing non-normalized PFNS evaluated spectrum shapes and corresponding covariances to satisfy constraints on spectral shapes as well as their covariance matrices that are dictated by normalization have been examined in this investigation. Methods for computing PFNS average neutron energy and its uncertainty from evaluated PFNS shape data and corresponding covariances are also discussed in this paper.

February 2015

TABLE OF CONTENTS

Contents

1. Introduction

Nuclear data evaluation is a pragmatic undertaking that is guided by three basic considerations: 1) what is sought by the evaluation, *i.e.*, the physical quantities to be evaluated; 2) the nature and availability of data to be used in the evaluation (both experimental and model-calculated); and 3) the chosen evaluation methodology. Nuclear data evaluation is as much art as science so there is no unique way of approaching this task. Various potential methods present both opportunities and disadvantages. Simplifying assumptions and approximations are generally involved. Evaluations are always hampered by shortcomings in the scope and accuracy of available experimental data as well as by limitations of the nuclear modeling algorithms used to supplement the experimental results. Furthermore, the outcomes from various evaluation schemes that utilize the same input data inevitably differ quantitatively to some extent. Nevertheless, some confidence in these evaluations can be gained if differences in the outcomes due solely to different choices of evaluation methodologies are comparable to or less than the uncertainties in the underlying data that are being evaluated.

The evaluation of neutron-emission spectra from ^{252}Cf spontaneous fission, or of the prompt neutrons from neutron-induced fission of actinides such as ^{235}U, ^{239}Pu, *etc.* (PFNS), entails technical aspects that in some respects resemble the evaluation of neutron cross-section data. However, there are significant differences that result in the evaluation of PFNS data being a somewhat more arbitrary undertaking in many instances. Cross-section data used in evaluations are assumed to be properly normalized, with various data sets then treated as comparable in the evaluation process. However, in contemporary evaluated nuclear data libraries, such as ENDF/B, quantitative specification of neutrons emitted by fissionable actinide nuclei is split into two multiplicative components: total neutron yield and a normalize energy distribution "shape" function [1]. They are assumed to be independent.

The shapes of neutron-emission spectra as a function of neutron energy are given in nuclear data libraries in tabular form, with iteration schemes specified such that the numerical spectrum representation, when it is integrated with respect to neutron energy, yields unity. Furthermore, all rows and columns of the corresponding covariance matrix should sum to zero [1]. Actually, the ENDF-6 format does make an allowance for limitations of numerical precision, *e.g.*, it requires that the covariance-matrix row and column sums must not exceed 10^{-5} [1]. In this paper, when we specify that a PFNS is "normalized", it is meant that the above stated conditions apply to both the spectrum representation and its covariance matrix. We shall see that there is an important distinction between "normalized" spectra and "scaled spectra".

The average total number of prompt neutrons emitted at all energies by fissionable actinide nuclei is referred to as prompt nu-bar, or often just nu-bar, although technically that is not exactly correct as is indicated in the discussion below. Nu-bar can be measured quite accurately with 4-pi detectors without regard to the emitted-neutron energies. Therefore, nu-bar uncertainties in the corresponding evaluated values, at least for the major actinides, tend to be quite small in comparison with those for the PFNS shapes. As mentioned above, evaluated values of nu-bar, along with their uncertainties, are specified in data libraries separately from shape information [1].

The total number of neutrons, *i.e.*, nu-bar, is multiplied times the PFNS shape to provide a representation of the effective evaluated neutron yield for application purposes. The

uncertainties from these two components are also combined. Accurate knowledge of nu-bar is essential in calculating important integral quantities for multiplicative physical systems such as fission reactors (*e.g.*, k_{eff}), since the total number of neutrons present in any multiplicative system at a particular instant is directly related to nu-bar.

Delayed neutrons are also emitted following fission from the decay, by neutron emission, of highly excited fission-product nuclei. Delayed nu-bar refers to these neutrons, and its value is always very small compared to prompt nu-bar [2,3]. The spectrum of emitted delayed neutrons for a fissionable actinide nucleus depends on isotopic yields and details of the nuclear structure of the various radioactive fission-product isotopes that emit these neutrons. Consequently, the delayed-neutron energy-spectrum shapes differ greatly from those for prompt fission neutrons. Total nu-bar is the sum of prompt nu-bar and delayed nu-bar. Delayed nu-bar is also provided for several actinides in evaluated data libraries [1] since delayed neutrons play a very important role in controlling nuclear reactors [4]. However, for present purposes we shall be concerned only with prompt-neutron spectra, *i.e.*, with PFNS, since these neutrons dominate the neutron spectra encountered in most applications.

The spectral shapes of the PFNS neutrons can have a significant effect on the reactivity for certain critical assemblies. In general, the softer the spectrum (lower average energy) the greater the reactivity in thermal assemblies [5,6]. Knowledge of the fission-neutron energy-spectrum shape is also essential for interpreting spectrum-average neutron-dosimetry data. For this purpose, the neutron spectrum shape is folded with the differential cross-section data for these reaction processes [7]. In both applications it is also required to know the corresponding uncertainties.

Prompt fission-neutron spectral shapes as a function of emitted-neutron energy are rather difficult to measure [8,9,10]. The yields of neutrons at high energies are very low (*e.g.*, by several orders of magnitude) compared to the yields near the spectral maxima, which typically occur around 0.7 to 0.8 MeV depending on the fissionable isotope. At low energies, secondary neutrons from scattering interfere with measuring the direct fission neutrons. Furthermore, calibration of neutron detectors is quite challenging. It must be possible experimentally to span a broad range of detectable energies from as low as a few tens of keV to as high as 12 MeV, above which the yields are generally too low to measure by contemporary means. Techniques for performing these difficult measurements have been described in the literature [8,9,10]. PFNS for various actinides are often measured as ratios to the well-known spectrum of spontaneous-fission neutrons from ^{252}Cf in order to avoid having to calibrate the detector efficiencies directly, and to minimize the uncertainties and applied corrections (*e.g.*, multiple scattering). The difficulties associated with these experiments result in relatively large uncertainties at the low- and high-energy regions of the measured spectra. Statistical uncertainties clearly dominate at the high energies while systematic uncertainties play an important role at low energies. Experimental results generally need to be supplemented by calculated values based on nuclear theory since evaluated data libraries require that numerical values be provided from zero to 20 MeV. Theoretical work on the nuclear fission process has a long history (*e.g.*, [11,12]), and the quest to develop reliable quantitative characterizations of PFNS, based on a more sophisticated understanding of the physics of fission, continues to be an active area of both theoretical and experimental nuclear research and development [13,14,15,16,17].

There are two conceptually distinct approaches to evaluating PFNS data, as described in the following two paragraphs.

The first approach to evaluating PFNS data involves adjusting the parameters of a nuclear model of PFNS by least-squares to yield the best possible agreement of the calculated results with available experimental data. The adjusted model parameters and their uncertainties are then used exclusively to derive evaluated PFNS values over the entire energy range of the evaluation, along with their uncertainties. PFNS results can be generated in this manner from zero up to 20 MeV on as fine an energy mesh as desired. Therefore, it is a very convenient approach. Another advantage provided by the exclusive use of models in PFNS evaluations is that they offer the desired "smoothness" in the calculated shapes and corresponding covariances as a function of energy. This feature is generally lacking in experimentally derived evaluated results. Reliance on model calculations to generate PFNS, when the model parameters are adjusted to "fit" experimental data, can be justified in situations where the model used is known, based on extensive experience, to be capable of providing an adequate representation of the physical processes involved. However, there are two significant sources of uncertainty to consider regarding such model-calculated PFNS values. One source of uncertainty stems from the fact that knowledge of the parameters in these models is uncertain [18,19]. This source of uncertainty can be addressed through the least-squares adjustment process described above or through straightforward deterministic or Monte Carlo uncertainty propagation techniques [20]. The second source of uncertainty in model-calculated PFNS results is attributable to the perceived inability of the nuclear models to reproduce the "true" spectral shapes, *i.e.*, the so-called "model-defects" uncertainty [21,22]. Discrepancies between the models and "reality" are mainly traceable to imperfect understanding of the underlying physics. Model-defect uncertainties are difficult to quantify since differences between the results from a utilized model and the "true" spectrum representation cannot be ascertained. In short, there is no way of knowing the "true" values. However, some practical attempts have been made recently to quantify these modeling defects in an approximate way by performing selected comparisons between model-predicted and independent good-quality experimental results [21,22,23,24]. Also, effort is being devoted to eliminating some inherent deficiencies in contemporary modeling of PFNS spectra by acquiring a better understanding of the underlying physics of the nuclear fission process, as mentioned above.

The second conceptual approach to evaluating PFNS data involves weighted averaging of model and experimental data in such a way that an evaluated representation of the spectrum is produced that presumably incorporates information from both sources in a reasonable manner, thereby achieving coverage of the whole energy range of emitted neutrons, including regions where no experimental data exist. In this hybrid approach, greater weight is given to the experimental information in energy regions where they are plentiful, accurate, and consistent. In energy regions where the data are sparse or lacking, the evaluations must rely primarily on nuclear modeling. This hybrid evaluation approach usually leads to structure in the evaluated spectral results as a function of neutron energy. Such "spurious" structure is usually considered to be non-physical, and it is generally viewed as a consequence of statistical effects rather than physical ones. Numerical PFNS evaluated results obtained this way are frequently smoothed artificially to produce continuous representations of the spectra that are devoid of significant structure at all energies where the neutron yield is significant. This process of smoothing would appear to be motivated solely by a desire to cosmetically eliminate what evaluators consider to be inconsequential artifacts of the evaluation process. However, it can also serve the practical goal of making it possible to more conveniently represent the evaluated data in a tabular form, along with a prescribed interpolation procedure, that is amenable to inclusion in an evaluated data library.

Both of these evaluation concepts generally entail applications of linear least-squares methods, either simple least-squares (SLS) or generalized least-squares (GLS) algorithms, to generated evaluated central values as well as covariance matrices that specify their uncertainties and correlations. Least-squares procedures are approximate by nature since they involve linearization of physical quantities whose values as a function of energy (or various other parameters) can be rather non-linear. Fortunately, evaluators are able in most practical situations to rely on the linear approximation, with benefits that accrue from simplification, to yield results of sufficient accuracy. However, there are instances when they do need to be concerned about non-linear effects, especially when dealing with highly discrepant data and large uncertainties.

For evaluation purposes, it is important to understand clearly the distinction between "normalized" PFNS data, as described earlier in this section, and merely "scaled" PFNS data. There are no inherent numerical differences between a PFNS spectrum shape that is normalized to unity and one that is scaled to unity. The distinction between "normalized" and "scaled" PFNS appears ONLY in the distinct properties of their corresponding covariance matrices. For normalized PFNS the rows and columns of the covariance matrix must sum to zero. This need not be the case for scaled PFNS covariance matrices. In subsequent sections of this paper the origins of this distinction are discussed in more specific terms. The question naturally arises as to whether normalized and scaled PFNS can be "mixed" in a least-squares evaluation procedure. As a general rule, it appears to be preferable that evaluations be performed either with only scaled PFNS (and their covariance matrices), but not necessarily scaled to unity, with the normalization condition then imposed *a posteriori* on the solution, or with only normalized PFNS data (and their corresponding normalized covariance matrices), rather than with mixtures of these two categories of spectral data. This supposition is based on the philosophical notion that, when possible, it is preferable to work with quantities having similar properties rather than those with mixed properties. However, for reasons that are discussed at some length in this paper, it is usually not possible to perform an evaluation with only normalized or only non-normalized, but scaled, PFNS, since experimental PFNS are difficult to normalize while most model-calculated PFNS are inherently normalized. Nevertheless, it has been suggested that if the shape uncertainties of the model-calculated PFNS are larger than those of the experimental PFNS data, then reasonable evaluated results should still be obtainable regardless of whether both normalized and merely scaled data are utilized in the evaluation process, *i.e.*, if "mixtures" are involved [5,25]. This is especially true in practice if the linear approximation is deemed to be adequate. This point is explored briefly in this paper through an example given in Appendix B. Thorough investigation of this point is needed at some point, but this is beyond the scope of the present work. However, it is certainly true that model-calculated PFNS with limited numbers of parameters tend to be "stiff", *i.e.*, to have strong uncertainty correlations, resulting in a tendency toward low shape uncertainties for normalized model PFNS. Thus, the conditions for use of "mixed" PFNS data in evaluations involving models should be verified in each case.

This paper is structured as follows: First, the steps needed to prepare the available PFNS data (including model-calculated results), so that they can be used properly in a least-squares evaluation procedure, are discussed. An important part of this process involves scaling the various data sets so that they can be treated as "comparable" in an evaluation. It will be seen that there is no unique procedure for scaling PFNS shape data. Eleven options that have been considered in the course of this investigation are described in Appendix A. Next, the least-squares algorithms that are widely used in PFNS evaluations are described. The mathematical procedure for normalizing a non-normalized evaluated PFNS and its

covariance matrix is described, as well as the procedure for calculating PFNS average energies and their uncertainties from the evaluated PFNS results. Numerical comparisons of evaluated results obtained using the same hypothetical input data collection but various data scaling and least-squares data evaluation options are discussed in Appendix B. Appendix C contains tables that summarize the results from the exercises presented in Appendix B.

2. Preparation of PFNS Data

As indicated in Section 1, data used in PFNS evaluations are generally acquired from both nuclear modeling and experiments. Before an evaluation can be performed it is necessary to prepare this information in a manner that is compatible with SLS or GLS evaluation procedures that are used for this purpose. The work described here involves two aspects of data preparation: spectrum energy grouping and spectrum scaling. The following sections discuss these procedures. It is quite common in realistic evaluations to represent PFNS data as ratios of actual neutron yield values to Maxwellian functions with average energies comparable to those expected for the particular data types being evaluated. The purpose for this mathematical approach is to reduce the dynamic range of numbers being manipulated, since actual PFNS values extend over several orders of magnitude as the neutron energy ranges from a few tens of keV upward to 20 MeV. Another common approach to avoid issues due to the large dynamic range of values is to transform the evaluation input observables into logarithmic space, perform the evaluation there, and then transform the evaluated output back to linear PFNS space. Neither of these two approaches has been incorporated in the present investigation. The procedures and numerical analyses discussed in this paper operate only with direct PFNS values.

2.A. *Energy Grouping*

There are two methods of representing evaluated data for continuous PFNS as a function of emitted neutron energy. One is the point method; the second is the group method. In the point method evaluated PFNS values are provided at certain discrete energies and an interpolation scheme is specified for calculating values at intermediate energies. In the group method, contiguous energy intervals are defined and average PFNS values are determined for each energy interval. Group values are then defined as average PFNS values multiplied times the energy-interval widths. Therefore, an integral of the PFNS over energy can be represented as a discrete sum of group values over the entire range of the spectrum. While values of PFNS can be expressed either way, corresponding covariance data are always expressed in a way that is directly consistent with the energy-group approach. Therefore, it has been chosen in the present work to approach the evaluation of PFNS entirely from a group-structure perspective.

The concepts mentioned in the preceding paragraphs can be expressed in mathematical terms. For this purpose non-normalized group values Ω_i (i = 1,m) for an evaluated PFNS that is characterized by the continuous function $\Omega(E)$ are defined for the i^{th} group as $\Omega_i = \int_{(ELi,EHi)} \Omega(E)\, dE$, where $\int_{(Eli,EHi)}$ signifies integration of the continuous function $\Omega(E)$ over the energy interval (E_{Li},E_{Hi}). It is also possible to write $\Omega_i = \langle\Omega(E)\rangle_i \Delta E_i$, where $\langle\Omega(E)\rangle_i$ is the average value of $\Omega(E)$ over the indicated energy interval. The group flux Ω_i corresponds to the non-normalized neutron flux encountered with energies between the limits specified by the i^{th} energy interval of width ΔE_i. If the energy group structure is sufficiently fine (*i.e.*, the total number of groups m is relatively large) so that the histogram defined by the

indicated energy intervals and average values $\langle\Omega(E)\rangle_i$ provides an adequate representation of the continuous point energy spectrum, then it may be the case that $\langle\Omega(E)\rangle_i \approx \Omega(\langle E\rangle_i) \approx \Omega[\frac{1}{2}(E_{Li} + E_{Hi})]$. Exact equality is appropriate if Ω is a linear function of E in the i^{th} interval. In reality this is rarely the case, but this approximation can be quite adequate in many practical situations for sufficiently fine group structures. Only at the higher energies, where the neutron yield decreases steeply with increasing energy by orders of magnitude relative to the maximum yield in the vicinity of 0.7 to 0.8 MeV, can this assumption be called into question. This was first pointed out by Madland and Nix [11]. Nevertheless, in the following discussion it is assumed that the average energy $\langle E_i\rangle$ for the i^{th} group is taken as equal to the group midpoint energy.

In the present approach, the individual data sets provided for an evaluation, including the one based on model calculations, should be prepared in such a way that they conform to a common energy-group structure. This must be carried out in a way that avoids excessively distorting the information provided by the experimenters and theoretical modelers. Only then can data from these different sources be treated as comparable, even when they span different energy ranges, fail to cover particular energy groups, or lack initial consistency in scaling (as discussed below). This preparatory step requires effort on the part of the evaluator and it is inevitable that some approximations will need to be made. This is familiar to cross-section evaluators [24], so the procedures are not discussed further here.

It is not required that each experimental PFNS data set to be included in the evaluation process spans the entire energy range of the spectrum and yields values for every energy group. In fact, this will rarely if ever be the case for reasons mentioned above. However, it is essential that at least one PFNS data set used in the evaluation process – either from experiment or model - does span the entire neutron energy range, or that the data sets considered partially overlap and their union spans the whole range. Of course, a data set based on modeling can always be generated to span the whole energy range. Inclusion of model-calculated data in the evaluation process therefore insures that an evaluation can be generated that provides sufficient data coverage of the fission-neutron spectrum so that the requisite normalization constraint of the final evaluation can be performed and numerical values provided for the full energy range, as required for evaluated nuclear data libraries such as ENDF/B [1]. This is especially important in the evaluation of PFNS for scenarios where experimental data are very sparse, *e.g.*, for spectra resulting from fission by neutrons with incident energies above the second chance fission threshold. In the absence of a specific theoretical model of PFNS, another possibility for fulfilling this requirement would be to introduce *ad hoc* extrapolated or interpolated values (augmentation) that are consistent with trends suggested by integral experimental data, for those regions that lack direct experimental PFNS data [5]. The uncertainties in those regions will then be determined by the uncertainties associated with the augmented data. However, one should be aware that if this approach is taken it may compromise the possibility of eventually using the evaluated spectra for integral data testing unless care is taken to utilize only a subset of all the available integral data for this purpose. Then, it will be legitimate to use the resulting evaluation to validate the remainder of the available integral data. An alternative method in such situations would be to augment the existing data with values that are consistent with general trends in the shape of PFNS based on broad theoretical considerations [6,18].

2.B. *Scaling*

The next issue to consider is the scaling of individual PFNS data sets that have been expressed on a common energy-group structure. Scaling, *i.e.*, multiplying the data sets by constants, will not alter the shape of the individual input sets. This is important since the goal of a PFNS evaluation is to obtain reliable shape information based on the available data. Scaling should not distort this information.

Since GLS is widely used for data evaluation, for convenience the present discussion of scaling is first framed primarily in this context. Extension of the basic concepts to situations where SLS can be used is fairly straightforward. Assume that there exist K+1 PFNS data sets, with one of them originating from nuclear modeling, as discussed in the preceding paragraph. This model data set provides values for each of the m defined energy groups mentioned in Section 2.A, so it serves as a convenient prior for the GLS evaluation procedure.

In giving consideration to the selection of an appropriate prior when employing a GLS procedure for an evaluation, it is proper for an evaluator to explore the impact of the assumed correlations associated with a model-based prior. For example, it could be decided to either include or exclude the off-diagonal correlations, or to arbitrarily soften them to some extent. Such trials might not necessarily be related to physics considerations but rather they might be based on certain assumptions or previous knowledge that the evaluator is willing to invoke for pragmatic reasons. Some options to consider might be: i) to use model uncertainty values without any correlations in the region where experimental data are present; ii) to use the actual calculated model-parameter based covariances as input to the evaluation everywhere; or iii) to soften the often "stiff" model covariances associated with the second approach to somewhat "softer" (lesser in magnitude) values over certain regions of the spectrum, but not to set them to zero. Differences seen in the GLS evaluated results obtained from exploring these three approaches could be very relevant to the eventual outcome of the evaluation process [25]. For example, it might be concluded by the evaluator that using the actual PFNS covariances propagated from model-parameter uncertainties "contaminates" the evaluation process excessively because of their excessive stiffness, *i.e.*, that these correlations are more detrimental than helpful to the evaluation process. In any event, by examining limiting cases such as the three just mentioned, an evaluator can gain a better understanding of the impact of the assumptions associated with the utilized priors. As for justifying the consideration of such an approach to evaluating PFNS, an evaluator should gain some comfort in knowing that it is consistent with the Bayesian concept of utilizing priors that the evaluator believes reflect "rational degrees of expectation" as to what is actually known about the situation in advance of considering new objective information (*e.g.*, data from experiments).

In this paper, vectors and matrices generally are shown in bold font while scalar quantities are indicated in normal (non-bold) font. Group-spectrum prior values are denoted by the vector $\mathbf{\Phi}_0$. There are m non-zero elements of $\mathbf{\Phi}_0$ corresponding to the m contiguous energy groups that span the complete range of non-negligible values for the evaluated PFNS spectrum. The m x m covariance matrix for $\mathbf{\Phi}_0$ is denoted by $\mathbf{V}_{\Phi 0}$. The vector $\mathbf{\Phi}_0$ is assumed for present purposes to be non-normalized, including its covariance matrix, so a multiplicative scalar factor c_0 may need to be assigned that serves for scaling purposes in the evaluation procedure. The value of c_0 is to be determined as part of the data preparation

procedure and it will depend on the scaling approach utilized by the evaluator (see Appendix A).

Furthermore, it is assumed that there are K remaining non-normalized data sets to be used in the evaluation, and that all of them are based on independent experiments. These data sets are denoted by $\mathbf{\Phi}_k$ (k = 1,K) and their covariance matrices are identified by $\mathbf{V}_{\Phi k}$. Actually these data sets need not be entirely independent, but assuming so simplifies the discussions here and in Appendices A and B considerably without invalidating the basic evaluation methods. In realistic situations there may be uncertainties in these data sets that are correlated between the various sets, *e.g.*, in the case of the experimental PFNS if their detector calibrations are based on a common characterization of the ^{252}Cf spontaneous-fission neutron spectrum.

For present purposes, it is assumed that the k^{th} data set ($k \geq 1$) has n_k elements and the corresponding covariance matrix has dimension n_k x n_k. The dimensions of these vectors will vary from one data set to another, but $n_k < m$ in each instance since in realistic situations none of the experimental data sets are likely to provide values for every energy group involved in representing the PFNS. The scaling factors for these spectra are denoted by c_k (k = 1,K). It is important to recognize that only the relative values of the scaling factors matter for the evaluation of these non-normalized data, since the evaluated solution will ultimately be normalized. Eleven procedures that have been examined in the present work for determining these scaling factors are described in Appendix A. They are compared through hypothetical numerical examples presented in the Appendix B.

At first thought it would seem reasonable to consider uncertainties associated with determining the scaling parameters c_k when evaluating PFNS data. However, a recent investigation of this issue revealed that uncertainties from this origin are eliminated completely when a non-normalized evaluated PFNS and its associated covariance matrix are ultimately normalized [25]. However, some uncertainty in the spectrum shapes might arise from variations in the methods of determining the scaling factors. This point is explored in the present investigation.

After the scaling parameters c_k (k = 0,K) have been determined, it is possible to define a new collection of non-normalized vectors $\mathbf{z}_k$ with corresponding covariance matrices $\mathbf{V}_{zk}$ to characterize the scaled PFNS data sets that are to be employed in executing an actual GLS evaluation. Thus:

$$\mathbf{z}_k = c_k \, \mathbf{\Phi}_k \; (k = 0,K), \tag{1}$$

$$\mathbf{V}_{zk} = c_k^2 \, \mathbf{V}_{\Phi k} \; (k = 0,K). \tag{2}$$

In this formalism $\mathbf{z}_0$ and $\mathbf{V}_{z0}$ play the role of prior information for the GLS procedure whereas the $\mathbf{z}_k$ and $\mathbf{V}_{zk}$ (k = 1,K) represent new information which, in this case, corresponds to the available collection of experimental data. The outcome from applying the GLS procedure is a posterior solution PFNS that is used to generate the desired evaluation after it is normalized.

Although the preceding discussion focuses on scaling in the framework of the generalized least-squares (GLS) procedure, a similar approach to scaling applies in PFNS evaluations that utilize simple least-squares (SLS) procedures. The main difference is that in SLS one does not designate a particular spectrum to be a prior but rather treats all the PFNS

on an equal basis. Then, it is appropriate to drop the notation "k = 0" that suggests special treatment for a particular spectrum. Eqns. (1) and (2) still apply for SLS, but only for k = 1,K. Nevertheless, in SLS one generally designates a particular spectrum from the collection to serve as the anchor shape for scaling purposes, and then scales the other PFNS to it. It is convenient to designate $\mathbf{\Phi}_1$ as this anchor shape and set $c_1 = 1$. The scaling exercise required prior to performing the evaluation by SLS therefore involves determining the various additional c_k (k = 2,K).

3. PFNS Evaluation

There are two approximate mathematical approaches to evaluating data (both model-calculated and experimental) that are assumed to be normally distributed. As mentioned above, these are the linear simple least-squares (SLS) and linear generalized least-squares (GLS) procedures. They are approximate in the sense that the mathematical process is taken to be linear where in reality relationships between various parameters that describe physical processes need not always be linear. The extent to which actual data are indeed normally distributed is another matter. Nevertheless, the mathematical procedures associated with SLS and GLS are widely applied in data evaluation.

We begin the discussion with the GLS procedure for evaluating a PFNS. It is embodied completely in the following set of matrix equations [26,27]:

$$\mathbf{\Omega} = \mathbf{z}_0 + \mathbf{V}_{z0}\,\mathbf{A}^{+}\,(\mathbf{Q} + \mathbf{V}_y)^{-1}\,(\mathbf{y} - \mathbf{y}_0), \tag{3}$$

$$\mathbf{Q} = \mathbf{A}\,\mathbf{V}_{z0}\,\mathbf{A}^{+}, \tag{4}$$

$$\mathbf{V}_\Omega = \mathbf{V}_{z0} - \mathbf{V}_{z0}\,\mathbf{A}^{+}\,(\mathbf{Q} + \mathbf{V}_y)^{-1}\,\mathbf{A}\,\mathbf{V}_{z0}, \tag{5}$$

$$\chi^2 = (\mathbf{y} - \mathbf{y}_0)^{+}\,(\mathbf{Q} + \mathbf{V}_y)^{-1}\,(\mathbf{y} - \mathbf{y}_0). \tag{6}$$

Some explanation is required to understand the roles of the quantities appearing in Eqns. (3) – (6).

In Eqn. (3), $\mathbf{\Omega}$ represents the solution of the GLS procedure; *i.e.*, it is the evaluated non-normalized PFNS. It has dimension m, which is the same as the prior scaled PFNS representation $\mathbf{z}_0$, since the group representation for the evaluated PFNS must span the entire energy range of the spectrum. Both $\mathbf{\Omega}$ and the prior $\mathbf{z}_0$ correspond to the same energy-group representation. The solution covariance matrix generated by this procedure is denoted in Eqn. (5) by $\mathbf{V}_\Omega$. It has dimension m x m, which clearly is the same as the dimension of the prior covariance matrix $\mathbf{V}_{z0}$. The vector $\mathbf{y}$ that appears in Eqns. (3) and (6) represents the entire collection of non-normalized but appropriately scaled experimental data, *i.e.*, $\mathbf{y}$ is a vector that consists of K sub-vectors $\mathbf{z}_1$, $\mathbf{z}_2$, … , $\mathbf{z}_k$, … , $\mathbf{z}_K$ organized in column form in the order indicated. The dimension of $\mathbf{y}$ is n, where $n = \Sigma_{k=1,K}\, n_k$. The covariance matrix $\mathbf{V}_y$ in Eqns. (3), (5), and (6) has dimension n x n, and it is constructed from the covariance matrices $\mathbf{V}_{zk}$ (k = 1,K) as shown in Table 1. Note that "n" also represents the degrees of freedom (d.o.f.) of the GLS problem in that it corresponds to the number of experimental data points (sources of new information) that are introduced in order to update the prior information [27].

Table 1: The structure of the experimental data covariance matrix $\mathbf{V}_y$ is shown here. The matrix is symmetric so the upper half values of $\mathbf{V}_y$ are not exhibited explicitly. Off-diagonal blocks of zero sub-matrices reflect the fact that it has been assumed for present purposes that the K distinct PFNS data sets are uncorrelated with each other. Of course it is also assumed that these experimental data sets are uncorrelated with the prior PFNS representation that is based on nuclear modeling.

$\mathbf{V}_{z1}$									
0	$\mathbf{V}_{z2}$								
0	**0**	.							
0	**0**	**0**	.						
0	**0**	**0**	**0**	.					
0	**0**	**0**	**0**	**0**	$\mathbf{V}_{zk}$				
0	**0**	**0**	**0**	**0**	**0**	.			
0	**0**	**0**	**0**	**0**	**0**	**0**	.		
0	**0**	**0**	**0**	**0**	**0**	**0**	**0**	.	
0	**0**	**0**	**0**	**0**	**0**	**0**	**0**	**0**	$\mathbf{V}_{zK}$

The vector $\mathbf{y}_0$ is the calculated equivalent of the experimental vector $\mathbf{y}$ that is derived from the prior values of the adjustable parameters, *i.e.*, the elements of $\mathbf{z}_0$. Vector $\mathbf{y}_0$ has dimension n as does $\mathbf{y}$, and their comparable elements have the same physical units. In the GLS procedure the elements of $\mathbf{y}$ and $\mathbf{y}_0$ should not differ by very much in magnitude since they represent corresponding measured values and quantities calculated from best-estimate values for the prior parameter values $\mathbf{z}_0$ using the model that relates the observable quantities to the adjustable parameters. Thus, $\mathbf{y} \approx \mathbf{y}_0 = \mathbf{f}(\mathbf{z}_0)$. $\mathbf{A}$ is an n x m linear sensitivity matrix whose values depend on specified functional relationships, denoted by $\mathbf{f}$, between $\mathbf{y}_0$ and $\mathbf{z}_0$. The elements of $\mathbf{A}$ are a_{vi} (v = 1,n; i =1,m), and they are derived from the formula $a_{vi} = \partial f_v(\mathbf{z}_0)/\partial z_{0i}$. Since in this exercise the adjustable parameters denoted by $\mathbf{z}$ are mathematically comparable to the physical quantities $\mathbf{y}$, the matrix $\mathbf{A}$ consists entirely of partial derivatives whose values are either 0 or 1. These 0's and 1's are strategically situated in the matrix $\mathbf{A}$ to insure compatibility of the measured data and the computed equivalent values that are based on the prior parameter values [27]. It is stressed that while the details discussed in this paragraph are not very difficult to conceptualize, the bookkeeping effort required to insure that $\mathbf{y}$, $\mathbf{y}_0$, and $\mathbf{A}$ are properly structured for compatibility can be quite tedious for the large data sets often encountered in realistic PFNS evaluations.

$\mathbf{Q}$ is a covariance matrix that provides the uncertainty and correlation information for $\mathbf{y}_0$ based on propagating uncertainties from the prior covariance matrix $\mathbf{V}_{z0}$. Its inclusion insures that the GLS evaluation procedure considers the uncertainties in the model-calculated PFNS spectrum as well as those from the experimental components. The symbols "+" and "$^{-1}$" that appear as superscripts in Eqns. (3) – (6) signify matrix transposition and matrix inversion, respectively [27].

The quantity χ^2 is a chi-square parameter associated with the GLS algorithm. It provides a consistency test of the input information, taking into consideration the uncertainties of the model-calculated prior PFNS as well as of the experimental values. As is evident from Eqn. (6), χ^2 can be calculated prior to executing the GLS procedure. Actually, it is the chi-square per degree of freedom (or chi-square per d.o.f.) that is of interest, *i.e.*, χ^2/n, since, as mentioned above, "n" represents the degrees of freedom of the mathematical problem as well as the number of experimental data values [27]. If the PFNS data used in the evaluation are consistent, in the context of the specified uncertainties, then $\chi^2/n \approx 1$. If $\chi^2/n << 1$, these data are most likely unrealistically consistent. This suggests that the assigned uncertainties may be too large. The PFNS data are considered to be inconsistent if $\chi^2/n >> 1$. There are several possible sources of inconsistency. One source might be inadequate scaling of the data prior to executing the GLS procedure. Another source could be that the specified uncertainties in the PFNS data are too small when compared to actual scatter of the data. Finally, significant shape inconsistencies for the assembled PFNS data that cannot be purged by scaling can lead to large values of χ^2/n. Whenever values of χ^2/n that are significantly greater than unity are encountered, an investigation as to the source of the problem needs to be undertaken. A PFNS evaluation should not be accepted for inclusion in an evaluated data library until the problem is resolved or a compromise reached.

A final comment here concerns the use of model-calculated PFNS in a GLS evaluation procedure. As alluded to earlier in this paper, there are unique features of model-calculated data covariance matrices when compared to results from experiments. In particular, the correlations for model-generated data covariances tend to be stronger (stiffer) than those corresponding to comparable experimental data. This can be problematic for two reasons. First, too-strong model correlations can lead to low evaluated uncertainties. Second, they can restrain the evaluated mean values such that they cannot reproduce reasonable experimental data.

The simple least-squares (SLS) approach to evaluating PFNS can be applied when the spectra to be considered can be treated on more or less equal footing, *e.g.*, when all the spectra originate from experiments and they collectively span the entire energy range of the PFNS without having to resort to the use of a model-based prior. Such non-model evaluations would be appropriate if there are extensive, comprehensive data as, *e.g.*, in the case of ^{252}Cf spontaneous fission PFNS. The equations used in SLS evaluations are as follows:

$$\mathbf{\Omega} = \mathbf{V}_\Omega \, \mathbf{A}^+ \, \mathbf{V}_y^{-1} \, \mathbf{y}, \tag{7}$$

$$\mathbf{V}_\Omega = (\mathbf{A}^+ \, \mathbf{V}_y^{-1} \, \mathbf{A})^{-1}, \tag{8}$$

$$\chi^2 = (\mathbf{y} - \mathbf{A}\,\mathbf{\Omega})^+ \, \mathbf{V}_y^{-1} \, (\mathbf{y} - \mathbf{A}\,\mathbf{\Omega}). \tag{9}$$

The symbols appearing in the SLS formalism, as embodied in Eqns. (7) – (9), have the same significance as they do in the preceding discussion for the GLS formalism. Vector $\mathbf{y}$ is the union vector of all the $\mathbf{z}_k$ (k = 1,K) and $\mathbf{V}_y$ is the corresponding covariance matrix constructed from the component matrices $\mathbf{V}_{zk}$. $\mathbf{A}$ is the design matrix that relates the elements of $\mathbf{y}$ to the appropriate PFNS groups. In SLS, the chi-square per d.o.f. is given by $\chi^2/(n - m)$, where m represents the number of grid intervals used in representing the PFNS and n is the total number of data values included as input to the evaluation process. Clearly, n > m is required, and this is a characteristic of SLS in comparison to GLS, where n, in principle,

could be any integer value greater than unity, and it applies only to the experimental values and not to the prior ones.

4. Normalization of the Evaluated PFNS

The evaluated PFNS $\mathbf{\Omega}$ and its covariance matrix $\mathbf{V}_\Omega$ are not likely to be properly normalized for inclusion as shape data in an evaluated data library, even if they are based on input data that have been scaled. What is ultimately required for present purposes is a truly normalized PFNS. This section demonstrates how this normalization is accomplished.

It is desired to transform an evaluated non-normalized discrete PFNS group representation $\mathbf{\Omega}$ to a normalized discrete group representation $\mathbf{\Psi}$ having the property that

$$\Sigma_{i=1,m}\, \Psi_i = 1. \tag{10}$$

The discrete sum of group-spectrum values in Eqn. (10) is equivalent to the integral of a continuous function $\Psi(E)$ over the complete energy range of the spectrum. The energy-group structure will have been chosen at the outset so that the first interval with width ΔE_1 will have a lower limit of zero and the upper-most interval with width ΔE_m will have an upper limit in a region where the functional values $\Psi(E)$ are vanishingly small (typically $\approx$ 12 MeV for actual PFNS). Of course, it may be necessary to provide evaluated PFNS values up to 20 MeV to satisfy the format requirements of data libraries, even though these numbers are vanishingly small and therefore of no practical consequence [1]. The evaluated, non-normalized group PFNS, consisting of values Ω_i obtained by the procedure described in Section 3, will generate a finite positive number (mostly likely not 1) when summed over all m groups (it can be denoted by G for convenience) [25]. Thus, for i = 1,m:

$$G \equiv \Sigma_{i=1,m}\, \Omega_i \,. \tag{11}$$

Therefore, Ω_i and Ψ_i are related by the expression

$$\Psi_i = [\Omega_i \,/\, (\Sigma_{i=1,m}\, \Omega_i)] = \Omega_i \,/\, G \quad (i = 1,m). \tag{12}$$

It is obvious that this step effectively normalizes the group spectrum values Ψ_i, according to Eqn. (10), as desired for the energy-group structure defined in the present evaluation procedure.

The collection $\{\Psi_i\}$ forms a vector $\mathbf{\Psi}$ with dimension m. The relationship between $\mathbf{\Psi}$ and $\mathbf{\Omega}$ given by Eqn. (12) is straightforward, but it is not a linear one. This has important implications when transforming the m x m covariance matrix $\mathbf{V}_\Omega$ for $\mathbf{\Omega}$ to the corresponding m x m covariance matrix $\mathbf{V}_\Psi$ for $\mathbf{\Psi}$. It is for this reason that the normalization procedure described in this section usually is carried out as the last step of the PFNS evaluation process, *i.e.*, after executing the SLS or GLS procedure that generates $\mathbf{\Omega}$ and $\mathbf{V}_\Omega$.

The covariance matrix $\mathbf{V}_\Psi$ can be obtained from $\mathbf{V}_\Omega$ by applying the well-known, linear (first-order) Law of Error Propagation (often referred to as the "Sandwich Rule") [25,26,28]:

$$\mathbf{V}_\Psi = \mathbf{T}\, \mathbf{V}_\Omega\, \mathbf{T}^+. \tag{13}$$

T is the m x m sensitivity matrix that implements the desired transformation. Its elements are defined as $(\mathbf{T})_{ij} = (\partial\Psi_i/\partial\Omega_j)$. It can be shown that:

$$(\mathbf{T})_{ij} = (\partial\Psi_i/\partial\Omega_j) = (G\,\delta_{ij} - \Omega_i) / G^2, \tag{14}$$

where δ_{ij} is the Kronecker Delta function: $\delta_{ii} = 1$ (i = 1,m) and $\delta_{ij} = 0$ for all $i \neq j$ (i,j = 1,m). This is the final step of the evaluation procedure that yields a normalized, evaluated neutron-emission spectrum representation $\mathbf{\Psi}$ along with its associated covariance matrix $\mathbf{V}_\Psi$ that can be included in an evaluated data library [1,28].

The number of groups, m, and the detailed group-energy interval structure, with interval boundaries and corresponding widths ΔE_i, must be specified in an evaluated data library if these results are to be useful for applications. Also, it may be required by data users for evaluators to produce a normalized point representation of the PFNS, $\Psi(E)$, along with an interpolation rule that can be used to approximate the continuous spectrum numerically. Care then needs to be taken to insure that this continuous point representation $\Psi(E)$ is consistent with the evaluated (normalized) group spectrum values represented by the vector $\mathbf{\Psi}$. The point representation of $\Psi(E)$ must also be normalized such that it integrates to unity over the same inclusive energy range as the group representation, with point values at arbitrary energies within this range obtained by invoking a clearly specified interpolation scheme.

Since covariance matrices can be defined only for discrete sets of values, corresponding to defined neutron-energy intervals, the covariance matrix $\mathbf{V}_\Psi$ should continue to apply in representing PFNS shape uncertainties regardless of how the central values are represented.

5. Smoothing of Evaluated PFNS Results

A GLS evaluation procedure inevitably generates evaluated group PFNS results $\mathbf{\Psi}$ such that the values $\Psi_i/\Delta E_i$ (i = 1,m) do not readily define a smooth curve as a function of energy. This is a consequence of statistical fluctuations in the experimental data employed in the evaluation process. In principle this is not a problem, but for practical as well as cosmetic reasons there is a preference by data users for smooth-curve representations of evaluated data. This is especially true if these results are represented in data libraries in point format [1].

Various smoothing procedures have been suggested and used for this purpose [5], but there is no clear basis for preferring any particular smoothing method as long as the resulting values differ from the actual evaluated values by amounts that are insignificant in comparison with the evaluated uncertainties. No smoothing is required for evaluated covariance data that are always represented in group format in evaluated data libraries [1], often as relative rather than absolute covariance matrices. This paper does not address the topic of PFNS data smoothing methods.

6. PFNS Average Energy

The average energy ε of a PFNS is a parameter that is frequently used to characterize PFNS for application purposes [5,18,23]. It is defined by $\varepsilon = \int E\,\Psi(E)\,dE$, where $\Psi(E)$ is the normalized PFNS and integration formally extends from 0 to infinity (or to an upper energy

limit beyond which the PFNS is vanishingly small). For completeness, this section examines two methods for calculating ε and determining its uncertainty based on evaluated group PFNS and average group energies. One method uses the normalized evaluated group-spectrum values while the other approach uses the non-normalized evaluated results. Both of these approaches should yield the same answer. Although not discussed here, it is obvious that similar calculations can be performed if given continuous point representations of these spectra, as described in Sections 3, 4, and 5.

6.A. *Normalized Spectrum Formalism*

The PFNS average energy ε can be expressed approximately as a function, denoted by "h", of the normalized group values $\mathbf{\Psi}$ and the selected point energy values $\langle\mathbf{E}\rangle$ that one chooses to associate with these groups. The vector $\langle\mathbf{E}\rangle$ corresponds to ($\langle E_1\rangle$, $\langle E_2\rangle$, … , $\langle E_i\rangle$, … , $\langle E_{m-1}\rangle$, $\langle E_m\rangle$). As discussed in Section 2, one possibility for defining each $\langle E_i\rangle$ – a choice that is likely to be adequate for most practical applications that utilize many groups – is $\langle E_i\rangle = \frac{1}{2}(E_{Li} + E_{Hi})$, where (E_{Li},E_{Hi}) defines the i^{th} group energy interval with width ΔE_i. In other words, $\langle E_i\rangle$ is taken to be the mean energy value of the i^{th} energy-group interval. As also mentioned in Section 2, the larger the number of groups involved, the better this approximation becomes. Thus,

$$\varepsilon \approx h(\langle\mathbf{E}\rangle,\mathbf{\Psi}) = \Sigma_{i=1,m} \langle E_i\rangle \Psi_i \, . \tag{15}$$

Since $\Sigma_{i=1,m} \Psi_i = 1$, the weighting values for the individual average group energies $\langle E_i\rangle$ that are exhibited in Eqn. (12) are automatically normalized in this formula. Of course, it is very important that the group representation span the entire energy range of significant neutron yield for the PFNS. In this formalism the $\langle E_i\rangle$ are not assigned uncertainties. However, the individual normalized spectrum values Ψ_i that form the weighting factors are taken to be uncertain. These uncertainties are characterized by the m x m covariance matrix $\mathbf{V}_\Psi$, as defined by Eqn. (13). Consequently, the uncertainty in the average energy ε based on Eqn. (15) can be derived using the Law of Error Propagation [26,28], namely,

$$V_\varepsilon \approx \mathbf{W}\, \mathbf{V}_\Psi\, \mathbf{W}^{+}. \tag{16}$$

The elements of the 1 x n sensitivity matrix $\mathbf{W}$ are given by the expression

$$(\mathbf{W})_{1j} = (\partial h/\partial \Psi_j) = \langle E_j\rangle, \quad (j = 1,m). \tag{17}$$

V_ε is a scalar quantity that corresponds to the estimated variance in the average energy ε. Therefore, the absolute uncertainty (standard deviation) e_ε in the average energy is given by $e_\varepsilon = (V_\varepsilon)^{1/2}$.

Three points that need to be stressed regarding this discussion of average energy are:

i) The uncertainty in the average energy can be traced directly to the uncertainty in the normalized spectrum representation.

ii) Once the average energy has been defined in this manner, its uncertainty can be computed in a straightforward way using the Law of Error Propagation.

iii) A fine energy-grid structure is required to obtain an accurate value for the average energy when it is calculated using group PFNS data in the manner described in this section. Even if a point representation is used, the results

will be quite sensitive to the assumed point mesh structure since the PFNS values at energies elsewhere need to be determined by interpolation.

6.B. *Non-normalized Spectrum Formalism*

The formalism for evaluating PFNS average energy ε in the case of non-normalized spectral information is very similar to that described for normalized spectra, as described in Section 6.A. The average energy is given by the expression

$$\varepsilon \approx (\Sigma_{i=1,m} <E_i> \Omega_i) / (\Sigma_{i=1,m} \Omega_i) = (\Sigma_{i=1,m} <E_i> \Omega_i) / G. \quad (18)$$

Ω is the collection of non-normalized evaluated group spectrum values. The covariance matrix (variance) for ε can be derived using the Law of Error Propagation. Thus,

$$V_\varepsilon \approx \mathbf{U}\, \mathbf{V}_\Omega\, \mathbf{U}^+ . \quad (19)$$

U is the 1 x n sensitivity matrix that is used to perform the transformation. The elements of **U** are given by the formula

$$(\mathbf{U})_{1j} = (\partial\varepsilon/\partial\Omega_j) = (E_j - \varepsilon) / G, \quad (j = 1,m). \quad (20)$$

The absolute uncertainty e_ε in ε is therefore given by $e_\varepsilon = (V_\varepsilon)^{1/2}$. This value is identical to the result obtained using the normalized evaluated PFNS.

7. Conclusions

It is inevitable that scale differences will exist in PFNS data sets employed in an evaluation, even if care is taken to calibrate the detectors used and determine all the other factors that influence the experimental results. Therefore, it is clear that different PFNS data sets in a collection that are used in an evaluation do need to be scaled in order to be able to evaluate these data properly and thereby provide recommended values of PFNS shapes for use in data libraries. There is no unique procedure for performing the necessary data scaling exercise. This paper investigates eleven approaches to scaling and evaluating PFNS data (Appendix A). They fall into two broad categories. In one category an anchor shape is generated for scaling purposes that is based on averaging input PFNS data over limited ranges of neutron emission energy where the neutron spectrum is represented by all the input data sets. The averaging process may or may not weight the values being averaged based on their uncertainties. The second category includes those methods that utilize one of the input spectra as the anchor shape for scaling purposes. Usually it is the one based on model calculations that can provide values for the entire energy range of the spectrum. Again, the scaling procedure may or may not take uncertainties of the input data into consideration, but all the available data can be considered if desired, not just those in a limited energy range. In both of these categories, the scaling is accomplished by multiplying the individual input PFNS by their corresponding derived scaling factors.

The methods described in this paper are compared by using a hypothetical ("toy") data set that illustrates many of the issues encountered in scaling, evaluating, and normalizing PFNS data (Appendix B). Most of these methods yield results that agree very well with each other. This suggests that PFNS evaluations may not be particularly sensitive to the choice of

scaling method used as long as the scaling procedure employed makes reasonable use of the available PFNS data. This is not a surprising conclusion since no matter which scaling approach is used, the shapes of the input PFNS are not altered by scaling.

If the data scaling is non-optimal, and this becomes evident if the least-squares evaluation procedure generates a chi-square value which is not as small as it could be, then the influence of individual input PFNS may become distorted and the evaluated results will be less reliable than they might be. The key, therefore, appears to be to achieve through the scaling process the lowest possible value of chi-square allowed by the input data. Of the eleven scaling methods considered in this paper, *Scaling Method 7* (Appendix A) is probably the one that could be viewed as the most "rigorous" one since it utilizes all the input information (PFNS values as well as covariance data) in a mathematically consistent manner with the fewest assumptions. However, this method is also mathematically the most complicated approach. In the examples considered in Appendix B, this additional complexity leads to only small differences in the obtained results from several other simpler ones, so it may not be worth the trouble. It is left to evaluators to decide which approach is the most practical one for the particular task involved. Furthermore, it may be prudent to try several approaches in a particular evaluation.

While there is a preference on philosophical grounds for performing PFNS evaluations with input data that are either all normalized or all non-normalized, the present investigation suggests that in practice these evaluations can often be performed with mixtures of normalized and non-normalized input PFNS as long as these data are properly scaled. The key is that the assumption of linearity inherent to SLS and GLS evaluation procedures be adequately fulfilled by the data being treated [25]. The normalization constraint is usually present with model-calculated PFNS. However, few difficulties should be encountered as long as the shape uncertainties of the model are larger than those of the experimental data (considered collectively). Care must be taken to avoid the pitfalls associated with strong correlations found in data generated by nuclear models that involve only a few variable parameters [18]. This requirement places a premium on developing physical models of PFNS with a sufficient number of parameters to insure that the minimum uncertainty at the pivot-point energy for a normalized PFNS will not be too small [5,18]. This practical need for applied evaluation purposes, as well as the desire, from a fundamental scientific perspective, to develop better models of neutron fission and PFNS, is a strong motivator of ongoing theoretical research on nuclear-fission physics in the nuclear science community [13,14,15,16].

Non-model evaluations based on SLS are possible in principle, and they will yield reasonable results as long as experimental data sets are available to span the entire energy range of significant PFNS yield [5]. If not, in some situations it may be possible to augment these data with estimated values as long as the impact of these introduced values on the evaluation process is modest [5]. However, in most cases it is necessary to employ nuclear models to generate prior PFNS spectra which can then be merged by a GLS procedure with experimental data to provide an evaluation.

Finally, since evaluated shape PFNS results and corresponding uncertainties are sought through the evaluation procedures discussed here, rather than absolute neutron-yield data, the normalization constraint should always be applied to the posterior solution PFNS data as a last step, regardless of which approach is used in performing the evaluation. Even when an obtained solution PFNS is found to be close to satisfying the normalization

constraint (with concurrent row-and-column sums close to zero for the covariance matrix), applying the transformation described in Section 4 one more time should yield a final result which is in even closer compliance with this constraint [1], with only very small changes in the evaluated numerical results.

Acknowledgments

The authors appreciate many fruitful discussions on this topic with Patrick Talou, Toshihiko Kawano, Vladimir Pronyaev and Andrej Trkov. Two of the authors (D.N. and D.L.S) are grateful for support from the IAEA that enabled this work to be undertaken. The work performed at Los Alamos National Laboratory was partly carried out under the auspices of the National Nuclear Security Agency of the U.S. Department of Energy under Contract No. DE-AC52-06NA25396.

References

[1] "ENDF-6 Formats Manual: Data Formats and Procedures for the Evaluated Nuclear Data Files ENDF/B-VI and ENDF/B-VII", written by the Members of the Cross Section Evaluation Working Group, Edited by M. Herman and A. Trkov, National Nuclear Data Center, Brookhaven National Laboratory, Upton, NY 11973-5000 (July 2010). Internet: www.bnl.gov/isd/documents/70393.pdf.

[2] "DOE Fundamentals Handbook - Nuclear Physics and Reactor Theory", Report DOE-HDBK-1019/1-93, U.S. Department of Energy (January 1993).

[3] John T. Mihalczo, "Radiation Detection from Fission", Report ORNL/TM-2004/234, Oak Ridge National Laboratory (November 19, 2004).

[4] H. Nifenecker *et al.*, "Basics of Accelerator Driven Subcritical Reactors", *Nucl. Instr. and Meth. in Phys. Research* **A463**, 428 (2001).

[5] A. Trkov. V. Pronyaev, and R. Capote, "Current Issues in Nuclear Data Evaluation Methodology: ^{235}U Prompt Fission Neutron Spectra and Multiplicity for Thermal Neutrons", *Nuclear Data Sheets* **123**, 8 (2015).

[6] T. Kawano *et al.*, "Statistical and Evaporation Models for Neutron Emission Energy Spectrum in the Center-of-Mass System from Fission Fragments", *Nucl. Phys.* **A913**, 51 (2013).

[7] R. Capote *et al.*, "Updating and Extending the IRDF-2002 Dosimetry Library", *Journal of the ASTM International* **9**(4), 197 (2012).

[8] H.-H. Knitter, "Measurement of the Energy Spectrum of Prompt Neutrons from the Fission of ^{239}Pu by 0.215-MeV Neutrons", *Atomkernenergie* **26**, 76 (1975).

[9] P. Staples *et al.*, "Prompt Fission Neutron Energy Spectra Induced by Fast Neutrons", *Nucl. Phys.* **A591**, 41 (1995).

[10] W. Boldeman, "Review of Measurements of the Prompt Fission Neutron Spectrum from the Spontaneous fission of ^{252}Cf", Report IAEA-TECDOC-410, International Atomic Energy Agency, Vienna, Austria, 127 (1987).

[11] D.G. Madland and J.R. Nix, "New Calculation of Prompt Fission Neutron Spectra and Average Prompt Neutron Multiplicities", *Nucl. Sci. Eng.* **81**, 213 (1982).

[12] P. Möller, J.R. Nix, W.D. Myers, and W.J. Swiatecki, *Atomic Data and Nuclear Data Tables* **59**, 185 (1995).

[13] T. Kawano *et al.*, "Effect of the Pre-equilibrium Process Upon Fast-Neutron Fission Spectra from ^{238}U", *Phys. Rev.* **C63**, 034601 (2001).

[14] R. Vogt *et al.*, "Event-by-Event Study of Prompt Neutrons from ^{239}Pu(n,f)", *Phys. Rev.* **C80**, 044611 (2009).

[15] O. Litaize and O. Serot, "Investigation of Phenomenological Models for the Monte Carlo Simulation of the Prompt Fission Neutron and γ Emission", *Phys. Rev.***C82**, 054616 (2010).

[16] B. Becker *et al.*, "Monte Carlo Hauser-Feshbach Predictions of Prompt Fission Gamma Rays: Applications to n + ^{235}U, n + ^{239}Pu, and ^{252}Cf (sf)", *Phys. Rev.* **C87**, 014617 (2013).

[17] M.B. Chadwick *et al.*, "The CIELO Collaboration: Neutron Reactions on ^{1}H, ^{16}O, ^{56}Fe, ^{235,238}U, and ^{239}Pu", *Nuclear Data Sheets* **118**(12) 1, (2014).

[18] P. Talou *et al.*, "Uncertainty Quantification of Prompt Fission Neutron Spectrum for n(0.5 MeV) + ^{239}Pu", *Nucl. Sci. Eng.* **166**, 254 (2010).

[19] R. Capote *et al.*, "Reference Input Parameter Library for Calculations of Nuclear Reactions and Nuclear Data Evaluations", *Nuclear Data Sheets* **110**(12), 3107 (2009).

[20] D. Rochman *et al.*, "Nuclear Data Uncertainty Propagation: Total Monte Carlo vs. Covariances", *Journal of the Korean Physical Society* **59**(2), 1236 (2011).

[21] H. Leeb *et al.*, "Consistent Procedure for Nuclear Data Evaluation Based on Modeling", *Nuclear Data Sheets* **109**(12), 2762 (2008).

[22] D. Neudecker *et al.*, "Impact of Model Defect and Experimental Uncertainties on Evaluated Output", *Nucl. Instr. and Meth.* **723A**, 163 (2013).

[23] D. Neudecker *et al.*, "Preliminary Evaluation and Uncertainty Quantification of the Prompt Fission Neutron Spectrum of ^{239}Pu", *Nuclear Data Sheets* **123**, 146 (2015).

[24] A.D. Carlson *et al.*, "International Evaluation of Neutron Cross Section Standards", *Nuclear Data Sheets* **110**(12), 3215 (2009).

[25] D. Neudecker *et al.*, "Impact of the Normalization Condition and Model Information on Evaluated Prompt Fission Neutron Spectra and Associated Uncertainties", *Nucl. Sci. and Eng.* (to be published).

[26] D.L. Smith, *Probability, Statistics, and Data Uncertainties in Nuclear Science and Technology*, American Nuclear Society, LaGrange Park, Illinois (1991).

[27] D.L. Smith, "A Least-Squares Computational Tool Kit", Report ANL/NDM-128, Argonne National Laboratory (1993).

[28] D.L. Smith and N. Otuka, "Experimental Nuclear Reaction Data Uncertainties: Basic Concepts and Documentation", *Nuclear Data Sheets* **113**(12), 3006 (2012).

[29] N.V. Kornilov, "Scale Method for Evaluation of Fission-Neutron Spectra", *Nucl. Sci. and Eng.* **169**, 290 (2011)

[30] "Maxwell-Boltzman Distribution", *Wikipedia*. Taken from the Internet at the following URL: http://en.wikipedia.org/wiki/Maxwell%E2%80%93Boltzmann_distribution (January 31, 2015).

Appendix A

PFNS Data Scaling

The reason for scaling PFNS data sets prior to performing an evaluation is that it is important to eliminate, to the extent possible, the effects of differences in the often unspecified scales of different group data sets so that the adjusted (*i.e.*, scaled) data can then be employed to evaluate spectral shapes using the GLS of SLS procedures discussed in Section 3. Section 2 describes in mathematical terms the precise role that scaling plays in preparing energy-grouped PFNS data for evaluation by the least-squares methods. The issue of scaling PFNS data for evaluation purposes has been discussed elsewhere (*e.g.*, [29]), and it has been investigated further in the present work. This appendix describes eleven different PFNS data scaling methods that have been examined in the present investigation. All of these techniques are essentially *ad hoc* in that they cannot be justified on the basis of any rigorous principles, but rather they are presented here for pragmatic purposes. There may be even better approaches than those mentioned here that could be applied in certain practical cases, but even then the basic concept should be the same. From a practical point of view, in any particular instance a viable scaling method should normally be viewed as one that is physically reasonable and leads to the smallest possible chi-square "goodness of fit" test parameter generated by a GLS or SLS procedure. For effectively scaled data sets, the major contributors to this chi-square test parameter should come from shape differences and scatter in the input data values rather than spectrum scale effects. This work explores the following question: "To what extent are the evaluated normalized PFNS results and their uncertainties dependent on the method used to scale the input spectral data?"

Such a pragmatic approach might not appeal to individuals for whom rigor is of paramount importance. However, the evaluation of nuclear data for the most part is conducted with applied objectives in mind. Evaluators are required to generate information that can be used for nuclear-reactor design studies and related applications. They cannot afford the luxury of refusing to undertake this important task simply because the data available to them are inadequate, uncertain, and possibly even discrepant. There appear to be no unique methods available for producing reasonable evaluated results in the presence of these existing limitations. The notion that the end justifies the means has unsavory connotations; however, that is quite often what evaluators are required to do. The challenge is in being able to apply experienced judgment to accomplish this task in a manner that yields evaluated data that data users will accept as reasonable, reliable, and therefore trustworthy for their applications.

A.1. Basic Concept of Scaling

The basic concept of data scaling can be illustrated by examining two separate plots of two hypothetical data sets that purport to represent the same physical information, but that clearly possess inherently distinct but unspecified scales. This is shown in Fig. A.1. One plot (left side) shows the original unscaled data while the second plot (right side) shows the scaled results. The first data set is identified by red squares while the second one is identified by blue diamonds. For convenience in illustrating the concept, each data set has the same number of values corresponding to a common collection of characterizing parameters (*e.g.*, energy groups), as indicated on the abscissa of each plot.

The method used here to scale these data so as to generate the results shown in the right-hand plot is as follows: First, simple (un-weighted) averages are calculated of the corresponding red and blue values, taken group-by-group. These average values are exhibited using the same dashed line in both plots. Second, separate sums are calculated of all the un-weighted red values, of all the un-weighted blue values, and of all the computed average values. The scaling factor c_red used to scale (multiply) the original red values equals the sum of all the average values divided by the sum of all the original red values. The scaling factor c_blue used to scale (multiply) the original blue values is the sum of all the average values divided by the sum of all the original blue values. Another way of looking at this is that the scaling factors c_red and c_blue are calculated as ratios of an average of the calculated average values divided by averages of the original red and blue values, respectively. It is evident from the plot on the right-hand side of Fig. A.1 that the simple scaling algorithm described in this instance does a reasonably good job of factoring out the differences in inherent scales of the two considered data sets, thereby preparing these data for a more rigorous shape evaluation procedure based on GLS. This simple example is designed only for the purpose of demonstrating the basic concept of scaling so it is given no further consideration in the ensuing discussion.

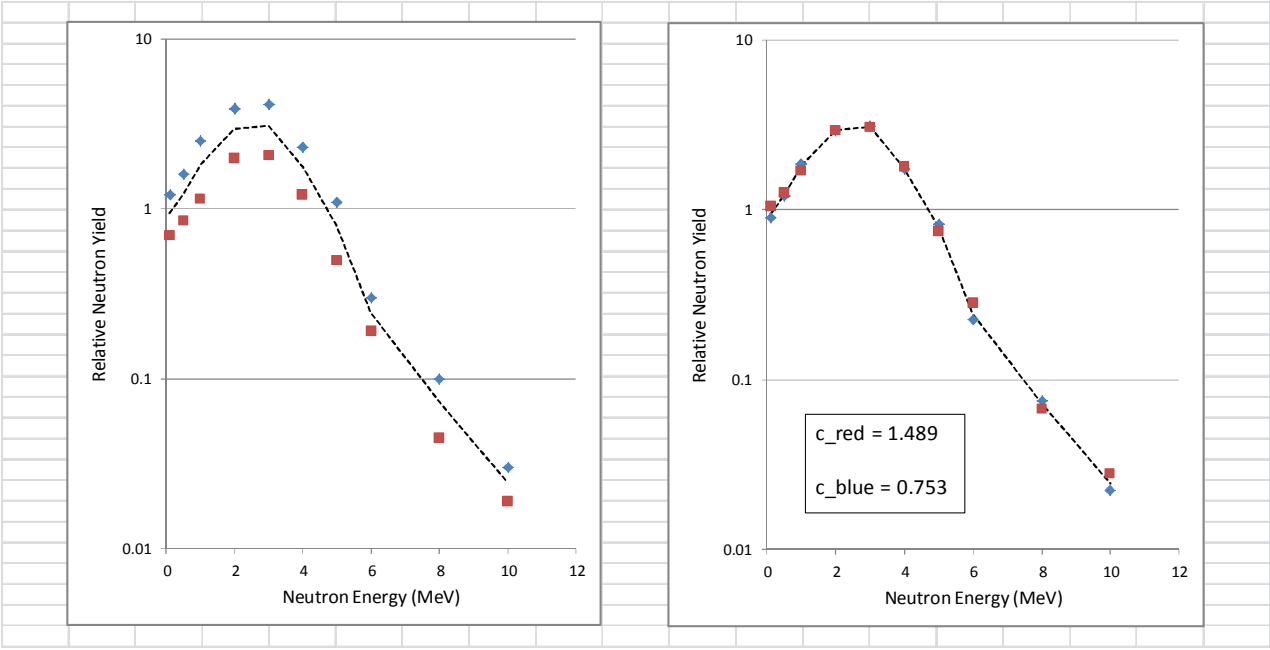

Figure A.1: Comparison of original data and scaled results, obtained as described in the Section A.1.

The eleven different scaling techniques that have been examined in the present investigation (denoted by *Scaling Method 1* through *Scaling Method 11*) are discussed sequentially in the following sections. All of the methods discussed here are assumed to apply to PFNS represented as direct neutron data (real or hypothetical) rather than spectra expressed relative to some reference shape such as a Maxwellian distribution [30]. Due to the wide dynamic range of PFNS neutron yield as a function of emission energy, there may be technical advantages to scaling these data to a reference shape so as to suppress the dynamic range. In particular, doing this clearly simplifies visualization of differences between various

measured and calculated versions of a particular PFNS. That is a peripheral issue that is not considered here, but it is certainly one that is worthy of consideration.

A.2. Scaling Method 1

Suppose that each of the K+1 data sets to be used in a PFNS evaluation (one set that is model-calculated and K that are experimental) provides spectrum values for every energy group within a specific limited energy range (E_L,E_H) that is unlikely to encompass the entire range of interest for the PFNS. Typically, this energy region will be in the range ≈1 – 5 MeV, since this is the energy regime of typical PFNS spectra that yields the most neutrons. Furthermore, it is also the range where PFNS spectrum shapes tend to not vary as dramatically with emitted neutron energy as is the case for other energy regions of these spectra. This is a scenario which occurs quite frequently, though certainly not universally, in PFNS evaluation situations. Model values can be calculated at any energy, and all the experiments considered will likely provide information in this high-neutron-yield region of the PFNS. Therefore, in this case the scaling factors could be determined by employing essentially the same procedure described in the simple hypothetical example given in Section A.1, except that now the energy range for this type of analysis is restricted to (E_L,E_H). This particular approach is described below in more concrete mathematical terms.

As in the main body of this paper, the input data are represented by the vector arrays of group values $\mathbf{\Phi}_k$ (k = 0,K). $\mathbf{\Phi}_0$ denotes the model-calculated values while the remaining arrays (k = 1,K) correspond to experimental data. The first step is to average all K+1 spectrum values for each contiguous energy group within the indicted energy range (E_L,E_H), so as to generate an additional vector $\boldsymbol{\xi}$, which we shall refer to as the anchor shape vector, whose components ξ_i are the averages of spectrum values Φ_{ki} for each group in that defined energy range.

Fig. A.2 illustrates how the energy interval is selected for an application of *Scaling Method 1* in the simple case of two spectra. In realistic situations, K+1 will be greater than two. In *Scaling Method* 1 it is assumed that simple averaging is used to generate the anchor shape vector $\boldsymbol{\xi}$, *i.e.*, identical weights are given to all the comparable data values in a particular group, irrespective of potentially wide variations in the scales of these PFNS representations. So, in essence, the data are un-weighted. Thus,

$$\xi_i = [\Sigma_{k=0,K}\, \Phi_{ki}]/(K+1). \quad (i = iL,iH) \tag{A.1}$$

Vector $\boldsymbol{\xi}$, which obviously needs to be defined only for those groups included in the energy range (E_L,E_H), serves as the anchor shape over this limited energy range for use in calculating the scaling factors c_k that are to be employed for all the input spectra. In *Scaling Method 1* these scaling factors are calculated using the following expression:

$$c_k = [\Sigma_{\{iL,iH\}}\, \xi_i] \,/\, [\Sigma_{\{iL,iH\}}\, \Phi_{ki}] \quad (k = 0,K). \tag{A.2}$$

The notation {iL,iH} denotes inclusion in the indicated sums of all the contiguous energy groups "i" in the energy range (E_L,E_H).

It is evident from the formula for c_k given in Eqn. (A.2) that if the data points for a specific data set $\mathbf{\Phi}_k$ tend to be larger, on average, than the comparable calculated average

values $\boldsymbol{\xi}$ for this energy range, then c_k <1 is obtained and all the original spectrum values in vector $\boldsymbol{\Phi}_k$, not only those for the energy range (E_L,E_H), should be scaled to lower values using the scaling factor c_k. The opposite holds true if the spectrum values for set $\boldsymbol{\Phi}_k$ tend to be lower than comparable ones for $\boldsymbol{\xi}$ in the given energy range. Then all the values of $\boldsymbol{\Phi}_k$ should be scaled toward higher values by multiplying them with c_k, since c_k >1 will be obtained from Eqn. (A.2). Thus, in applying *Scaling Method 1*, the scaling factors determined from information for the limited energy range (E_L,E_H) are applied over the entire energy range of the PFNS, *i.e.*, for all groups in that are populated with non-zero spectrum values.

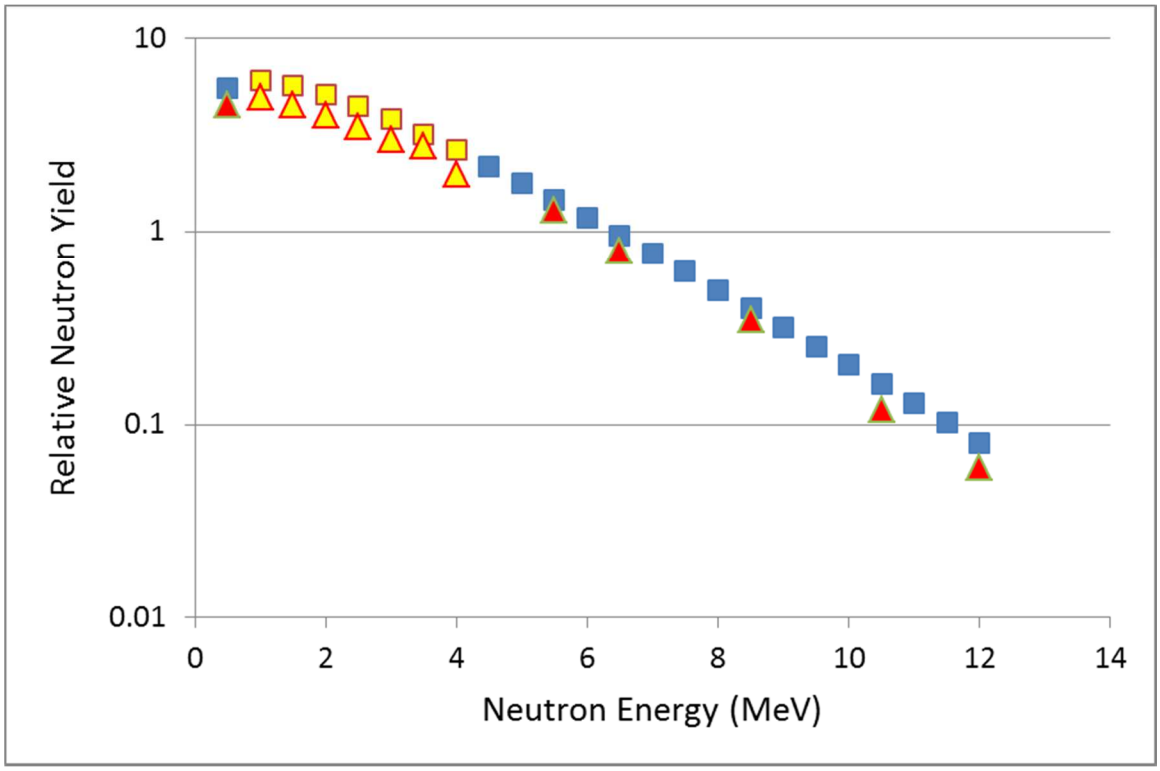

Figure A.2: This figure illustrates *Scaling Method 1* for calculating scaling factors based on un-weighted averaging of the spectrum values for all the considered spectra within a specific range of energies where spectral data are available for all the contiguous groups covering this energy range. The two distinct hypothetical spectra illustrated here are identified by triangles and squares. The values to be included in the scaling analysis for the two considered spectra are identified by yellow-filled symbols, whereas those not included in the scaling analysis are shown in blue-filled squares and red-filled triangles, respectively, for the two data sets.

As indicated in Section 2 in this paper, no consideration is given to assigning uncertainties to the derived scaling factors c_k since an earlier study that is reported elsewhere has shown that such scaling uncertainties ultimately cancel when evaluated PFNS shape data and their covariances are normalized [25].

A.3. Scaling Method 2

One assumption of *Scaling Method 1* might be viewed as too simplistic. Determination of an anchor shape $\boldsymbol{\xi}$ and subsequent calculation of scaling factors c_k is carried out in *Scaling Method 1* with no consideration given to the variable quality of the individual

PFNS data sets employed in the analysis. All the spectral data values are treated equally. Therefore, a refinement to *Scaling Method 1*, which is referred to here as *Scaling Method 2*, involves taking the uncertainties in these data into consideration through the use of weighting factors derived from these uncertainties. Otherwise, the present approach (*Scaling Method 2*) is essentially the same as *Scaling Method 1*.

For *Scaling Method 2*, the values ξ_i that define the anchor shape are determined by means of weighted-averaging, using standard deviations of the spectrum values to calculate the weighting factors w_{ki}. These standard deviations are denoted by e_{ki} ($k = 0,K$; $i = iL,iH$) and the selected weights w_{ki} are defined by $w_{ki} = f_{ki}^{-2}$, with $f_{ki} = (e_{ki} / \Phi_{ki})$. The choice is made to use fractional (or percent) uncertainties rather than absolute uncertainties in order to minimize the potential negative impact of the Peelle's Pertinent Puzzle (PPP) phenomenon that might be encountered if presumably comparable values, *i.e.*, the input PFNS values, actually differ considerably in magnitude (*e.g.*, [26,28]). The average values ξ_i that define the anchor shape $\boldsymbol{\xi}$ are therefore obtained in *Scaling Method 2* using the expression:

$$\xi_i = [\Sigma_{k=0,K}\, w_{ki}\Phi_{ki}] \,/\, [\Sigma_{k=0,K}\, w_{ki}] \quad (i = iL,iH). \tag{A.3}$$

The scaling factors c_k are then calculated using the following formula:

$$c_k = \{[\Sigma_{\{iL,iH\}}\, \xi_i]/\nu\} \,/\, \{[\Sigma_{\{iL,iH\}}\, w_{ki}\Phi_{ki}]/[\Sigma_{\{iL,iH\}}\, w_{ki}]\} \quad (k = 0,K). \tag{A.4}$$

The integer $\nu = (iH - iL + 1)$ corresponds to the number of energy groups in the energy range (E_L,E_H). Eqn. (A.4) states that the scaling factor c_k should be calculated as the ratio of the average value of the elements of anchor shape $\boldsymbol{\xi}$ to the weighted average of the k^{th} PFNS values. Only those values that correspond to the specific energy range (E_L,E_H) are considered in this analysis.

No consideration is given here to the influence of uncertainty correlations for the group PFNS values Φ_{ki} in the formalism that constitutes *Scaling Method 2*, as defined by Eqns. (A.3) and (A.4). It would be possible in principle to take such correlations into consideration in evaluating the scaling factors c_k, but that would entail calculations considerably more complicated than those indicated by Eqns. (A.3) and (A.4). Whether or not the neglect of such correlations might have a significant impact on determinations of the scaling factors c_k, and hence on the overall evaluation procedure discussed here, is a topic for further investigation. This possibility has not been explored in the present work.

A.4. Scaling Method 3

A matter of concern in applying *Scaling Method 2*, as well as in applying the overall PFNS evaluation procedure described in Section 3 of this paper, stems from the unique characteristics of the uncertainties of model-calculated PFNS in comparison with typical experimental PFNS data uncertainties. This point was already stressed in Section 3. It has been observed that the uncertainties of model-calculated PFNS can be very small at certain energies when compared to corresponding experimental data uncertainties, mainly as a consequence of the relative simplicity of most contemporary PFNS computational models (few variable parameters). In particular, this appears to stem from limited sensitivity of the calculated spectral values in certain energy regions of the PFNS to variations of certain PFNS model parameters [18,25]. At these energies, applying a weighted averaging procedure to

define an anchor shape in *Scaling Method 2* could lead to average values of the anchor shape values ξ_i that are dominated to an unreasonable extent by the model-calculated results.

This issue can be illustrated by examining a very simple theoretical model of a PFNS that provides an approximate representation of the shape of a typical PFNS. It is the Maxwell-Boltzmann (M-B) function which has the mathematical form $f(E) = C\ E^{1/2}\ \exp(-E/T)$, where C is treated as an arbitrary scaling constant [30]. This spectrum-shape representation has a single variable parameter T which corresponds to the nuclear temperature expressed in energy units. The inherently normalized M-B spectrum representation has the form $f_n(E) = C_n\ E^{1/2}\ \exp(-E/T)$, where $C_n = 2\ \pi^{-1/2}\ T^{-3/2}$. While the functions f and f_n have the same shape with respect to energy for a particular value of T, there is a difference between them which is pertinent to the present discussion. For the non-normalized M-B function f (where C is an arbitrary constant), the relationship between the fractional uncertainty in f and the fractional uncertainty in T is given by the expression $(\Delta f/f) = (E/T)\ (\Delta T/T)$. For E = 0, the fractional uncertainty in f is zero, but it increases linearly with energy with a slope given by 1/T. However, for the inherently normalized M-B function f_n, the relationship between the fractional uncertainties in f_n and T is given by $(\Delta f_n/f_n) = [(E/T)-(3/2)]\ (\Delta T/T)$. The sensitivity factor $[(E/T)-(3/2)]$ clearly goes to zero when E = 3T/2. This value of E also corresponds to the average energy <E> of the M-B function. The specific energy where the sensitivity of the PFNS to the parameter T vanishes is commonly called the pivot point [18,25]. The behavioral differences in the fractional uncertainties for the non-normalized and inherently normalized representations of the M-B spectrum, as a function of energy E, are shown graphically in Fig. A.3 for the case where T = 1.32, $\Delta T/T = 0.05$, and <E> = 1.98.

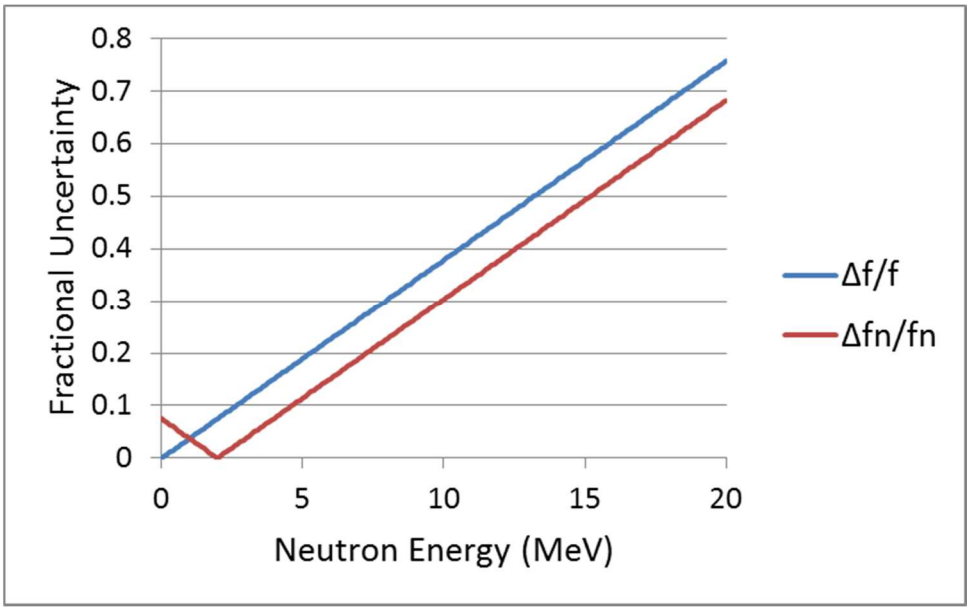

Figure A.3: Comparisons of fractional uncertainties for a non-normalized M-B PFNS ($\Delta f/f$) and an inherently normalized M-B PFNS ($\Delta f_n/f_n$), both with T = 1.32 and fractional uncertainty $\Delta T/T = 0.05$.

Since the M-B function has a single parameter, in the non-normalized case the uncertainties at all energies are 100% correlated (a very stiff covariance matrix!). For the inherently normalized version, the correlation pattern is more complicated. The uncertainties for PFNS values at energies above the pivot point are 100% correlated to each other. The

same holds true for the uncertainties of PFNS values below the pivot point. However, the uncertainties for PFNS values above the pivot point are 100% anti-correlated to PFNS values at energies below the pivot point. This situation can cause serious difficulties for using a normalized model-calculated PFNS such as the fully normalized M-B function in a GLS or SLS evaluation procedure. This possibility led us to focus mainly on evaluation approaches that utilize non-normalized PFNS in conjunction with scaling procedures to adjust the data used for the evaluation. Normalization is then carried out after applying a GLS or SLS evaluation procedure. Of course, it may not always be possible to work with non-normalized PFNS, especially when utilizing nuclear models where inherently normalized algorithms are generally encountered.

Contemporary models of PFNS (*e.g.*, the Los Alamos Model [11]) are considerably more complicated than the M-B function, and they involve more than one variable parameter. However, they nevertheless are essentially phenomenological in nature although they do reflect more detailed underlying physics. Still, due to the somewhat limited numbers of parameters in these more sophisticated PFNS models, they also tend to be afflicted with mathematical features resembling those seen for the M-B function, *e.g.*, low uncertainties close to the pivot point and covariance matrices with strong correlations and anti-correlations. However, these undesirable features tend not to be quite as severe as they are for the inherently normalized M-B function.

One way to avoid potential problems that might be associated with including model-calculated PFNS data in applying *Scaling Method 2* would be to limit the determination of an anchor shape $\boldsymbol{\xi}$ to inclusion of only experimental PFNS data. In order to apply this approach, denoted here as *Scaling Method 3*, it is required that more than just one experimental PFNS data set be available, *i.e.*, $K \geq 2$. The formulas for ξ_i and c_k corresponding to *Scaling Method 3* are:

$$\xi_i = [\Sigma_{k=1,K}\, w_{ki}\Phi_{ki}] \,/\, [\Sigma_{k=1,K}\, w_{ki}] \quad (i = iL,iH), \tag{A.5}$$

$$c_0 = [\Sigma_{\{iL,iH\}}\, \xi_i] \,/\, [\Sigma_{\{iL,iH\}}\, \Phi_{0i}], \tag{A.6}$$

$$c_k = \{[\Sigma_{\{iL,iH\}}\, \xi_i]/\nu\} \,/\, \{[\Sigma_{\{iL,iH\}}\, w_{ki}\Phi_{ki}]/[\Sigma_{\{iL,iH\}}\, w_{ki}]\} \quad (k = 1,K). \tag{A.7}$$

The weighting factors w_{ki} are defined in an identical manner as for *Scaling Method 2*.

As in *Scaling Method 2*, no consideration is given in these formulas to the influence of uncertainty correlations in the spectrum values Φ_{ki}. Eqn. (A.5) is very similar to Eqn. (A.3) associated with *Scaling Method 2*. The only difference is that the $k = 0$ term is excluded from the sums for the numerator and denominator. The scaling factor c_0 to be applied to the model-generated PFNS data is calculated using Eqn. (A.6) rather than Eqn. (A.7). It uses un-weighted spectrum values for the sum in the denominator of Eqn. (A.6) to avoid overweighting group-spectrum values for energy groups near the pivot point. The scaling factors c_k ($k = 1,K$) are obtained for *Scaling Method 3* using Eqn. (A.7), which is identical to Eqn. (A.4) that is used in *Scaling Method 2*. It may seem odd that although the calculation of all scaling factors c_k ($k = 0,K$) utilize the same anchor shape defined by the ξ_i values given by Eqn. (A.5), actual computation of the scaling factor c_0 is treated differently from calculations of the c_k scaling factors for the experimental PFNS ($k = 1,K$). This exemplifies the use of an *ad hoc* approach for pragmatic reasons that can only be justified based on whether "reasonable" results are ultimately produced by its application.

A.5. Scaling Method 4

Scaling Methods 1, *2*, and *3* involve calculating scaling factors c_k using only PFNS data from a defined limited energy region of a PFNS spectrum where group values are available for each individual data set and each energy group in that range. Furthermore, these three approaches involve constructing distinct anchor shapes $\boldsymbol{\xi}$ by three different methods. PFNS data in other energy regions are neglected by these three methods of calculating scaling factors.

Scaling Method 4 takes advantage of the fact that the model-calculated component of the available data base for performing a PFNS evaluation provides values in all m energy groups of the spectrum. Therefore, it could be selected to play the role of an anchor shape for scaling each experimental PFNS, thereby avoiding the need to construct a distinct anchor shape $\boldsymbol{\xi}$, as is the case for *Scaling Methods 1*, *2*, and *3*. Furthermore, doing this would enable PFNS data over the entire energy range of the spectrum to be employed for scaling purposes, at least to the extent that these data, especially experimental data, are trustworthy. The fact that the model PFNS may be normalized (which is often the case) does not impact on its use as an anchor shape. Of course, if it is suspected that the experimental data are more trustworthy than the model, and that the model should be used only for extrapolation and interpolation where data are absent, this would not be the approach one should choose. Nevertheless, we explore this approach as an option that is worthy of consideration if one attaches reasonable credence to the model shape information. In this approach it is assumed that $c_0 = 1$ and all the other (experimental) PFNS are scaled so as to be consistent scale-wise with the model-generated spectrum shape. Use is made of the fact that the K experimental PFNS data sets are assumed to be independent of each other and of the model-calculated spectrum. No consideration is given to uncertainties in the model-calculated spectrum in this scaling method. It simply plays the role of anchor shape for scaling all the other (experimental) PFNS data.

Scaling Method 4 involves calculating individual un-weighted sums of PFNS values for each of the K experimental PFNS spectra $\boldsymbol{\Phi}_k$ (k = 1,K), and for each group that is represented in the spectrum by non-zero values over the entire energy range of the PFNS. No experimental data values are excluded unless the evaluator decides that some are unworthy. This concept is illustrated in Fig. A.4.

The number of terms in these sums will generally be smaller than the total number of groups (m) since none of the experimental spectra are likely to provide data for every group of the PFNS. A typical sum for the k^{th} experimental PFNS $\boldsymbol{\Phi}_k$ is $s_k = [\Sigma_{\{i\}k}\, \Phi_{ki}]$, where the notation "{i}k" indicates that the sum includes all n_k non-zero PFNS group values for the k^{th} spectrum over the entire energy range of the PFNS. In the same way, a second sum is calculated for the model-calculated spectrum $\boldsymbol{\Phi}_0$ over the same groups populated by non-zero representation in the sum for the k^{th} experimental PFNS. This sum is $t_k = [\Sigma_{\{i\}k}\, \Phi_{0i}]$. Clearly, s_k and t_k differ for each individual experimental PFNS since these sums over the model-spectrum are tailored to correspond to the specific energy groups represented in the individual experimental spectra (k = 1,K).

The resulting scale factors are then calculated using the expression $c_k = t_k/s_k$ (k = 1,K). In *Scale Method 4* each experimental PFNS is individually scaled to the fixed model-calculated PFNS so that collectively all experimental data will tend to group around the

model-calculated PFNS shape provided as input to the evaluation procedure. The main advantage of this approach is that all experimental data can be employed in the scaling procedure if desired.

A.6. Scaling Method 5

An alternative to *Scaling Method 4*, denoted as *Scaling Method 5*, utilizes weighted-averaging of all the input PFNS values Φ_{ki} (k = 0,K) in calculating the scale factors c_k (k = 1,K). All the available PFNS data can be used in this method as well. Furthermore, as in *Scaling Method 4*, $c_0 = 1$ since $\mathbf{\Phi}_0$ is treated as the anchor shape for scaling purposes. The weighting factors are derived from standard deviations expressed in the form of fractional uncertainties f_{ki} (k = 0,K; i = 1,m) for reasons mentioned earlier. These weighting factors are defined by $w_{ki} = f_{ki}^{-2}$. Thus, for *Scaling Method 5* the formula for c_k (k = 1,K) is:

$$c_k = \{[\Sigma_{\{i\}k}\, w_{0i}\Phi_{0i}] / [\Sigma_{\{i\}k}\, w_{0i}]\} / \{[\Sigma_{\{i\}k}\, w_{ki}\Phi_{ki}] / [\Sigma_{\{i\}k}\, w_{ki}]\} \quad (k = 1,K). \tag{A.8}$$

No consideration is given to uncertainty correlations in applying *Scaling Method 5*.

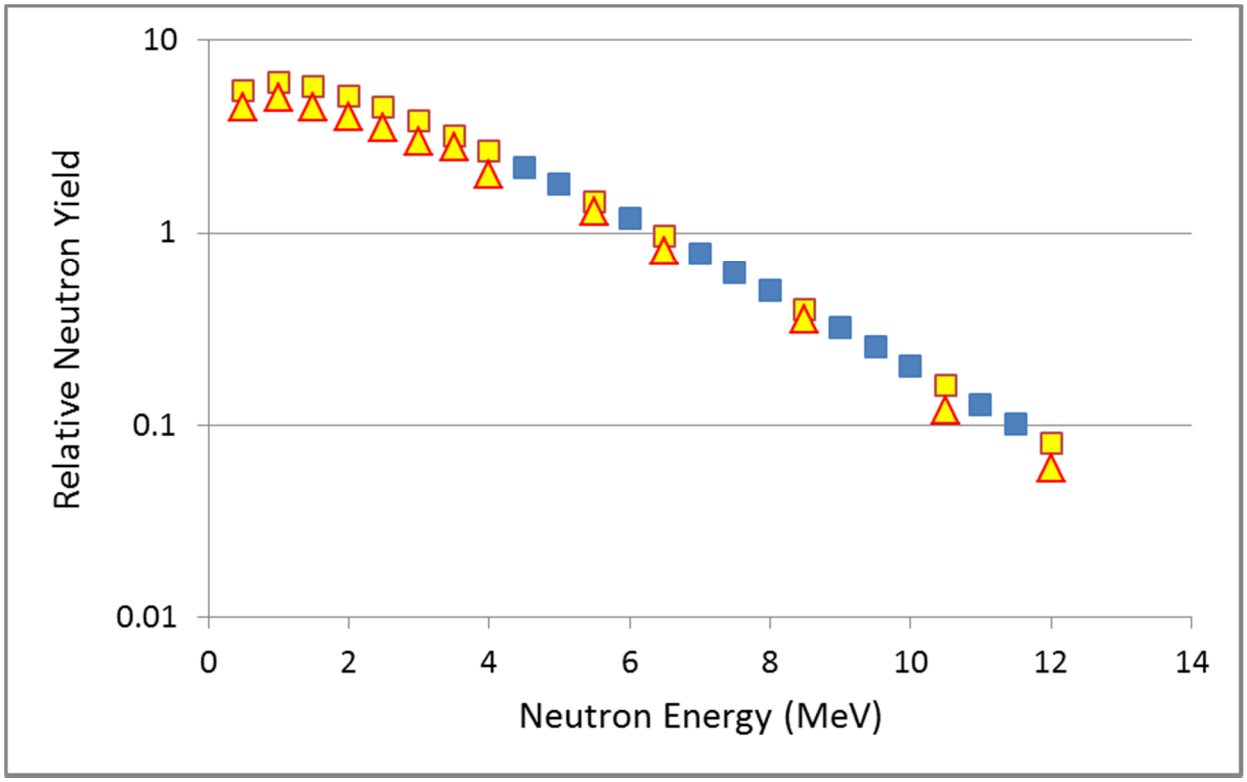

Figure A.4: This figure illustrates *Scaling Method 4* for calculating scaling factors, where one considers all the experimental group values of a specific experimental data set along with those values from the model-calculated results that correspond to the same groups as the experimental set. The yellow-filled triangles represent the values of a particular experimental data set. The yellow-filled squares correspond to the model-calculated anchor shape data set values that are used for scaling, whereas the blue-filled squares are the model-calculated values that are not used in the scaling calculation for this particular experimental data set.

A.7. Scaling Method 6

Scaling Method 6 is one of two possible SLS approaches for scaling experimental PFNS data sets $\mathbf{\Phi}_k$ to the non-normalized anchor shape defined by spectrum $\mathbf{\Phi}_0$ that have been investigated in the present work. The SLS calculations yield c_k values for the individual $\mathbf{\Phi}_k$ (k = 1,K). The factor c_0 is exactly 1 since the model-calculated spectrum serves as the anchor shape, as is the case in *Scaling Method 4* and *Scaling Method 5*. Use is made in *Scaling Method 6* of covariance information for the input PFNS data, including that for the anchor shape $\mathbf{\Phi}_0$. This is accomplished here by defining hybrid covariance matrices $\mathbf{W}_{\Phi k} = \mathbf{V}_{\Phi k} + \underline{\lambda}_k^2 \underline{\mathbf{V}}_{\Phi 0k}$ for use in the SLS scaling factor calculations. The significance of underlining $\underline{\lambda}_k$ and $\underline{\mathbf{V}}_{\Phi 0k}$ in this expression is explained in more detail below. The factor $\underline{\lambda}_k$ is introduced in *Scaling Method 6* to compensate for the fact that the scales of the PFNS data sets $\mathbf{\Phi}_k$ and $\mathbf{\Phi}_0$ may differ so widely that, without employing these factors, it would be unreasonable to try and treat the covariance matrices $\mathbf{V}_{\Phi k}$ and $\underline{\mathbf{V}}_{\Phi 0k}$ on equal footing in generating $\mathbf{W}_{\Phi k}$ for use in the SLS procedure. In *Scaling Method 6* it is explicitly assumed that $\underline{\lambda}_k = \langle \Phi_{ki} \rangle / \langle \underline{\Phi}_{0ki} \rangle$, where <…> signifies un-weighted averages of the indicated collections of variables over regions of the spectrum where both anchor and experimental data are represented.

It is convenient to define the parameter $p_k = 1/c_k$, where c_k is the desired scale factor for the k^{th} experimental PFNS (k = 1,K). Parameter p_k (k = 1,K) is to be derived using the SLS procedure [27]. The solution is obtained from the matrix equations

$$p_k = V_{pk}\, \underline{\mathbf{\Phi}}_{0k}^{+}\, \mathbf{W}_{\Phi k}^{-1}\, \mathbf{\Phi}_k, \tag{A.9}$$

$$V_{pk} = (\underline{\mathbf{\Phi}}_{0k}^{+} \mathbf{W}_{\Phi k}^{-1}\, \underline{\mathbf{\Phi}}_{0k})^{-1}, \tag{A.10}$$

$$\chi_k^2/(n_k - 1) = [(\mathbf{\Phi}_k - \underline{\mathbf{\Phi}}_{0k}\, p_k)^{+}\, \mathbf{W}_{\Phi k}^{-1}\, (\mathbf{\Phi}_k - \underline{\mathbf{\Phi}}_{0k}\, p_k)] / (n_k - 1). \tag{A.11}$$

The components of Eqns. (A.9) – (A.11) are defined as follows: V_{pk} is the variance of parameter p_k. It is a scalar quantity. $\chi_k^2/(n_k - 1)$ is the chi-square per d.o.f. parameter that measures the scatter of the experimental PFNS data set $\mathbf{\Phi}_k$ relative to the model-calculated anchor shape $\mathbf{\Phi}_0$. No further consideration is given to the derived uncertainty in p_k, *i.e.*, $e_{pk} = V_{pk}^{½}$, or to the uncertainty in the corresponding scaling parameter c_k, since scaling uncertainties are eliminated when non-normalized evaluated PFNS are normalized [25]. The least-squares scaling procedure is repeated K times, corresponding to the K experimental data sets.

At this point it is appropriate to explain the use of bold underlining for several of the variables appearing in the preceding two paragraphs. The vector $\underline{\mathbf{\Phi}}_{0k}$ is marked with a bold underline to indicate that it is actually a subset of dimension $n_k \leq m$ of the full vector $\mathbf{\Phi}_0$ of model-calculated values which has dimension m and is specifically constructed for the calculation of p_k. The corresponding covariance matrix of this subset is $\underline{\mathbf{V}}_{\Phi 0k}$. Thus, the elements of $\underline{\mathbf{\Phi}}_{0k}$ correspond specifically to the energy groups that are populated with non-zero values in the experimental PFNS data set $\mathbf{\Phi}_k$. The same explanation applies to the factor $\underline{\lambda}_k$. Only those values from the subset vector $\underline{\mathbf{\Phi}}_{0k}$ are averaged in calculating this factor. The dimension of the k^{th} experimental PFNS data covariance matrix $\mathbf{V}_{\Phi k}$ is n_k x n_k. The dimension of $\underline{\mathbf{V}}_{\Phi 0k}$ is also n_k x n_k. Therefore, the dimension of $\mathbf{W}_{\Phi k}$ is n_k x n_k.

A.8. Scaling Method 7

Scaling Method 7 is the second SLS approach to deriving the scaling factors c_k for the experimental PFNS (k = 1,K) that is examined in this paper. Again it is assumed that the factor c_0 is exactly 1 since the spectrum $\mathbf{\Phi}_0$ serves as the anchor shape. This is also the case for *Scaling Methods 4*, *5*, and *6*. For *Scaling Method 7* it is assumed that the following information is available to an evaluator: $\mathbf{\Phi}_0$, $\mathbf{V}_{\Phi 0}$, [$\mathbf{\Phi}_k$, $\mathbf{V}_{\Phi k}$ (k = 1,K)]. In this approach, for a particular PFNS "k" (k = 1,K) ratio values r_{ki}, that collectively form a vector $\mathbf{r}_k$, are calculated using the formula $r_{ki} = \underline{\Phi}_{0ki}/\Phi_{ki}$ (k = 1,K; i = 1, n_k). Thus, only certain values from $\mathbf{\Phi}_0$ are applicable here, namely those corresponding to the specific energy groups for which there are corresponding data available from $\mathbf{\Phi}_k$ and from the defined subset $\underline{\mathbf{\Phi}}_{0k}$ of $\mathbf{\Phi}_0$, in a similar fashion to *Scaling Method 6*. Then it is possible to generate a covariance matrix $\mathbf{V}_{rk}$ for the calculated ratio set $\mathbf{r}_k$ using the Law of Error Propagation and the given PFNS data [28]. The elements v_{rkij} of $\mathbf{V}_{rk}$ are then calculated using the formula

$$\begin{aligned} v_{rkij} &= (\partial r_{ki}/\partial \underline{\Phi}_{0ki})\, \underline{v}_{\Phi 0kij}\, (\partial r_{kj}/\partial \underline{\Phi}_{0kj}) + (\partial r_{ki}/\partial \Phi_{ki})\, v_{\Phi kij}\, (\partial r_{kj}/\partial \Phi_{kj}) \\ &= (1/\Phi_{ki})\, \underline{v}_{\Phi 0kij}\, (1/\Phi_{kj}) + (-\underline{\Phi}_{0ki}/\Phi_{ki}^2)\, v_{\Phi kij}\, (-\Phi_{0kj}/\Phi_{kj}^2). \end{aligned} \tag{A.12}$$

In these equations $\underline{\Phi}_{0ki}$ is an element of $\underline{\mathbf{\Phi}}_{0k}$, $\underline{v}_{\Phi 0kij}$ is an element of $\underline{\mathbf{V}}_{\Phi 0k}$, and $v_{\Phi kij}$ is an element of $\mathbf{V}_{\Phi k}$. Eqn. (A.12) is derived from the assumption that the PFNS $\mathbf{\Phi}_0$ and $\mathbf{\Phi}_k$ are uncorrelated.

A further assumption of *Scaling Method 7* is that each of the n_k ratios value r_{ki} should be representative of the scaling parameter c_k that is sought from the analysis. Therefore, $c_k \approx r_{ki}$ (i = 1,n_k), and c_k can thus be thought of as a type of least-squares weighted average of the n_k ratios of the k^{th} experimental PFNS to the anchor shape, with full consideration given in the computational procedure to the uncertainties and correlations for the PFNS sets $\mathbf{\Phi}_0$ and $\mathbf{\Phi}_k$. Clearly, *Scaling Method 7* is a more sophisticated approach to scaling than *Scaling Method 6*, and it involves fewer assumptions.

The set of derived ratio values $\mathbf{r}_k$ and their covariance matrix $\mathbf{V}_{rk}$ can be treated as input data for the SLS analysis that aims to provide a recommended value of c_k based on the given input data. The least-squares criterion in *Scaling Method 7* involves minimizing the quadratic form $(\mathbf{r}_k - \mathbf{A}_k\, c_k)^+\, \mathbf{V}_{rk}^{-1}\, (\mathbf{r}_k - \mathbf{A}_k\, c_k)$. The SLS solution is given by the equations

$$c_k = V_{ck}\, \mathbf{A}_k^+\, \mathbf{V}_{rk}^{-1}\, \mathbf{r}_k, \tag{A.13}$$

$$V_{ck} = (\mathbf{A}_k^+ \mathbf{V}_{rk}^{-1}\, \mathbf{A}_k)^{-1}, \tag{A.14}$$

$$\chi_k^2/(n_k - 1) = [(\mathbf{r}_k - \mathbf{A}_k\, c_k)^+\, \mathbf{V}_{rk}^{-1}\, (\mathbf{r}_k - \mathbf{A}_k\, c_k)] \,/\, (n_k - 1). \tag{A.15}$$

The sensitivity matrix $\mathbf{A}_k$ that appears in Eqns. (A.13) – (A.15) is a column vector consisting of n_k elements all equal to 1. This is a result of the assumption that $c_k \approx r_{ki}$ (k = 1,K) [27].

This scaling procedure is repeated independently K times, once for each of the K experimental data sets. As mentioned elsewhere in this paper, the uncertainties in the c_k derived in this manner are of no particular interest since scaling uncertainties are eliminated when non-normalized evaluated PFNS are normalized [25]. However, the derived values of

chi-square are of interest since they yield useful information on the scatter of the ratio values $\mathbf{r}_k$.

The approach described here is not the most general one in this particular category of SLS derivations of scaling factors. For example, it would be possible to evaluate all the scaling factors c_k (k = 1,K) simultaneously using SLS in a way that takes into consideration correlations between them that are introduced by the use of a common anchor shape. The mathematics would involve a straightforward extension of that discussed for *Scaling Method 7*, but the bookkeeping would be considerably more tedious. This approach was not explored in the present investigation.

A.9. Scaling Method 8

If it happens that the union of all the experimental PFNS available for consideration in an evaluation covers essentially the entire energy range of significance for applications, excepting possibly the very highest and lowest energies, and if there is an energy region where all these spectra overlap, or if they overlap in segments such that there are no "orphaned" data sets that do not overlap with other sets to provide comprehensive coverage for scaling, then the present approach, denoted by *Scaling Method 8*, could be applied. In this approach no use is made of data from a nuclear model, therefore it can be described as a "non-model" PFNS evaluation procedure. As in the preceding discussions, the experimental data sets to be considered are denoted by $\mathbf{\Phi}_k$ (k = 1,K). No model is used, so no mention is made of $\mathbf{\Phi}_0$ since this notation is generally reserved in this paper to represent a model-calculated PFNS used in GLS evaluation procedures.

The first step in *Scaling Method 8* is to select one of the experimental PFNS data sets to serve as the anchor shape to which the other experimental PFNS are scaled so that all the experimental data will be comparable, albeit non-normalized. One possible choice would be the spectrum with the largest representation with respect to its range in energy, and therefore that offers the most options for spectral overlap with the remaining experimental PFNS. However, the procedure described here need not fulfill this particular requirement. For example, it might also be the case that the evaluator would want to pick as the anchor shape the PFNS data set viewed as the most trustworthy. Regardless of how it is chosen, this PFNS is then denoted as $\mathbf{\Phi}_1$. Its scaling factor is therefore $c_1 = 1$ by convention. In the simplest case where all the other spectra $\mathbf{\Phi}_k$ ($k \geq 2$) overlap $\mathbf{\Phi}_1$, a value for the k^{th} PFNS scaling factor can be obtained from the expression $c_k = (\Sigma_{\{\text{“i” overlap}\}k}\ \Phi_{1i}) / (\Sigma_{\{\text{“i” overlap}\}k}\ \Phi_{ki})$. The notation {“i” overlap}k signifies summation over those PFNS spectrum groups where Φ_{1i} and Φ_{ki} overlap. This scaling approach resembles *Scaling Method 4* in the sense that no attention is paid to the uncertainties in these data for scaling purposes. More complicated expressions for c_k will be necessary if the PFNS overlap patterns are more complicated, but the concept remains unchanged.

Once the c_k values have been determined, the PFNS are scaled to generate the vectors $\mathbf{z}_k = c_k\ \mathbf{\Phi}_k$ (k = 2,K) and their corresponding covariance matrices are $\mathbf{V}_{zk} = c_k^2\ \mathbf{V}_{\Phi k}$ (k = 2,K), in the same manner as discussed earlier. If the total number of experimental data values exceeds the number of groups in the spectrum, *i.e.*, if $n = \Sigma_{k=1,K}\ n_k > m$, then the SLS procedure can be applied to perform the next step in the evaluation process [27]. This contrasts with use of the GLS method for the main part of the evaluation, as discussed for

Scaling Methods 1 through *7*. The formulas to carry out the SLS evaluation are given in Eqns. (7) – (9).

The final step in this evaluation process, *i.e.*, the one taken to obtain the normalized evaluated PFNS $\mathbf{\Psi}$ and its covariance matrix $\mathbf{V}_{\Psi}$, is accomplished as discussed in Section 4. However, if the evaluator decides that the solution $\mathbf{\Omega}$ obtained by using only experimental data needs to be augmented slightly to provide coverage of the very highest and lowest emitted neutron energies, then for completeness a simple shape extrapolation or theoretical model could be used for this purpose, leading to a non-normalized, augmented PFNS $\mathbf{\Omega}_a$ and its associated covariance matrix $\mathbf{V}_{\Omega a}$ [5]. Typically, a very large uncertainty (say 100%) would be assigned to the added components required to deal with the extreme low and high ends of the PFNS. Then, the normalization transformation discussed in Section 4 would be applied to $\mathbf{\Omega}_a$ and $\mathbf{V}_{\Omega a}$ to obtain the final normalized solution.

The appeal of this approach stems from the fact that the present state of development of reliable theoretical models of PFNS is such that whenever it is possible to generate an evaluated PFNS representation based entirely on experimental data (with at most minor extensions based on theory), then that is preferable to relying heavily on a questionable theoretical PFNS spectrum [5]. Unfortunately, there are relatively few cases where this is possible. They correspond to PFNS for certain major actinides at a few specific incident neutron energies, *e.g.*, thermal or 0.5 MeV [5].

A.10. Scaling Method 9

Suppose that an evaluator has produced a non-normalized PFNS evaluation based on experimental data alone, *e.g.*, $\mathbf{\Omega}$ and its covariance matrix $\mathbf{V}_{\Omega}$, as discussed for *Scaling Method 8*. However, the evaluator may later wish to take into consideration in an updated evaluation the information provided by a recently improved nuclear model. This can be accomplished in a straightforward manner by scaling the earlier non-model evaluated solution vector $\mathbf{\Omega}$ and its covariance matrix $\mathbf{V}_{\Omega}$ to the model-calculated PFNS shape $\mathbf{\Phi}_0$ and its covariance matrix $\mathbf{V}_{\Phi 0}$, *e.g.*, by utilizing *Scaling Method 4*. The SLS procedure described in Section 3 can be used for performing the actual evaluation. The result of this least-squares analysis would then need to be normalized, as described in Section 4. This approach constitutes *Scaling Method 9*. Note that in this approach the evaluator is essentially overlooking the fact that the model-calculated PFNS may be inherently normalized and is treating it as if it were non-normalized.

In applying this method when $\mathbf{\Phi}_0$ and its covariance matrix $\mathbf{V}_{\Phi 0}$ are actually normalized one needs to be concerned with whether the uncertainties in $\mathbf{\Phi}_0$ are excessively small near the pivot point and the correlations in $\mathbf{V}_{\Phi 0}$ are too strong, since this might compromise the evaluation process, as discussed in Section A.4. Under these circumstances, it may be preferable to pursue the following scaling approach, *i.e.*, *Scaling Method 10*.

A.11. Scaling Method 10

PFNS models such as the Los Alamos Model [11] are often "hard wired" to satisfy the normalization criterion in such a manner that the normalization constraint cannot be bypassed in a straightforward manner. Then one would not be able to perform an evaluation

based entirely on non-normalized data. We have already seen earlier in this appendix how the normalization criterion affects the mathematical expression for the M-B function. Therefore, it may be preferable to first normalize an evaluated PFNS based on the available experimental data (as described for *Scaling Method 8*), along with its covariance matrix, according to the procedure described in Section 4, before combining it with an inherently-normalized, model-generated PFNS using either a GLS or SLS procedure. In this manner, the experimental and model-generated input to the evaluation procedure can be treated *a priori* on the same footing, and the concern expressed in Section A.10 can be completely averted. In this case there is no need at all for scaling the PFNS. So, *Scaling Method 10* is basically a "no scaling" option.

The solution PFNS from the least-squares procedure in this situation would likely not be perfectly normalized, perhaps due to numerical round-off effects in the least-squares analysis, so the normalization procedure discussed in Section 4 would need to be applied subsequently to both the solution vector and its covariance matrix to obtain the desired results.

Sequential applications of the normalization criterion to a PFNS and its covariance matrix (as described in Section 4) any number of times, even when the initial result is close to being normalized, should produce no discernable negative consequences on the final obtained numerical values as long as the linear approximation is adequate.

A.12. Scaling Method 11

It is often the case that model-calculated PFNS are intrinsically normalized, as discussed in Sections 2,3, and 4. *Scaling Method 10*, discussed in Appendix A.11, describes a scenario whereby the model-calculated PFNS and the experimental PFNS (there may be more than one) are all assumed to be normalized prior to performing an evaluation using SLS.

However, it is of interest to explore the consequences of performing an evaluation whereby the model-calculated PFNS is acknowledged to be intrinsically normalized while the experimental PFNS data sets are definitely not normalized. The experimental PFNS data sets could be scaled to the normalized model-calculated PFNS (used as the anchor shape) by one of the procedures described earlier in this paper, allowing them to be properly compared to the model-calculated PFNS prior to performing an evaluation using a SLS or GLS procedure. The obtained scaling factors are needed to scale the experimental PFNS covariance matrices as well. This constitutes what is referred to here as *Scaling Method 11*. Since this approach unabashedly mixes an inherently normalized model-calculated PFNS with comparably scaled (but not normalized) experimental PFNS data sets in the evaluation process, the evaluator needs to be on the lookout for any potential negative consequences. The validity of such a "mixed" PFNS data evaluation approach can then be validated qualitatively only by observing whether the results obtained in a specific application appear to be "reasonable".

It should be evident from the discussions associated with the eleven PFNS data scaling and evaluation approaches considered in this appendix that they by no means encompass all the possibilities. Other varieties of scaling techniques could be conceived that might be more appropriate in certain situations. It is instructive to gain some understanding of the sensitivity of the final evaluated results to the scaling method selected by examining

numerical examples. This topic is addressed in Appendix B where the eleven approaches described in the present appendix are applied in eleven separate examples that employ a single, common collection of three hypothetical "toy" PFNS data sets. Two of them are "experimental" and one plays the role of the "model-calculated" PFNS.

Appendix B

Numerical Examples

Eleven numerical examples are presented in this appendix. They have been designed to illustrate the eleven PFNS data scaling and evaluation techniques discussed in Appendix A. Numerical examples do not constitute mathematical proofs of the validity of particular evaluation procedures, but they can offer some insight on their practical viability. Use is made of "toy" data sets in these examples to facilitate the numerical analyses. Note that the numbers of decimal places given for the numerical results usually exceed the accuracy of the obtained results. These values were taken directly from the calculations, with no attempt to round them to reflect perceived numerical significance.

B.1. "Toy" PFNS Data Collection

A common collection of "toy" PFNS data is employed in all the calculations presented in this appendix in order to facilitate comparisons of the performance of the various scaling methods considered in this investigation. Three hypothetical PFNS data sets that purport to characterize a particular, unspecified PFNS are considered. These data sets are in no way intended to actually correspond to real PFNS data, although they have been designed to reflect features that to some extent do resemble real data. In fact, the values in this collection were generated to resemble roughly a Maxwell-Boltzmann distribution with temperature T ≈ 1.333 MeV, corresponding to a spectrum average energy of ≈ 2 MeV. However, some alterations in the shapes were introduced *ad hoc* to add realism to the exercises. These "toy" PFNS data collectively span a neutron energy range from 0 to 12 MeV. For present purposes this is assumed to be broad enough to include all emitted neutrons. The information is represented in group format, as discussed in the main body of this paper. The chosen energy range is divided into 15 contiguous energy groups. The widths of these energy groups and their midpoint energies are indicated in Table B.1. This is too crude a grid structure to adequately represent real PFNS data, but it is sufficient for demonstrating the various procedures discussed herein.

Table B.1: Energy-group structure and midpoint energies for the numerical examples.

Group # (i)	Ei-low (MeV)	Ei-high (MeV)	ΔEi (MeV)	<E>i
1	0	0.05	0.05	0.025
2	0.05	0.1	0.05	0.075
3	0.1	0.2	0.1	0.15
4	0.2	0.3	0.1	0.25
5	0.3	0.5	0.2	0.4
6	0.5	1	0.5	0.75
7	1	1.5	0.5	1.25
8	1.5	2	0.5	1.75
9	2	3	1	2.5
10	3	4	1	3.5
11	4	5	1	4.5
12	5	6	1	5.5
13	6	8	2	7
14	8	10	2	9
15	10	12	2	11

The three hypothetical ("toy") group PFNS data sets considered here are denoted by the vectors $\mathbf{\Phi}_0$, $\mathbf{\Phi}_1$, and $\mathbf{\Phi}_2$, respectively. The uncertainties in these data are comprised of two components: a random uncertainty and a fully correlated uncertainty. By fully correlated it is meant that the indicated uncertainty is a systematic uncertainty (given in percent) that applies to each PFNS value in the tables. Tables B.2, B.3, and B.4 provide the numerical values, including the group values and their uncertainties, for these "toy" PFNS. Figs. B.1, B.2, and B.3 show plots of the uncertainty components and total uncertainties for these data. The covariance matrices $\mathbf{V}_{\Phi 0}$, $\mathbf{V}_{\Phi 1}$, and $\mathbf{V}_{\Phi 2}$ can be constructed readily from this information [28].

Table B.2: $\mathbf{\Phi}_0$ PFNS data.

Group # (i)	Φ0i	% Rand Unc	% Correl Unc	% Tot Unc
1	0.077588	8.00%	3.00%	8.54%
2	0.129441	7.00%	3.00%	7.62%
3	0.346089	6.00%	3.00%	6.71%
4	0.414515	5.00%	3.00%	5.83%
5	0.937069	4.00%	3.00%	5.00%
6	2.467232	4.00%	3.00%	5.00%
7	2.189142	4.00%	3.00%	5.00%
8	1.780236	5.00%	3.00%	5.83%
9	2.424755	6.00%	3.00%	6.71%
10	1.355224	7.00%	3.00%	7.62%
11	0.725876	8.00%	3.00%	8.54%
12	0.379068	10.00%	3.00%	10.44%
13	0.277673	13.00%	3.00%	13.34%
14	0.070253	16.00%	3.00%	16.28%
15	0.01733	20.00%	3.00%	20.22%

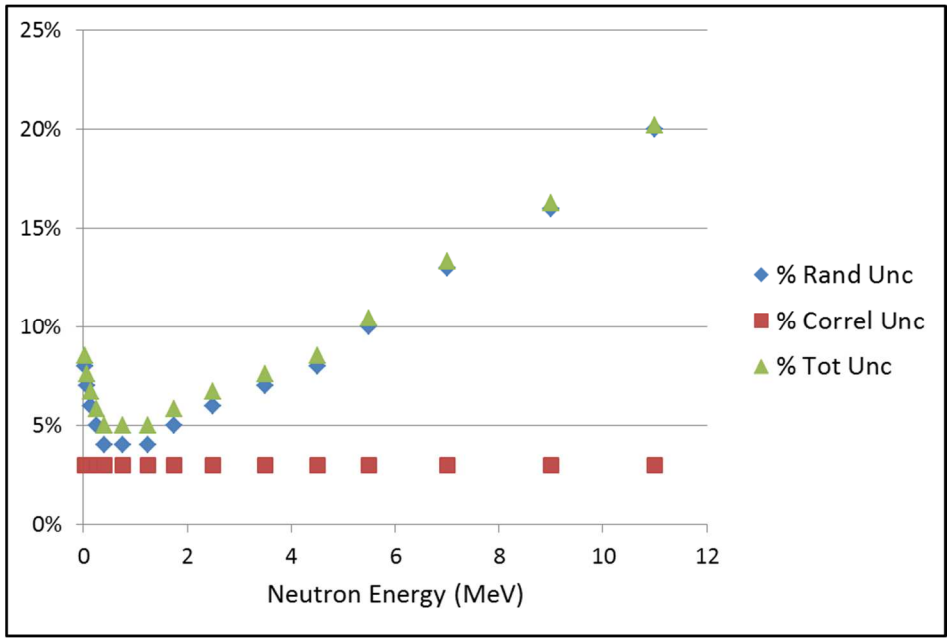

Figure B.1: Plot of uncertainty components and total uncertainties for $\mathbf{\Phi}_0$ PFNS data.

Notice that $\mathbf{\Phi}_0$ provides PFNS data for each of the twelve energy groups that collectively span the entire energy range of the spectrum. Consequently, $\mathbf{\Phi}_0$ is well suited to play the role of a prior whenever the generalized least-squares (GLS) evaluation procedure is employed. However, this data set was not generated using any model. By design it avoids some of the problems typically associated with model-generated data, as discussed in Section 3 and Appendix A.

Notice that data set $\mathbf{\Phi}_1$ has only ten PFNS values, and therefore it is not represented in every energy group of the spectrum. This is a very common situation for experimental PFNS. The data set $\mathbf{\Phi}_2$ provides values for just eleven of the energy groups that characterize the "toy" PFNS.

Table B.3: $\mathbf{\Phi}_1$ PFNS Data.

Group # (i)	Φ1i	% Rand Unc	% Correl Unc	% Tot Unc
1				
2	0.495	15.00%	3.00%	15.30%
3	1.42	8.00%	3.00%	8.54%
4				
5	3.76	4.00%	3.00%	5.00%
6	9.7	3.00%	3.00%	4.24%
7	9.05	3.00%	3.00%	4.24%
8	7	3.00%	3.00%	4.24%
9	10.2	3.00%	3.00%	4.24%
10	5.2	5.00%	3.00%	5.83%
11				
12	1.7	8.00%	3.00%	8.54%
13	1	12.00%	3.00%	12.37%
14				
15				

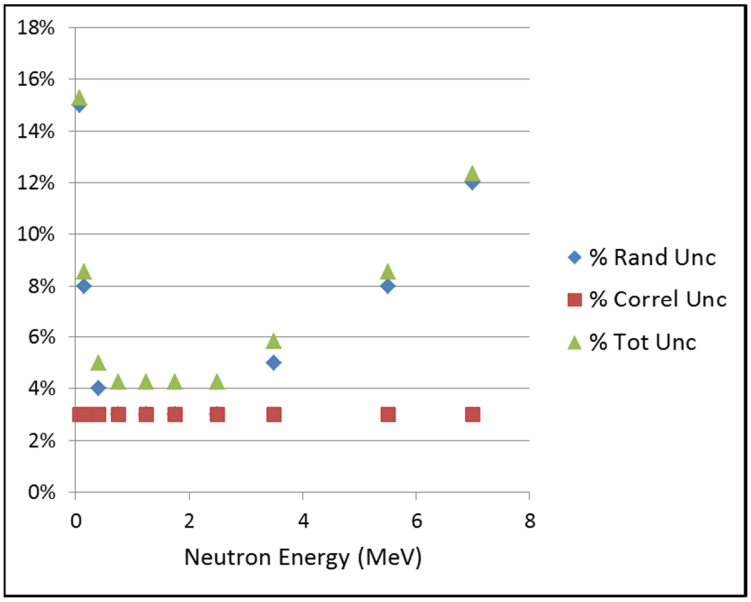

Figure B.2: Plot of uncertainty components and total uncertainties for $\mathbf{\Phi}_1$ PFNS data.

Table B.4: Φ_2 PFNS Data.

Group # (i)	Φ2i	% Rand Unc	% Correl Unc	% Tot Unc
1	0.00685	17.00%	4.00%	17.46%
2				
3	0.032	10.00%	4.00%	10.77%
4				
5	0.0852	6.00%	4.00%	7.21%
6	0.2325	5.00%	4.00%	6.40%
7	0.21	5.00%	4.00%	6.40%
8	0.18	5.00%	4.00%	6.40%
9	0.25	5.00%	4.00%	6.40%
10	0.145	6.00%	4.00%	7.21%
11	0.08	10.00%	4.00%	10.77%
12				
13	0.032	15.00%	4.00%	15.52%
14				
15	0.002	25.00%	4.00%	25.32%

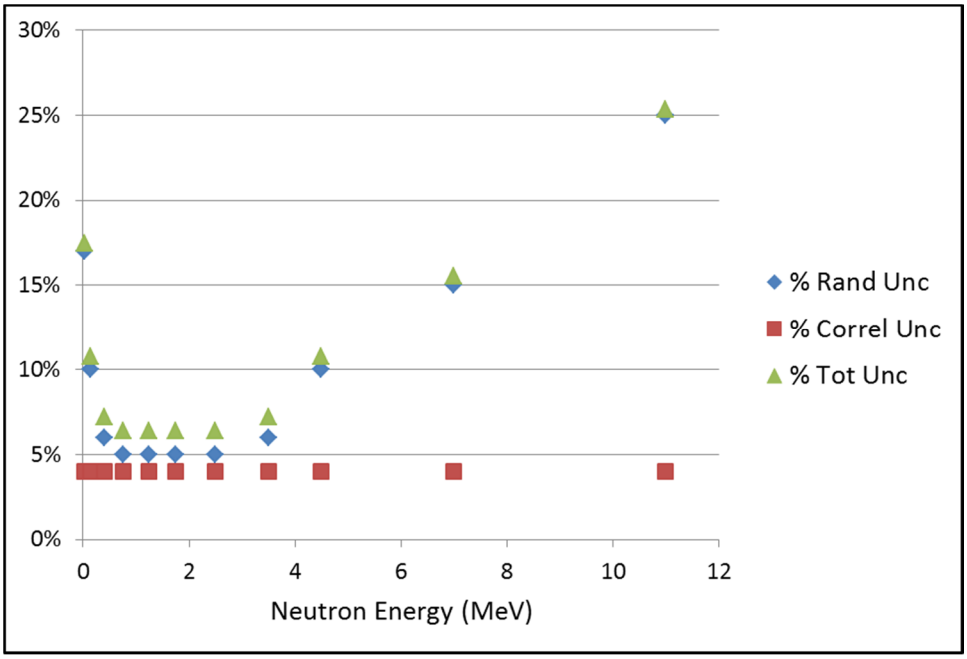

Figure B.3: Plot of uncertainty components and total uncertainties for Φ_2 PFNS data.

The three hypothetical spectral data sets considered in the following examples are plotted in Fig. B.4. Group values are plotted at the group midpoint energies. The discontinuity observed for the spectral shapes in the vicinity of 2 MeV is the result of a change in energy-group width (see Table B.1). It is clear that these data cannot be treated as comparable for evaluation purposes without first being scaled.

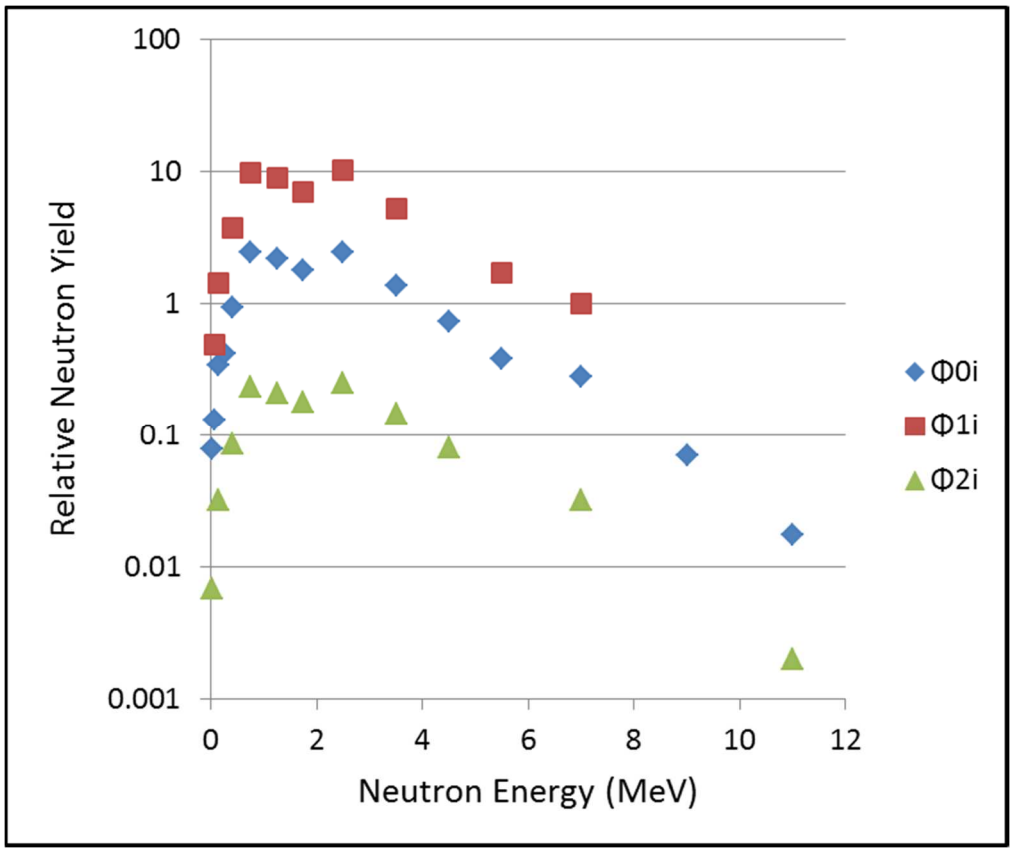

Figure B.4: Plots of group values for PFNS data sets $\mathbf{\Phi}_0$, $\mathbf{\Phi}_1$, and $\mathbf{\Phi}_2$ prior to scaling.

The calculations shown for all the following examples were carried out using various EXCEL and MATLAB routines. This simple computational approach was enabled by the limited numbers of energy groups and PFNS data values in the examples. Due to the relatively small number of energy groups, only matrices of modest dimensions needed to be manipulated (*e.g.*, inverted) in the various data scaling and evaluation procedures.

B.2. Example 1

This example demonstrates *Scaling Method 1* which is described in Section A.2. An anchor shape represented by $\boldsymbol{\xi}$ is used in scaling the three given PFNS data sets. Vector $\boldsymbol{\xi}$ is generated by un-weighted averaging of the values from the three input PFNS data sets, group-by-group, for groups 5 through 10. This method can be used since each of the PFNS data sets provides values for all these particular groups. Fig. B.5 shows the values for $\boldsymbol{\xi}$ in comparison to those for $\mathbf{\Phi}_0$, $\mathbf{\Phi}_1$, and $\mathbf{\Phi}_2$ in this range of energy groups. *Scaling Method 1* yields the values $c_0 = 1.70845$, $c_1 = 0.43430$, and $c_2 = 17.28072$ for the three scaling factors. The scaled PFNS data sets, denoted by $\mathbf{z}_k$ (k = 0, 1, and 2), are generated from the formula $\mathbf{z}_k = c_k \mathbf{\Phi}_k$ (k = 0, 1, and 2). The derived scaling factors are then applied to the PFNS data sets over all their respective energy groups. Segments of the scaled spectra corresponding to groups 5 through 10 are shown in Fig. B.6 compared with the derived anchor shape $\boldsymbol{\xi}$.

The covariance matrices for the $\mathbf{z}_k$ (k = 0, 1, and 2) are obtained from the formula $\mathbf{V}_{zk} = c_k^2 \mathbf{V}_{\Phi k}$ (k = 0, 1, and 2). The evaluation was then performed using these scaled PFNS data

and the GLS formalism discussed in Section 3. The data set $\mathbf{z}_0$ serves as the prior for this analysis since it provides values for each energy group.

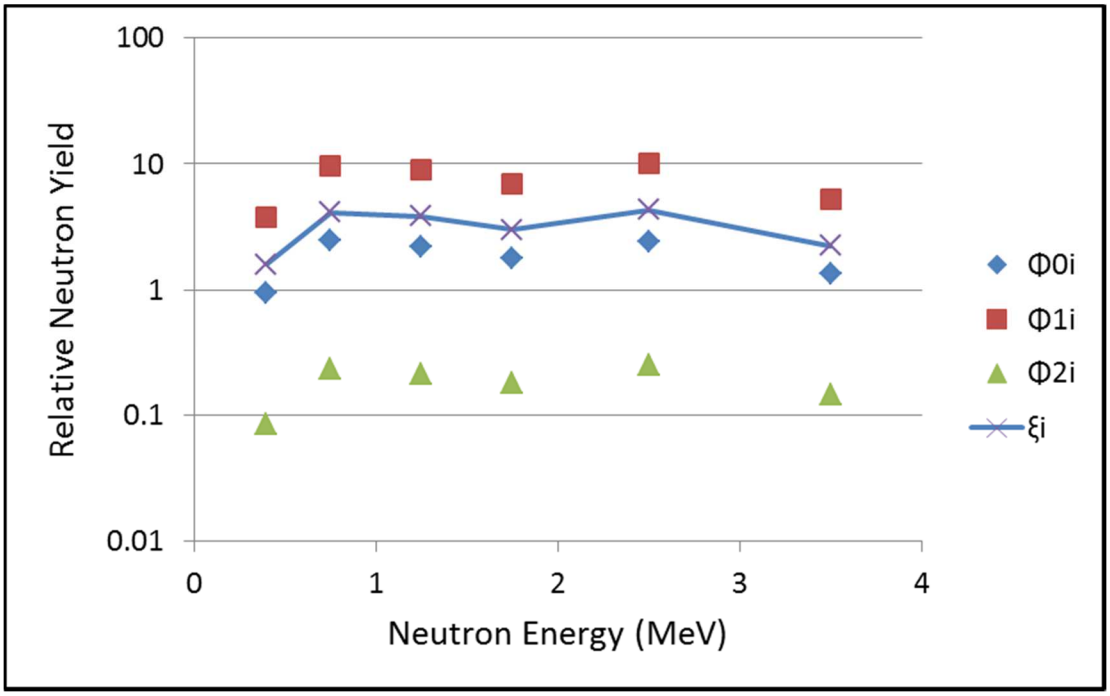

Figure B.5: Example 1: Comparison of $\mathbf{\Phi}_0$, $\mathbf{\Phi}_1$, and $\mathbf{\Phi}_2$ PFNS with anchor shape $\boldsymbol{\xi}$ for groups 5 – 10.

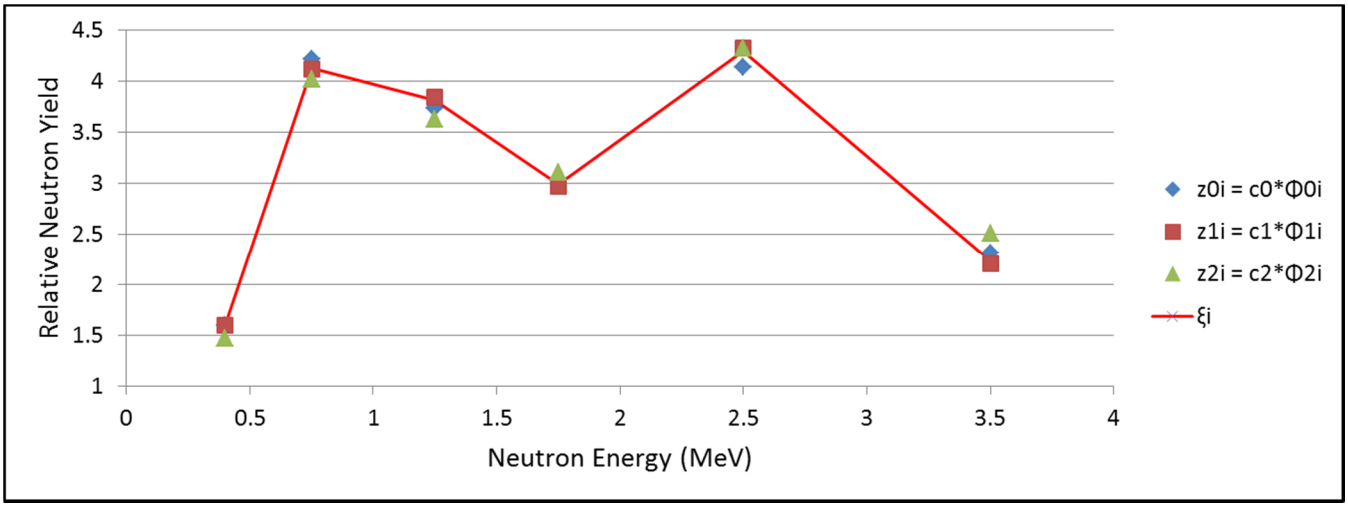

Figure B.6: Example 1: Comparison of $\mathbf{z}_0$, $\mathbf{z}_1$, and $\mathbf{z}_2$ PFNS with anchor shape $\boldsymbol{\xi}$ for groups 5 – 10.

The results of the GLS evaluation procedure are shown in Tables B.5 and B.6 for the spectra and their uncertainties, respectively. The evaluated, non-normalized PFNS is denoted by $\mathbf{\Omega}$. The chi-square per d.o.f. value for the evaluated solution is 0.535747. This signifies good consistency of the scaled input data, considering the assigned uncertainties. These results are also shown graphically in Figs. B.7, B.8, and B.9. Fig. B.8 is a scatter plot that exhibits differences of the data sets $\mathbf{z}_1$ and $\mathbf{z}_2$, as well as the evaluated solution $\mathbf{\Omega}$, from the assumed prior $\mathbf{z}_0$. It is evident that PFNS data set $\mathbf{z}_1$ exhibits a shape that is consistent with

the prior $\mathbf{z}_0$, but its values scatter considerably relative to that prior. The solution $\mathbf{\Omega}$ also has a shape that is similar to the prior. However, the shape of $\mathbf{z}_2$ is noticeably inconsistent with the other PFNS data. Fig. B.9 shows that the solution PFNS $\mathbf{\Omega}$ has noticeably smaller uncertainties than the input PFNS data.

Table B.5: Example 1: Comparison of the scaled input PFNS data and the evaluated spectrum results.

Group # (i)	<E>i	z0i	z1i	z2i	Ωi
1	0.025	0.132555864		0.118372948	0.128899803
2	0.075	0.221143169	0.210030038		0.217936481
3	0.15	0.59127492	0.602510412	0.552983115	0.583899285
4	0.25	0.708176885			0.704639291
5	0.4	1.600934651	1.595379683	1.472317545	1.565748297
6	0.75	4.215139459	4.115740139	4.017767948	4.108309588
7	1.25	3.740036943	3.83994312	3.628951695	3.753068831
8	1.75	3.041441582	2.97012175	3.110530024	3.001029442
9	2.5	4.142569552	4.327891693	4.320180589	4.279469245
10	3.5	2.315330353	2.206376157	2.505704742	2.303649035
11	4.5	1.24012179		1.382457788	1.283297983
12	5.5	0.647617484	0.721315282		0.685742059
13	7	0.474389364	0.424303107	0.552983115	0.462635852
14	9	0.12002327			0.119424742
15	11	0.029607301		0.034561445	0.031064668

Table B.6: Example 1: Comparison of the scaled input and evaluated PFNS data uncertainties.

Group # (i)	<E>i	% Unc z0i	% Unc z1i	% Unc z2i	% Unc Ωi
1	0.025	8.54%		17.46%	7.55%
2	0.075	7.62%	15.30%		6.69%
3	0.15	6.71%	8.54%	10.77%	4.74%
4	0.25	5.83%			5.48%
5	0.4	5.00%	5.00%	7.21%	3.18%
6	0.75	5.00%	4.24%	6.40%	2.88%
7	1.25	5.00%	4.24%	6.40%	2.88%
8	1.75	5.83%	4.24%	6.40%	2.99%
9	2.5	6.71%	4.24%	6.40%	3.06%
10	3.5	7.62%	5.83%	7.21%	3.88%
11	4.5	8.54%		10.77%	6.59%
12	5.5	10.44%	8.54%		6.57%
13	7	13.34%	12.37%	15.52%	7.90%
14	9	16.28%			16.23%
15	11	20.22%		25.32%	15.86%

The evaluated results, for both the PFNS spectrum and its covariance matrix, can then be normalized, as described in Section 4. This converts $\mathbf{\Omega}$ to $\mathbf{\Omega}_N$ (denoted by $\mathbf{\Psi}$ in Section 4). It is evident from Fig. B.10 that this exercise further reduces the uncertainty since the normalization process "washes out" residual fully-correlated uncertainty from the evaluated solution yielding what amounts to pure "shape" uncertainty. The correlation pattern for the normalized solution $\mathbf{\Omega}_N$ (generated by MATLAB) is shown in Fig. B.11.

Finally, the PFNS average energy and its uncertainty were calculated using Eqns. (15) – (17) and the normalized evaluated PFNS $\mathbf{\Omega}_N$ and its covariance matrix $\mathbf{V}_{\Omega N}$. The result is $\varepsilon = 2.0189$, with an uncertainty of 0.848%. Although this average-energy value is rather close to 2 MeV, it must be acknowledged that the 15 energy grids employed in the present calculations are insufficient to permit proper integration of the energy with respect to the spectrum shape in any realistic evaluation. For present purposes, ε should be viewed as a mathematical quantity that can be used to compare the results obtained by using the various scaling methods discussed in this paper.

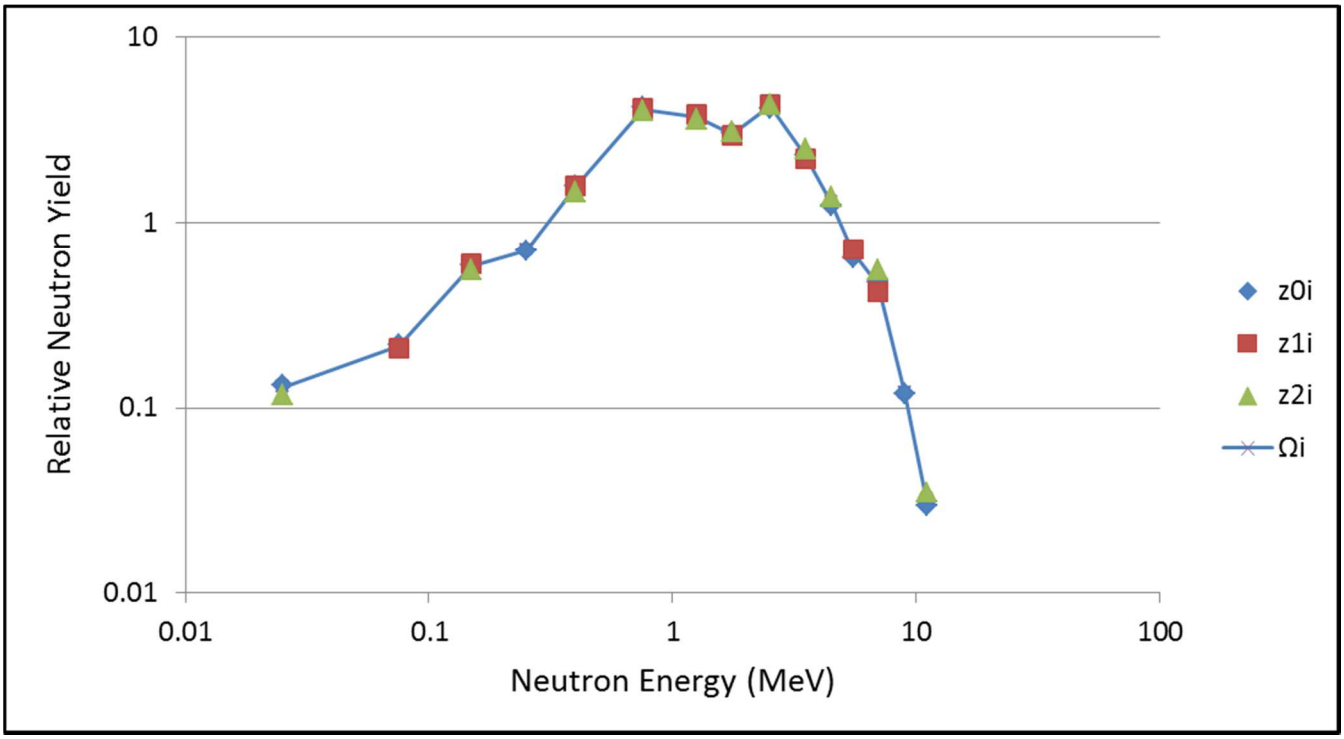

Figure B.7: Example 1: Comparison of $\mathbf{z}_0$, $\mathbf{z}_1$, $\mathbf{z}_2$, and $\mathbf{\Omega}$.

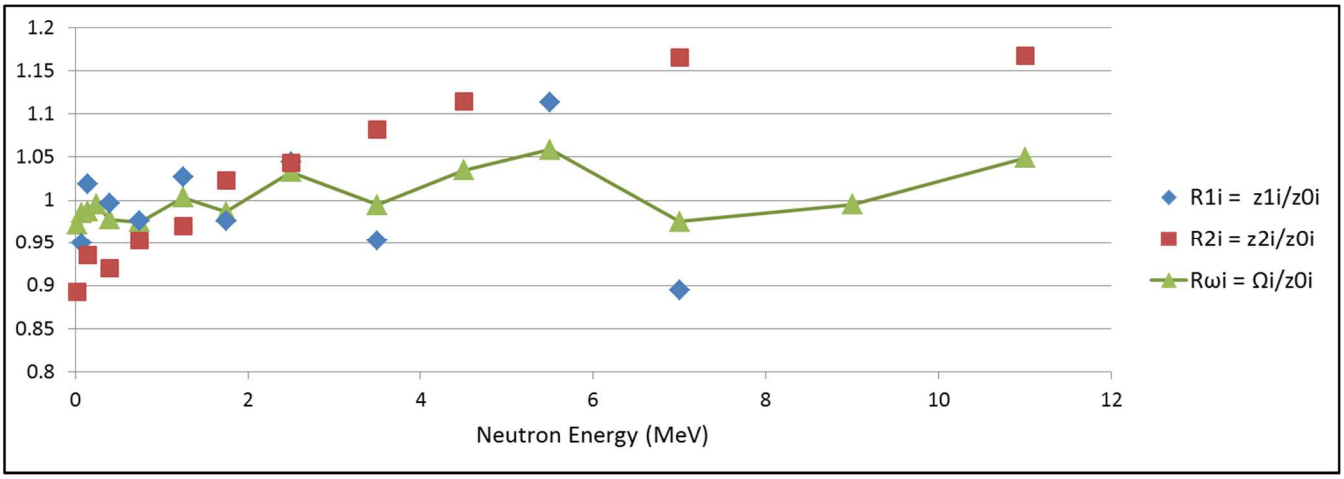

Figure B.8: Example 1: PFNS data $\mathbf{z}_1$, $\mathbf{z}_2$, and $\mathbf{\Omega}$ are plotted relative to $\mathbf{z}_0$. $R_{1i} = z_{1i}/z_{0i}$, $R_{2i} = z_{2i}/z_{0i}$, and $R_{\Omega i} = \Omega_i/z_{0i}$ (for all applicable energy groups i = 1 to 15).

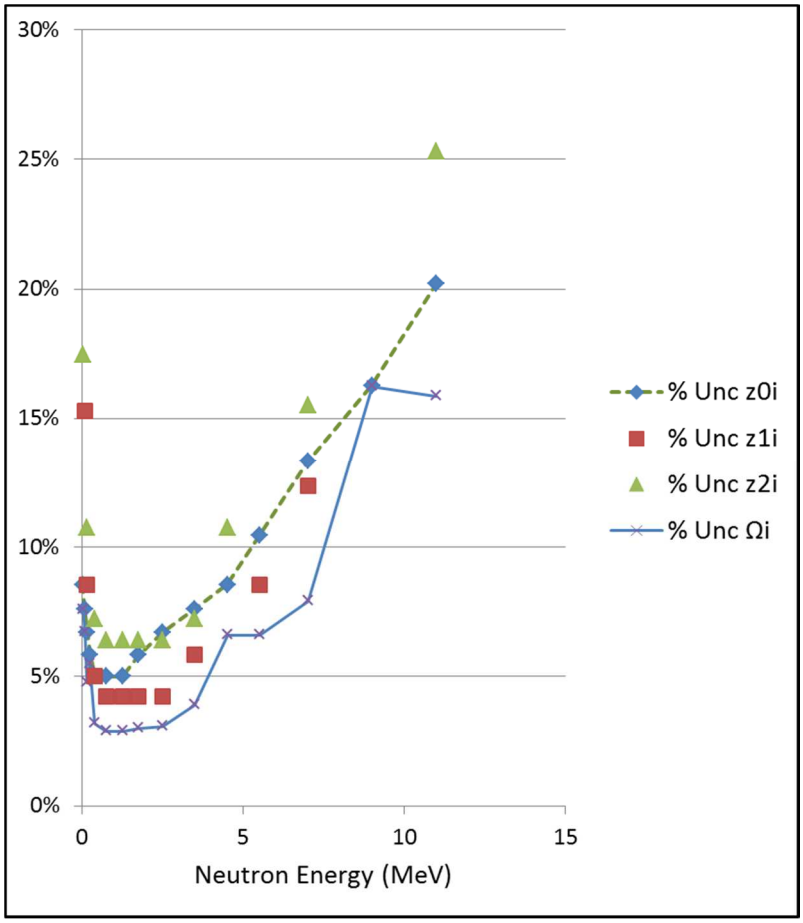

Figure B.9: Example 1: Comparison of the uncertainties for $\mathbf{z}_0$, $\mathbf{z}_1$, $\mathbf{z}_2$, and $\mathbf{\Omega}$.

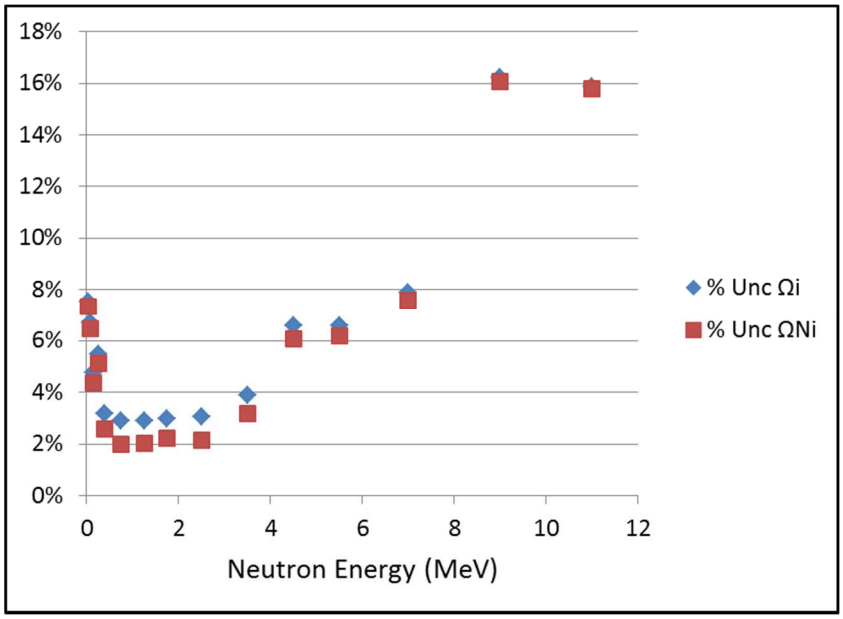

Figure B.10: Example 1: Comparison of uncertainties for the non-normalized ($\mathbf{\Omega}$) and normalized ($\mathbf{\Omega}_N$) solution.

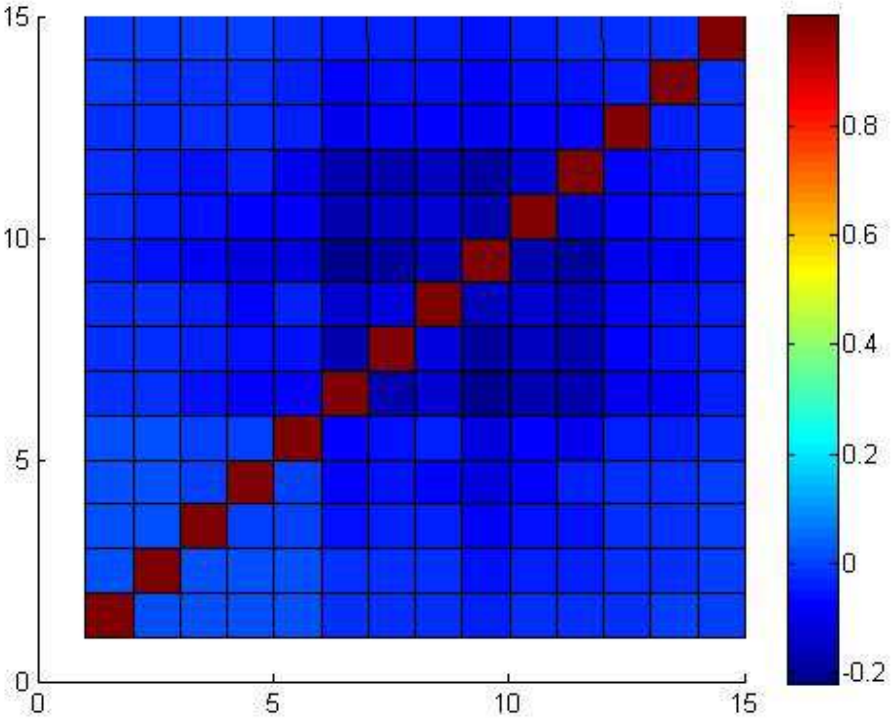

Figure B.11: Example 1: Uncertainty correlations for the normalized evaluated PFNS $\mathbf{\Omega}_N$. The ordinate and abscissa values correspond to energy group numbers.

B.3. Example 2

This example demonstrates *Scaling Method 2* which is described in Section A.3. The approach is similar to *Scaling Method 1*. It differs only in the fact that weighted rather than un-weighted averaging is used to generate the anchor shape $\boldsymbol{\xi}$ that serves in scaling the input PFNS data. No consideration is given to uncertainty correlations in this approach. This example employs PFNS data from energy groups 5 through 10 for scaling purposes, as is the case for Example 1. The analyses for these two examples are similar so the details for Example 2 are omitted here. This procedure leads to noticeably different scaling factors for Example 2 when compared to Example 1, *i.e.*, $c_0 = 2.24184$, $c_1 = 0.53166$, and $c_2 = 22.19130$. However, in spite of these considerable differences in the scaling factors derived from the two methods, the evaluation procedure used for Example 2 generates normalized spectrum shape results which are close to those obtained in Example 1 (< 0.6% difference for any single energy group). This is insignificant for most practical purposes. This outcome is evident from Table B.7 where the normalized PFNS values and their uncertainties are compared for Examples 1 and 2. The chi-square per d.o.f. value for the evaluated solution is 0.58397 which signifies good consistency of the scaled input data. The calculated PFNS average energy obtained using *Scaling Method 2* is $\varepsilon = 2.0192$ with an uncertainty of 0.855%. This value and its uncertainty also differ very little from the corresponding results in Example 1 that were obtained using *Scaling Method 1*.

Scaling Method 2 is more complicated than *Scaling Method 1* and, at least for the data considered in the present examples, it would appear that there is no practical advantage to using *Scaling Method 2* when compared with *Scaling Method 1*. The similar outcomes

obtained in these two examples suggest that the evaluated results obtained are rather insensitive to the scaling approach used. This proposition is further tested in the additional examples considered in this paper.

Table B.7: Comparison of normalized evaluated PFNS and their uncertainties for Examples 1 and 2.

Group # (i)	<E>i	ΩNi (Method 1)	Unc ΩNi (Method 1)	ΩNi (Method 2)	Unc ΩNi (Method 2)
1	0.025	0.005549134	7.36%	0.005571076	7.48%
2	0.075	0.009382161	6.45%	0.009412512	6.52%
3	0.15	0.025136852	4.36%	0.025189061	4.38%
4	0.25	0.030334707	5.12%	0.030516167	5.21%
5	0.4	0.067405433	2.58%	0.067452369	2.58%
6	0.75	0.176862645	1.99%	0.176729759	1.99%
7	1.25	0.161569537	2.03%	0.161605228	2.02%
8	1.75	0.129194257	2.21%	0.128980589	2.20%
9	2.5	0.184231065	2.14%	0.184038058	2.12%
10	3.5	0.099172044	3.19%	0.099004489	3.18%
11	4.5	0.055245952	6.06%	0.055519305	6.12%
12	5.5	0.029521182	6.18%	0.02959247	6.16%
13	7	0.019916464	7.58%	0.019872481	7.57%
14	9	0.005141233	16.07%	0.005171812	16.37%
15	11	0.001337333	15.77%	0.001344624	15.93%

B.4. Example 3

This example demonstrates *Scaling Method 3* which is the same as *Scaling Method 2* with one exception. Only data sets $\mathbf{\Phi}_1$ and $\mathbf{\Phi}_2$ are employed to derive the anchor shape $\boldsymbol{\xi}$. Data set $\mathbf{\Phi}_0$ is not considered for this purpose. The reason for this choice is discussed in Section A.4. Briefly, this approach might be selected when it happens that the uncertainties associated with $\mathbf{\Phi}_0$ are considerably smaller than those for $\mathbf{\Phi}_1$ and $\mathbf{\Phi}_2$, as is frequently the case if $\mathbf{\Phi}_0$ is generated from nuclear models. Since many of the details in the present analysis are very similar to those encountered in Examples 1 and 2, they are omitted here for brevity.

The scaling factor values obtained by this method are $c_0 = 2.78086$, $c_1 = 0.65531$, and $c_2 = 27.35256$. These scaling factors are again noticeably different from comparable values obtained in Examples 1 and 2. The normalized evaluated results obtained for this example are presented in Table B.8, where a comparison is also made with the outcome from Example 1. In spite of the considerable differences in the scaling factors for the two methods, the evaluation procedure for Example 3 generates normalized spectrum-shape results which are close to those obtained in Example 1 (< 0.7% difference for any single group). These differences are insignificant for most practical purposes. The chi-square per d.o.f. value for the evaluated solution is 0.59878, signifying good consistency of the scaled data. The calculated PFNS average energy obtained for Example 3 using *Scaling Method* 3 is ε = 2.0193 with an uncertainty of 0.854%. This value and its uncertainty differ insignificantly from the results obtained for Example 1 using *Scaling Method 1*.

There seems to be no justification for preferring *Scaling Method 3* to *Scaling Method 1*, at least for the present data collection. However, it should be noted that for the common data collection utilized in the present examples, the uncertainties for data set $\mathbf{\Phi}_0$ are comparable to those for data sets for $\mathbf{\Phi}_1$ and $\mathbf{\Phi}_2$. If they happened to be significantly smaller, the evaluated results might differ between the two methods by noticeable amounts. Therefore, it behooves evaluators to compare the outcomes of various scaling approaches in their PFNS evaluations when dealing with realistic data.

Table B.8: Comparison of normalized evaluated PFNS and their uncertainties for Examples 1 and 3.

Group # (i)	<E>i	ΩNi (Method 1)	Unc ΩNi (Method 1)	ΩNi (Method 3)	Unc ΩNi (Method 3)
1	0.025	0.005549134	7.36%	0.005573532	7.49%
2	0.075	0.009382161	6.45%	0.009418082	6.54%
3	0.15	0.025136852	4.36%	0.025193938	4.38%
4	0.25	0.030334707	5.12%	0.03054665	5.23%
5	0.4	0.067405433	2.58%	0.067452317	2.58%
6	0.75	0.176862645	1.99%	0.176704256	1.99%
7	1.25	0.161569537	2.03%	0.161600087	2.02%
8	1.75	0.129194257	2.21%	0.128954642	2.20%
9	2.5	0.184231065	2.14%	0.184007455	2.12%
10	3.5	0.099172044	3.19%	0.098989181	3.17%
11	4.5	0.055245952	6.06%	0.055561019	6.13%
12	5.5	0.029521182	6.18%	0.02960552	6.16%
13	7	0.019916464	7.58%	0.019870552	7.57%
14	9	0.005141233	16.07%	0.005177082	16.42%
15	11	0.001337333	15.77%	0.001345687	15.96%

B.5. Example 4

Example 1, which is based on *Scaling Method 1*, employs only energy groups 5 through 10 for scaling purposes. Un-weighted averages of the data sets $\mathbf{\Phi}_0$, $\mathbf{\Phi}_1$, and $\mathbf{\Phi}_2$ are used to generate an anchor shape $\boldsymbol{\xi}$ so that scaling factors c_0, c_1, and c_2 can be calculated. Example 4 utilizes all the available PFNS data in conjunction with *Scaling Method 4*. It differs considerably from Example 1 (using *Scaling Method 1*) in that the data set $\mathbf{\Phi}_0$ serves as the anchor shape for scaling purposes, and data sets $\mathbf{\Phi}_1$ and $\mathbf{\Phi}_2$ are scaled to this anchor shape. Consequently, $c_0 = 1$ exactly. This approach is facilitated by the fact that data set $\mathbf{\Phi}_0$ provides values for all 15 energy groups. As in Example 1, no weighting factors based on uncertainties are considered in this process, so all the PFNS data are treated equally.

The values for the other two scaling factors obtained by this procedure are $c_1 = 0.2480753$ and $c_2 = 10.0340195$. The normalized results of the evaluation for this example are given in Table B.9, where they are also compared with values obtained in Example 1. The chi-square per d.o.f. value for the evaluated solution is 0.54054, again reflecting good consistency of the scaled data. The comparable evaluated PFNS values obtained in Example 4 are almost identical to those for Example 1, differing by < 0.05% for any single energy group of the normalized PFNS. The uncertainties for Examples 1 and 4 are similar, according to Table B.9. The calculated PFNS average energy obtained for Example 4 using *Scaling*

Method 4 is ε = 2.0191 with an uncertainty of 0.849%. This value and its uncertainty differ very little from the results obtained for Example 1 using *Scaling Method 1*.

There are two reasons why Examples 1 and 4 yield similar results. First, in both methods there is no weighting of the data based on their uncertainties in determining the scaling factors. Second, it appears that inclusion of additional PFNS values at the low- and high-energy ranges of the spectrum has little influence on the relative scaling factors. PFNS values are much smaller at the spectrum extremes than in the region of peak neutron yield, so these data have negligible influence on scaling.

Of course, if the data in the region of peak yield show significant discrepancies, then the evaluator might wish to reconsider and use a different region of the spectrum for normalization where the data are more consistent.

Table B.9: Comparison of normalized evaluated PFNS and their uncertainties for Examples 1 and 4.

Group # (i)	<E>i	ΩNi (Method 1)	Unc ΩNi (Method 1)	ΩNi (Method 4)	Unc ΩNi (Method 4)
1	0.025	0.005549134	7.36%	0.005548182	7.37%
2	0.075	0.009382161	6.45%	0.009386042	6.46%
3	0.15	0.025136852	4.36%	0.025133597	4.36%
4	0.25	0.030334707	5.12%	0.030349706	5.13%
5	0.4	0.067405433	2.58%	0.067392945	2.58%
6	0.75	0.176862645	1.99%	0.17684345	1.99%
7	1.25	0.161569537	2.03%	0.161549478	2.03%
8	1.75	0.129194257	2.21%	0.129196407	2.21%
9	2.5	0.184231065	2.14%	0.184216499	2.14%
10	3.5	0.099172044	3.19%	0.099185147	3.18%
11	4.5	0.055245952	6.06%	0.055260699	6.05%
12	5.5	0.029521182	6.18%	0.029531184	6.19%
13	7	0.019916464	7.58%	0.01992499	7.58%
14	9	0.005141233	16.07%	0.005143737	16.10%
15	11	0.001337333	15.77%	0.001337938	15.75%

B.6. Example 5

Example 5 employs *Scaling Method 5*. In many ways it resembles *Scaling Method* 4 that is used in Example 4. The difference is that weighted group values of the PFNS $\mathbf{\Phi}_0$, $\mathbf{\Phi}_1$, and $\mathbf{\Phi}_2$ are employed in scaling $\mathbf{\Phi}_1$ and $\mathbf{\Phi}_2$ to the anchor shape $\mathbf{\Phi}_0$.

The resulting scale factors are $c_0 = 1$ (since $\mathbf{\Phi}_0$ serves as the anchor shape), $c_1 = 0.212441$, and $c_2 = 9.164120$. The normalized evaluated results for Example 5 are given in Table B.10 where they are also compared with the values from Example 1. The evaluated solution chi-square per d.o.f. in Example 5 is 1.05521. This value, although it would appear to be quite reasonable (*e.g.*, see Section 3), is noticeably larger than the comparable results

obtained in Examples 1 through 4. This suggests that under certain conditions normalized evaluated results may be sensitive to the selected method of scaling the PFNS data.

Table B.10: Comparison of normalized evaluated PFNS and their uncertainties for Examples 1 and 5.

Group # (i)	<E>i	ΩNi (Method 1)	Unc ΩNi (Method 1)	ΩNi (Method 5)	Unc ΩNi (Method 5)
1	0.025	0.005549134	7.36%	0.005623437	7.77%
2	0.075	0.009382161	6.45%	0.009496423	6.74%
3	0.15	0.025136852	4.36%	0.025293729	4.43%
4	0.25	0.030334707	5.12%	0.031038668	5.47%
5	0.4	0.067405433	2.58%	0.06750264	2.58%
6	0.75	0.176862645	1.99%	0.176337925	1.98%
7	1.25	0.161569537	2.03%	0.161584063	2.01%
8	1.75	0.129194257	2.21%	0.128497138	2.18%
9	2.5	0.184231065	2.14%	0.183547842	2.10%
10	3.5	0.099172044	3.19%	0.098655771	3.15%
11	4.5	0.055245952	6.06%	0.056235637	6.28%
12	5.5	0.029521182	6.18%	0.029768828	6.12%
13	7	0.019916464	7.58%	0.019793008	7.57%
14	9	0.005141233	16.07%	0.005260447	17.22%
15	11	0.001337333	15.77%	0.001364444	16.37%

The calculated PFNS average energy obtained for Example 5 using *Scaling Method* 5 is $\varepsilon = 2.02037$ with an uncertainty of 0.869%. This value and its uncertainty differ rather little from the value of ε obtained for Example 1 using *Scaling Method 1*.

The normalized, evaluated PFNS values for Examples 1 and 5 differ by as much as 2.3% for some energy groups. It is not surprising that differences of this magnitude should occur if one compares the scaling factor ratios for these two examples. It is also evident from Fig. B.12 that for most of the energy groups, the values of vectors $\mathbf{z}_1$ and $\mathbf{z}_2$ are correspondingly smaller than those of $\mathbf{z}_0$. This suggests that the *Scaling Method 5* algorithm does a rather poor job of scaling these PFNS. This is consistent with the larger chi-square value seen for this example compared with Examples 1 through 4.

It was stated earlier in this paper that an important measure of a "good" scaling procedure is that it should lead to relatively small values of chi-square when performing a least-squares evaluation of the scaled PFNS data. Therefore, the present outcome clearly indicates that *Scaling Method 5* is not the most appropriate scaling option for the data collection considered in this paper.

Further insight into this situation can be gained by comparing scatter plots of the non-normalized, scaled data and evaluated results for Examples 1 and 5. Fig. B.13 is a scatter plot of $\mathbf{z}_0$, $\mathbf{z}_1$, $\mathbf{z}_2$, and $\mathbf{\Omega}$ for Example 5 while Fig. B.8 shows the corresponding results for Example 1. It is evident from an inspection of these two figures that the values for $\mathbf{z}_1$, $\mathbf{z}_2$, and $\mathbf{\Omega}$ tend to be systematically lower than $\mathbf{z}_0$ in Example 5 whereas vectors $\mathbf{z}_1$, $\mathbf{z}_2$, and $\mathbf{\Omega}$ appear to be reasonably consistent with $\mathbf{z}_0$ for Example 1. This would again explain the larger value

of chi-square per d.o.f. obtained in Example 5 when compared with Example 1. A closer examination of chi-square sensitivity to scaling would be justified in order to gain further insight regarding this particular case. However, this matter was not pursued in the present investigation.

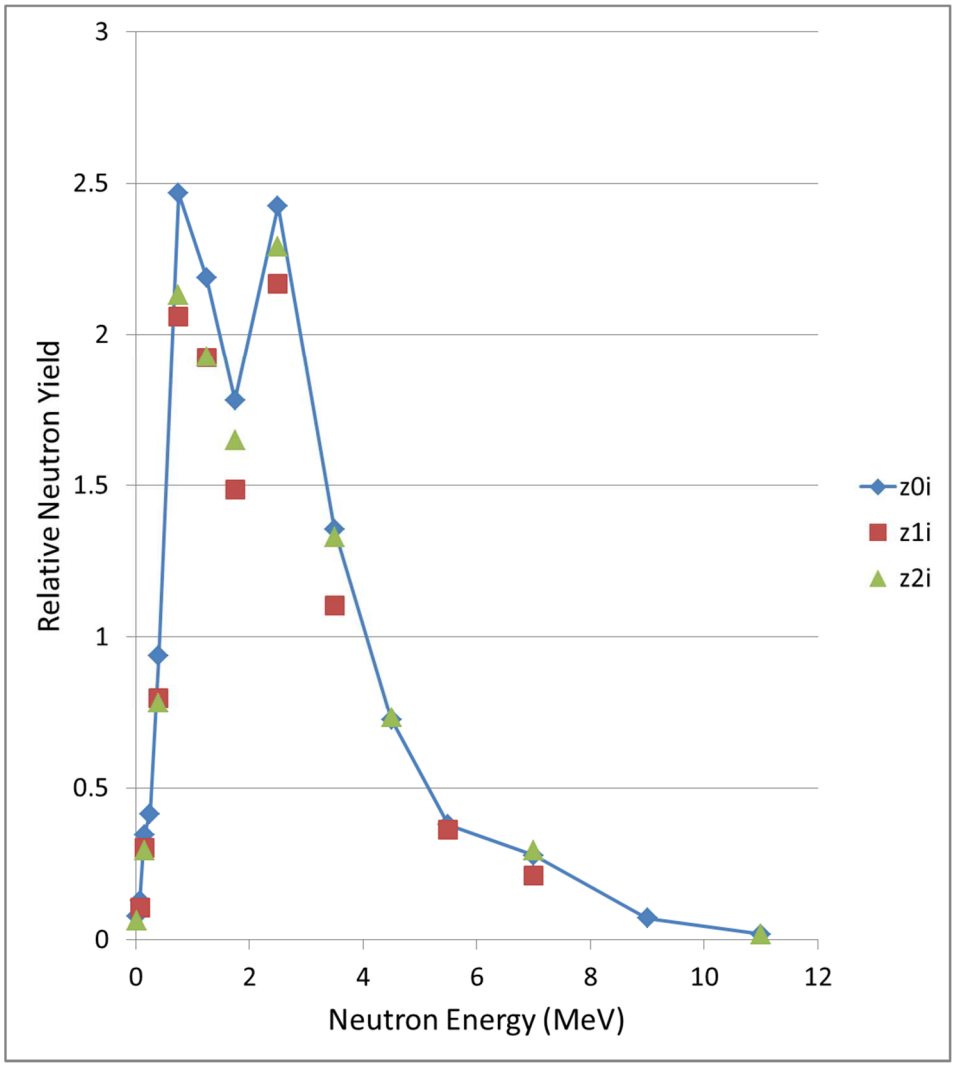

Figure B.12: Example 5: Plot of scaled PFNS $\mathbf{z}_0$, $\mathbf{z}_1$, and $\mathbf{z}_2$.

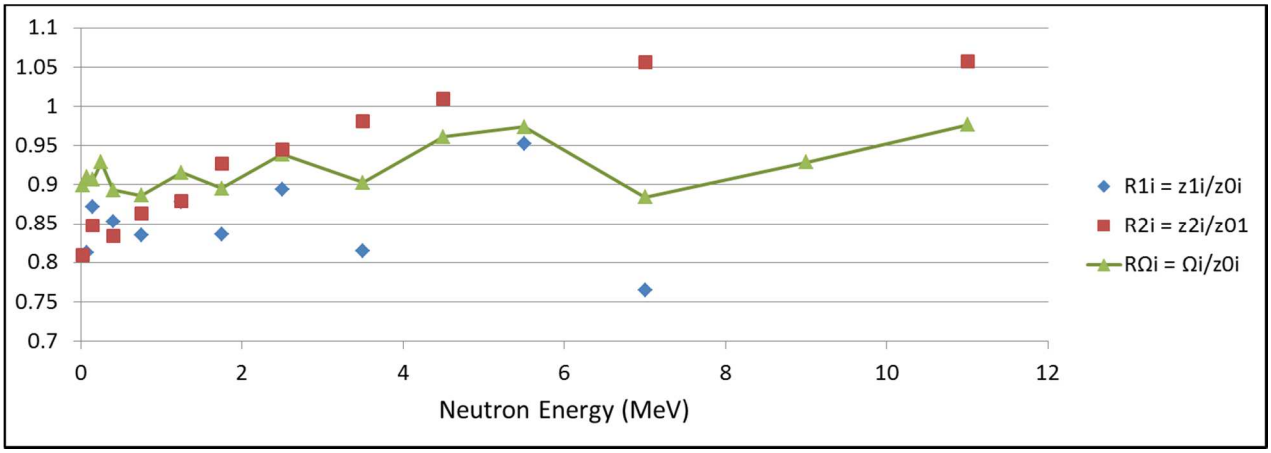

Figure B.13: Example 5: PFNS data $\mathbf{z}_1$, $\mathbf{z}_2$, and $\mathbf{\Omega}$ plotted relative to $\mathbf{z}_0$. $R_{1i} = z_{1i}/z_{0i}$, $R_{2i} = z_{2i}/z_{0i}$, and $R_{\Omega i} = \Omega_i/z_{0i}$ (for all applicable energy groups i = 1 to 15).

The fact that Examples 1 and 5 generate spectrum-average energies that differ rather little, while yielding noticeably different normalized evaluated PFNS, suggests that the spectrum-average energy is not a particularly effective parameter for characterizing a PFNS. This is an important point because the assumed strong correlation between k_{eff} for benchmark nuclear systems and source PFNS average energy are often invoked as a means to validate whether the evaluated PFNS data in a particular nuclear data library are adequate for the intended applications.

B.7. Example 6

Example 6 employs *Scaling Method 6* which involves a SLS procedure to determine the individual scaling factors. The results are $c_0 = 1$ (since $\mathbf{\Phi}_0$ serves as the anchor shape), $c_1 = 0.249137875$, and $c_2 = 10.31067784$. The chi-square per d.o.f. value obtained from the GLS evaluation procedure is 0.5327201 indicating that the scaled PFNS are very consistent. Table B.11 provides a comparison of the results obtained from Example 1 and Example 6. It evident that these results are in close agreement (<0.4% difference for any of the energy groups).

The calculated PFNS average energy obtained for Example 6 using *Scaling Method* 6 is $\varepsilon = 2.01848$ with an uncertainty of 0.848%. This value and its uncertainty differ very little from the results obtained for Example 1 using *Scaling Method 1*.

Table B.11: Comparison of normalized evaluated PFNS and their uncertainties for Examples 1 and 6.

Group # (i)	<E>i	ΩNi (Method 1)	fNi (Method 1)	ΩNi (Method 6)	fNi (Method 6)
1	0.025	0.005549134	7.36%	0.005550535	7.35%
2	0.075	0.009382161	6.45%	0.009373162	6.43%
3	0.15	0.025136852	4.36%	0.025143598	4.36%
4	0.25	0.030334707	5.12%	0.030298708	5.10%
5	0.4	0.067405433	2.58%	0.06743376	2.58%
6	0.75	0.176862645	1.99%	0.176909378	1.99%
7	1.25	0.161569537	2.03%	0.161615299	2.03%
8	1.75	0.129194257	2.21%	0.12919177	2.21%
9	2.5	0.184231065	2.14%	0.184267571	2.14%
10	3.5	0.099172044	3.19%	0.099142928	3.19%
11	4.5	0.055245952	6.06%	0.055207866	6.07%
12	5.5	0.029521182	6.18%	0.029497375	6.17%
13	7	0.019916464	7.58%	0.019897206	7.58%
14	9	0.005141233	16.07%	0.005135087	16.01%
15	11	0.001337333	15.77%	0.001335756	15.79%

B.8. Example 7

Example 7 employs *Scaling Method 7* which involves a SLS procedure to determine the individual scaling factors. However, this procedure differs considerably from *Scaling Method 6* used in Example 6. The results are $c_0 = 1$ (since $\mathbf{\Phi}_0$ serves as the anchor shape), $c_1 = 0.246767497$, and $c_2 = 9.991857664$. The chi-square per d.o.f. value obtained from the GLS evaluation procedure is 0.543153989 indicating that the scaled PFNS are very consistent. Table B.12 provides a comparison of the results obtained from Example 1 and Example 7. These results agree to within ≈ 0.1% for all of the energy groups. The uncertainty values obtained using the *Scaling Method 7* approach are also very close to the corresponding values obtained in Examples 1 and 6 using *Scaling Method 1* and *Scaling Method 6*, respectively.

The calculated PFNS average energy obtained for Example 7 using *Scaling Method* 7 is $\varepsilon = 2.01916$ with an uncertainty of 0.849%. This value and its uncertainty also differ very little from the results obtained for Example 1 using *Scaling Method 1*.

Table B.12: Comparison of normalized evaluated PFNS and their uncertainties for Examples 1 and 7.

Group # (i)	<E>i	ΩNi (Method 1)	fNi (Method 1)	ΩNi (Method 7)	fNi (Method 7)
1	0.025	0.005549134	7.36%	0.005550183	7.38%
2	0.075	0.009382161	6.45%	0.009390161	6.47%
3	0.15	0.025136852	4.36%	0.025138554	4.36%
4	0.25	0.030334707	5.12%	0.030372196	5.14%
5	0.4	0.067405433	2.58%	0.067395229	2.58%
6	0.75	0.176862645	1.99%	0.176824822	1.99%
7	1.25	0.161569537	2.03%	0.161549257	2.03%
8	1.75	0.129194257	2.21%	0.129173809	2.21%
9	2.5	0.184231065	2.14%	0.18419229	2.13%
10	3.5	0.099172044	3.19%	0.099170278	3.18%
11	4.5	0.055245952	6.06%	0.055293069	6.06%
12	5.5	0.029521182	6.18%	0.029541555	6.19%
13	7	0.019916464	7.58%	0.019922269	7.57%
14	9	0.005141233	16.07%	0.005147542	16.14%
15	11	0.001337333	15.77%	0.001338784	15.76%

B.9. Example 8

This example illustrates a situation where there is no prior PFNS and the evaluation is based solely on experimental data that have been augmented by introducing additional group values in such a way that all the groups are represented by data values for all the PFNS included in the evaluation. These added values are *ad hoc* in the present instance, but they have been chosen to have plausible magnitudes. This is a situation where a "non-model" PFNS evaluation approach could be applied.

This example, which utilizes *Scaling Method 8*, differs significantly from Examples 1 through 7 in a number of ways. Therefore, the results of the present analysis cannot be

compared directly with those from the preceding examples. Only two PFNS data sets are considered here rather than all three sets of the complete collection of "toy" data sets.

Table B.l3 shows the group PFNS values and uncertainties included in Example 8 for the first data set (also referred to here as $\mathbf{\Phi}_1$ although it differs from the original collection). The data values introduced here to augment the data used for Examples 1 through 7 are shown in red font in this table. The values in black font are identical to those from the preceding examples. It is assumed that these *ad hoc* values have 100% uncertainty, and that these uncertainties are uncorrelated to all other data, including to each other. Table B.14 shows the corresponding values for a second data set that was generated in a similar way (referred to here as $\mathbf{\Phi}_2$ although it differs from the original collection).

The information in these two tables is used to construct the covariance matrices that are required for a least-squares evaluation. Fig. B.14 is a plot of these two sets of group PFNS data. Spectrum $\mathbf{\Phi}_1$ is selected here as the anchor spectrum for scaling. Basically, a version of *Scaling Method 4* is applied here, with Groups 5 through 10 included in the scaling analysis since there are no *ad hoc* augmented data for any of these groups to distort the scaling process.

The results from this analysis are $c_1 = 1$ (since $\mathbf{\Phi}_1$ is the anchor spectrum) and $c_2 = 40.7273057$. Fig. B.15 is a linear plot of the scaled data $\mathbf{z}_1$ and $\mathbf{z}_2$.

The two scaled PFNS data sets and their (scaled) covariance matrices are then employed in a SLS evaluation procedure, as discussed in Sections 3 and A.9. The actual numerical PFNS values from this analysis are of limited interest to us since they cannot be compared with data from Examples 1 through 7. However, it is interesting to compare the evaluated results $\mathbf{\Omega}$ with $\mathbf{z}_1$ and $\mathbf{z}_2$ as well as their corresponding uncertainties. To do this, it is useful to define $R_{1i} = z_{1i}/\Omega_i$ and $R_{1i} = z_{1i}/\Omega_i$. The values of R_{ki} (k = 1,2) are plotted in Fig. B.16. Uncertainties obtained from this analysis appear in Table B.15. The chi-square per d.o.f. value obtained from the present procedure is 0.5416724, which is quite reasonable.

Table B.13: Group PFNS values for data set $\mathbf{\Phi}_1$ employed in Example 8. The original data shown in black font are augmented by the values shown in red font.

Group # (i)	<E>i	Φ1i	% Rand Unc	% Correl Unc	% Tot Unc
1	0.025	0.3	100.00%	0.00%	100.00%
2	0.075	0.495	15.00%	3.00%	15.30%
3	0.15	1.42	8.00%	3.00%	8.54%
4	0.25	1.7	100.00%	0.00%	100.00%
5	0.4	3.76	4.00%	3.00%	5.00%
6	0.75	9.7	3.00%	3.00%	4.24%
7	1.25	9.05	3.00%	3.00%	4.24%
8	1.75	7	3.00%	3.00%	4.24%
9	2.5	10.2	3.00%	3.00%	4.24%
10	3.5	5.2	5.00%	3.00%	5.83%
11	4.5	3.5	100.00%	0.00%	100.00%
12	5.5	1.7	8.00%	3.00%	8.54%
13	7	1	12.00%	3.00%	12.37%
14	9	0.24	100.00%	0.00%	100.00%
15	11	0.06	100.00%	0.00%	100.00%

Table B.14: Group PFNS values for data set $\mathbf{\Phi}_2$ employed in Example 8. The original data shown in black font are augmented by the values shown in red font.

Group # (i)	<E>i	Φ2i	% Rand Unc	% Correl Unc	% Tot Unc
1	0.025	0.00685	17.00%	4.00%	17.46%
2	0.075	0.012	100.00%	0.00%	100.00%
3	0.15	0.032	10.00%	4.00%	10.77%
4	0.25	0.038	100.00%	0.00%	100.00%
5	0.4	0.0852	6.00%	4.00%	7.21%
6	0.75	0.2325	5.00%	4.00%	6.40%
7	1.25	0.21	5.00%	4.00%	6.40%
8	1.75	0.18	5.00%	4.00%	6.40%
9	2.5	0.25	5.00%	4.00%	6.40%
10	3.5	0.145	6.00%	4.00%	7.21%
11	4.5	0.08	10.00%	4.00%	10.77%
12	5.5	0.05	100.00%	0.00%	100.00%
13	7	0.032	15.00%	4.00%	15.52%
14	9	0.012	100.00%	0.00%	100.00%
15	11	0.002	25.00%	4.00%	25.32%

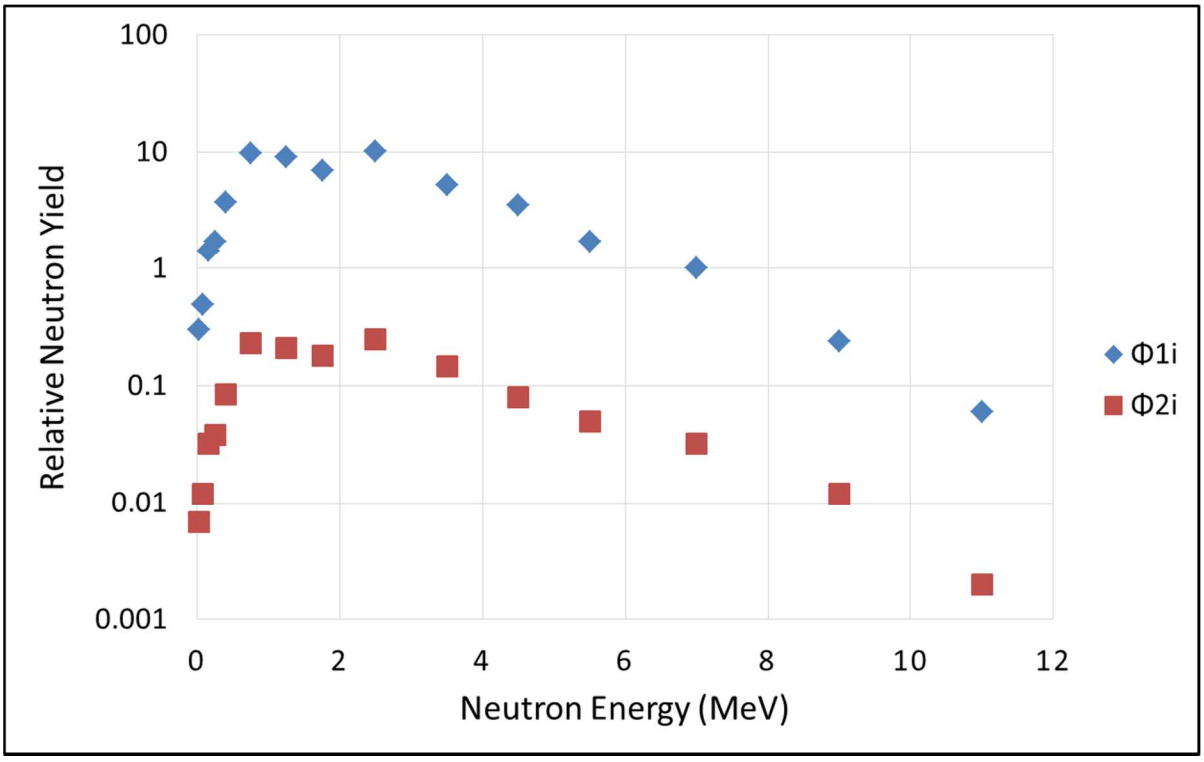

Figure B.14: Example 8: Plot of group spectrum values $\mathbf{\Phi}_1$ and $\mathbf{\Phi}_2$.

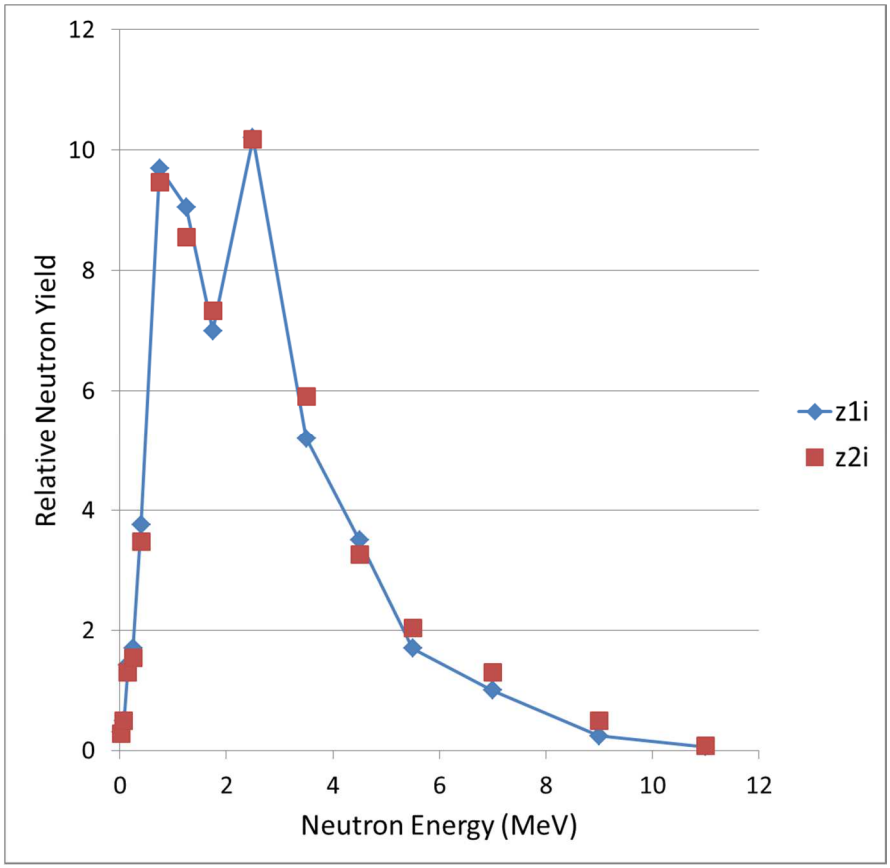

Figure B.15: Example 8: Plot of scaled PFNS group values $\mathbf{z}_1$ and $\mathbf{z}_2$.

Table B.15: Comparison of total uncertainties for the input and solution PFNS.

Group # (i)	<E>i	% Unc z1i	% Unc z2i	% Unc Ωi
1	0.025	100.00%	17.46%	17.03%
2	0.075	15.30%	100.00%	15.12%
3	0.15	8.54%	10.77%	6.73%
4	0.25	100.00%	100.00%	70.79%
5	0.4	5.00%	7.21%	4.12%
6	0.75	4.24%	6.40%	3.53%
7	1.25	4.24%	6.40%	3.53%
8	1.75	4.24%	6.40%	3.54%
9	2.5	4.24%	6.40%	3.54%
10	3.5	5.83%	7.21%	4.55%
11	4.5	100.00%	10.77%	10.35%
12	5.5	8.54%	100.00%	8.40%
13	7	12.37%	15.52%	9.79%
14	9	100.00%	100.00%	74.72%
15	11	100.00%	25.32%	24.54%

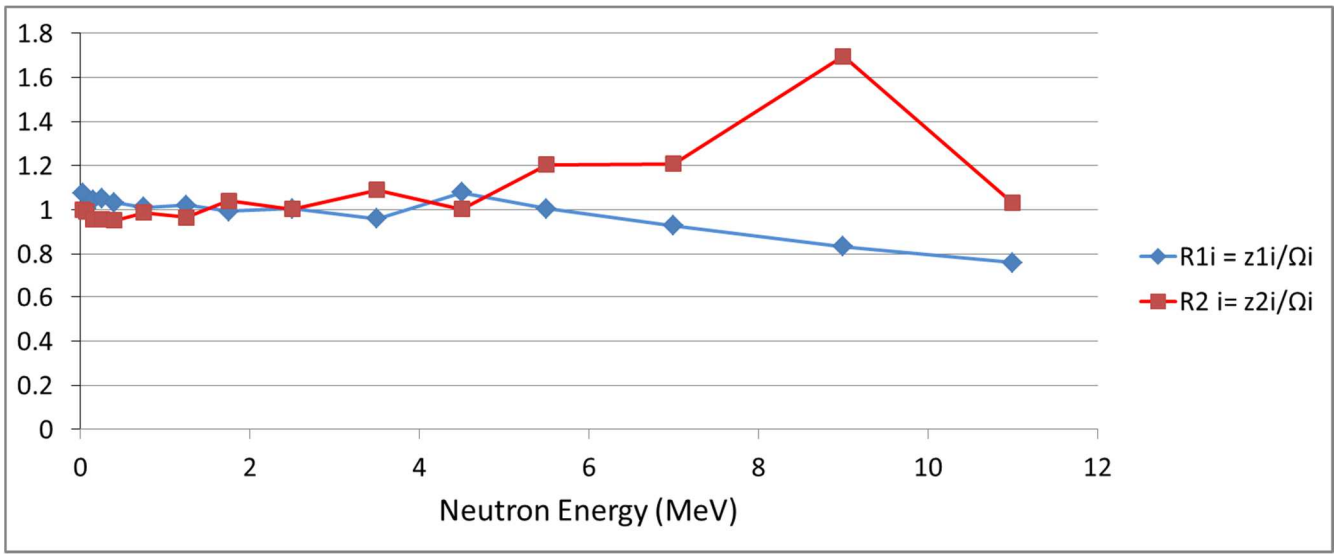

Figure B.16: Example 8: Plot of the ratios R_{1i} and R_{2i}.

The results obtained from Example 8 (Table B.15 and Fig. B.16) suggest that the SLS evaluation procedure used here yields reasonable solution values, considering the given uncertainties. These evaluated results can then be normalized in the manner described in Section 4. The uncertainty correlation pattern generated by this procedure is illustrated in Fig. B.17. Strong positive and negative correlations are evident in this pattern.

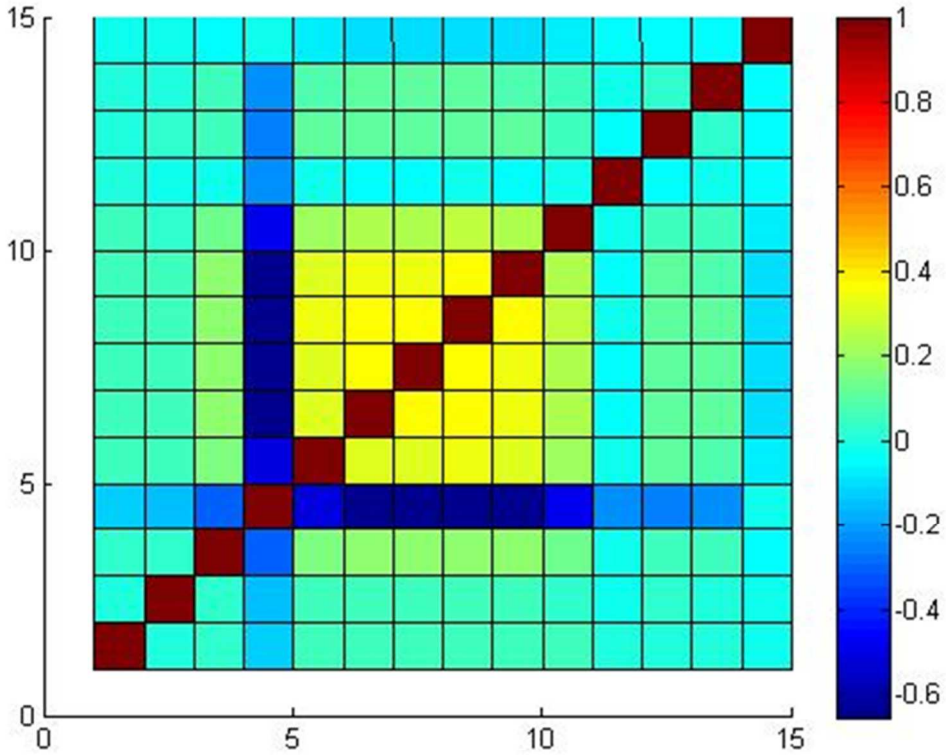

Figure B.17: Example 8: Uncertainty correlations for the normalized solution covariance matrix. The ordinate and abscissa values correspond to energy group numbers.

The calculated PFNS average energy obtained for Example 8 using *Scaling Method* 8 is $\varepsilon = 2.04186$ with an uncertainty of 2.517%. As is to be anticipated, this value and its uncertainty differ significantly from the results obtained for Example 1 using *Scaling Method 1* since only two of the three PFNS (the "experimental" ones) are used in the evaluation and extra data have been added.

There is an additional way to view the material of Example 8 that is quite interesting. An examination of Tables B.13, B.14, and B.15 shows that Groups 1, 2, 11, 12, and 15 are each represented by only one "real" data value from the original input data collection. The second value in each instance is an *ad hoc* one from the augmented set that has been introduced somewhat arbitrarily (but with plausible magnitude). Furthermore, Groups 4 and 14 are each represented by only the augmented data. The remaining groups of the PFNS are represented by "real" data from both original PFNS. If one examines Fig. B.16 and Table B.15 it is seen that for those groups where there is representation by "real" data from either of the original PFNS plus one *ad hoc* value from the augmented set, the evaluated non-normalized PFNS results and their uncertainties are based almost entirely on the "real" value represented in that group. The *ad hoc* values have little impact on the evaluated results for those groups or on their uncertainties. The *ad hoc* information provided for Groups 4 and 14 have negligible impact on the overall evaluation results for all the other groups. Indeed, this is quite reasonable since 100% uncertainty is assumed for all the *ad hoc* values. Consequently, they have little influence on the evaluation procedure, and the values for Groups 4 and 14 could be excluded from the final results. Or, perhaps better *a posteriori* estimates could be made of these values thereby leading to a smaller chi-square.

The introduction of *ad hoc* values with large assigned uncertainties to fill "gaps" in the provided "real" data collection offers a convenient way to generate an evaluation which is based on the "real" data alone, with introduction of the *ad hoc* values serving as a technique to facilitate the SLS evaluation process. This technique could be considered as a "trick", but in nuclear data evaluations such tricks are often very useful even though they may be difficult to justify rigorously. Generally speaking, if these tricks lead to reasonable results they can be viewed as pragmatically acceptable.

B.10. Example 9

It is seen from Example 8 that the approach labeled *Scaling Method 8* produces a "non-model" PFNS evaluation denoted by $\mathbf{\Omega}$ that is based, for all practical purposes, on "experimental" data. No use is made of the original model-calculated PFNS $\mathbf{\Phi}_0$. Therefore, the results cannot be compared with those from Examples 1 through 7. However, if the non-normalized PFNS results $\mathbf{\Omega}$ and $\mathbf{V}_\Omega$ from such a procedure are then combined by least-squares with a non-normalized prior PFNS representation $\mathbf{\Phi}_0$ and $\mathbf{V}_{\Phi 0}$, then it should be possible to generate a "complete" PFNS evaluation that can be compared directly with results obtained in Examples 1 through 7. In order to carry out this exercise it is necessary to scale these two spectra so that they are comparable. This procedure is denoted as *Scaling Method 9*, although the actual scaling approach is essentially the same as *Scaling Method 8*.

In the present example, $\mathbf{\Phi}_0$ is selected to be the anchor shape and $\mathbf{\Omega}$ is then scaled to this prior PFNS using a version of *Scaling Method 4* that involves all 15 energy groups, as in Example 8. Recall that the outcome of Example 8 involves inclusion of the *ad hoc* data from the augmented data set introduced in that example. These augmented data do not have any

influence on Examples 1 through 7 since they were not introduced in those examples. Therefore, the present exercise tests whether these *ad hoc* data have any influence on comparisons of the present results with those from Examples 1 through 7 that do not incorporate any of the augmented data values.

The scaling factors that are applicable in this example are $c_0 = 1$ and $c_\Omega = 0.249434431$. PFNS $\mathbf{\Omega}$ is multiplied by c_Ω to scale it to the anchor shape $\mathbf{\Phi}_0$. As in Example 8, the analysis is performed using the SLS method. The details of this analysis are similar to those considered in Example 8 so they are omitted here. The main results from this exercise appear in Table B.16. The calculated PFNS average energy obtained for Example 9 using *Scaling Method* 9 is $\varepsilon = 2.01894$ with an uncertainty of 0.844%. The ratios of the normalized solution PFNS values from Example 9 to the corresponding values from Example 1 are almost indistinguishable from unity. Furthermore, the uncertainties from Examples 1 and 9 are almost identical. The chi-square per d.o.f. value for the evaluated solution is 0.228598. This suggests that these two distinct approaches to evaluating the PFNS data collection lead to essentially the same outcome. In other words, GLS can be used to simultaneously consider the prior data and "experimental" data, or SLS can be used to first evaluate the "experimental" data (by introducing severely down-weighted augmented values to fill gaps) and then combining these results with the prior representation $\mathbf{\Phi}_0$, again using SLS. The *ad hoc* augmented values introduced with large uncertainties are seen to have a negligible influence on the outcome in Example 9.

In general, evaluation approaches that utilize GLS, with $\mathbf{\Phi}_0$ treated as a prior and $\mathbf{\Phi}_1$ and $\mathbf{\Phi}_2$ introduced as experimental data, *i.e.*, as in Examples 1 through 7, are to be preferred since then it is not necessary to augment the data sets with *ad hoc* values to satisfy the mathematical requirements of SLS. However, it is useful to know that the procedure employed in the present example can be used in situations where the experimental data base is nearly complete.

Table B.16: Comparison of evaluated normalized PFNS results from Examples 1 and 9.

Group # (i)	<E>i	Norm PFNS Ratio Ex9 to Ex1	Tot Unc Ex1	Tot Unc Ex9
1	0.025	0.999551522	7.36%	7.33%
2	0.075	0.999355625	6.45%	6.43%
3	0.15	0.999821554	4.36%	4.36%
4	0.25	0.999176715	5.12%	5.09%
5	0.4	0.999953922	2.58%	2.58%
6	0.75	1.000066505	1.99%	1.99%
7	1.25	0.999978756	2.03%	2.03%
8	1.75	1.000105376	2.21%	2.21%
9	2.5	1.000070513	2.14%	2.14%
10	3.5	1.000072762	3.19%	3.19%
11	4.5	0.999952142	6.06%	6.04%
12	5.5	1.000291499	6.18%	6.17%
13	7	1.000009992	7.58%	7.58%
14	9	1.000416546	16.07%	15.68%
15	11	0.993006608	15.77%	15.56%

B.11. Example 10

In Example 9 two non-normalized, scaled PFNS data sets, each of which provides representative values for every energy group of the spectrum, are used to generate a non-normalized PFNS evaluation. The normalization constraint is applied subsequently to this spectrum and its covariance matrix. In this section, the two input spectra are first normalized, as well as with their respective covariance matrices. This is possible since both of these spectra are "complete" in that they are represented in each spectral energy group. Then, an evaluation is performed by the SLS method and a comparison is made to the results of Example 9. It should be possible for collections of spectra, all which have the imposed normalization constraint, to be evaluated in the same way as collections of all non-normalized data. This approach is denoted here as *Scaling Method 10*. Of interest is whether two equivalent data collections, one which is non-normalized and the other normalized, yield the same evaluated results after the normalization criterion is applied following the SLS procedures. One would expect this to be the case within the confines of the linear approximation.

The identical, mutually scaled PFNS data sets (and their covariance matrices) utilized in Example 9 were first normalized before performing the SLS evaluation procedure. The sum of the solution PFNS values from this exercise, with no further change of normalization, is G = 1.000003003 which is very close to unity. The calculated PFNS average energy obtained for Example 10 using *Scaling Method* 10 is $\varepsilon = 2.0191865$ with an uncertainty of 0.845%. The sums of rows and columns of the solution covariance matrix are also very close to zero (typically on the order of $\pm 10^{-11}$ to 10^{-8}). For interest, the normalization algorithm from Section 4 was applied again to the results generated by the SLS method. The changes in the solution PFNS due to the application of this procedure are extremely small, but the value of G obtained as a consequence is precisely 1. Furthermore, the matrix row and column sums are reduced to values on the order of $\pm 10^{-17}$ to 10^{-14} by this additional step. Table B.17 compares the results from Examples 9 and 10 in terms of PFNS ratios. This table also shows the uncertainties obtained using these two approaches. The differences are very small.

The point is made in Section A.11 that multiple applications of the normalization procedure described in Section 4 introduce only very small changes in the PFNS values and corresponding covariance matrix when both are already close to satisfying the normalization criterion, as long as the linear assumption is applicable. This point is demonstrated numerically in the present example.

B.12. Example 11

Example 11 demonstrates *Scaling Method 11*, as discussed in Appendix A.12. This example is very closely related to Example 10 and it utilizes the same input data for an SLS analysis, with one exception. While in Example 10 both the PFNS and their respective covariance matrices satisfy the normalization constraint, as discussed in Section 4, in the present example the covariance matrix for the second PFNS (representing the experimental information) is not normalized but is merely scaled to be consistent with the spectrum itself, which has been scaled to a sum-to-unity status. So, this second covariance matrix has rather different character in that it does not by necessity have zero sums for the rows and columns. The sum of the solution PFNS values from this exercise, with no further change of normalization, is G = 1.000001202 which is very close to unity. Nevertheless, the normalization transformation was applied to this solution, as well as to the solution

covariance matrix, so as to force G to equal 1 exactly. The final results from this exercise are shown in Table B.18 where a comparison is also made to the comparable values from Example 10. It is seen that the differences in the outcomes from these two examples are very small. The calculated PFNS average energy obtained for Example 11 using *Scaling Method* 11 is $\varepsilon = 2.0193933$ with an uncertainty of 0.843%.

The distinction between "scaling" and "normalizing" a covariance matrix, as discussed in earlier sections of this paper, is somewhat subtle. However, at least in the present situation, it appears that the evaluated outcome is not particularly sensitive to whether the normalization constraint is or is not applied to the second (experimental) PFNS covariance matrix, when the first (model-calculated) PFNS and its covariance matrix do satisfy this condition, as long as the experimental PFNS and its covariance matrix are scaled to a sum-to-unity condition.

Table B.17: Comparison of evaluated normalized PFNS results from Examples 9 and 10.

Group # (i)	<E>i	Norm PFNS Ratio Ex10 to Ex9	Tot Unc Ex9	Tot Unc Ex10
1	0.025	0.999195036	7.33%	7.35%
2	0.075	0.99925469	6.43%	6.46%
3	0.15	0.999445385	4.36%	4.36%
4	0.25	0.999264948	5.09%	5.80%
5	0.4	0.999872599	2.58%	5.23%
6	0.75	0.999842199	1.99%	1.86%
7	1.25	1.00005908	2.03%	1.76%
8	1.75	1.000022338	2.21%	2.21%
9	2.5	1.000155543	2.14%	2.14%
10	3.5	1.000107569	3.19%	3.18%
11	4.5	1.000366553	6.04%	6.06%
12	5.5	1.000366649	6.17%	6.17%
13	7	1.000191084	7.58%	7.58%
14	9	0.999541732	15.68%	15.74%
15	11	0.999913961	15.56%	15.58%

Table B.18: Comparison of evaluated normalized PFNS results from Examples 10 and 11.

Group # (i)	<E>i	Norm PFNS Ratio Ex11 to Ex10	Tot Unc Ex10	Tot Unc Ex11
1	0.025	0.999894232	7.35%	7.36%
2	0.075	1.000023831	6.46%	6.46%
3	0.15	1.000044745	4.36%	4.36%
4	0.25	1.000374463	5.80%	5.73%
5	0.4	0.999590292	5.23%	5.23%
6	0.75	1.000015652	1.86%	1.85%
7	1.25	0.999825274	1.76%	1.76%
8	1.75	0.999787171	2.21%	2.20%
9	2.5	1.000030907	2.14%	2.14%
10	3.5	1.000091311	3.18%	3.18%
11	4.5	1.000882991	6.06%	6.01%
12	5.5	1.000158557	6.17%	6.16%
13	7	0.999915024	7.58%	7.57%
14	9	1.00044021	15.74%	15.73%
15	11	0.999750377	15.58%	15.58%

Appendix C

Summary of Results for Examples 1 to 11 from Appendix B

Tables C.1 through C.6 summarize all the evaluated results obtained for Examples 1 through 11, as discussed in Appendix B. The following notation is used in these tables: Ex1 through Ex11 denote Examples 1 through 11; ΩN Ex1 through ΩN Ex11 denote the normalized group PFNS values for Examples 1 through 11; ΩN2/ΩN1 through ΩN11/ΩN1 denote the indicated ratios of the normalized PFNS values for Examples 1 through 11; fN1 through fN11 denote the indicated normalized group PFNS uncertainties (in percent) for Examples 1 through 11; fN2/fN1 through fN11/fN1 denote the indicated group PFNS uncertainty ratios for Examples 1 through 11.

The evaluated values obtained in Example 8 cannot be compared directly with those obtained from the other examples for reasons mentioned in Section B.9 so they are highlighted in pink color.

Table C.1: Scale factors and normalized chi-square per d.o.f. values for Examples 1 through 11.

	Ex1	Ex2	Ex3	Ex4	Ex5	Ex6	Ex7	Ex8	Ex9	Ex10	Ex11
c0	1.7084	2.2418	2.7809	1.0000	1.0000	1.0000	1.0000	NA	NA	NA	NA
c1	0.4243	0.5317	0.6553	0.2481	0.2124	0.2491	0.2468	1.0000	1.0000	NA	NA
c2	17.2807	22.1913	27.3526	10.0340	9.1641	10.3107	9.9919	40.7273	0.2494	NA	NA
c1/c0	0.2484	0.2372	0.2357	0.2481	0.2124	0.2491	0.2468	NA	NA	NA	NA
c2/c0	10.1149	9.8987	9.8360	10.0340	9.1641	10.3107	9.9919	NA	NA	NA	NA
c2/c1	40.7273	41.7396	41.7396	40.4475	43.1366	41.3854	40.4910	40.7273	0.2494	NA	NA
χ^2/dof	0.5357	0.5840	0.5988	0.5405	1.0552	0.5327	0.5432	0.5417	0.2286	0.1138	0.2290

Table C.2: Normalized evaluated group PFNS values for Examples 1 through 11.

Grp #	ΩN Ex1	ΩN Ex2	ΩN Ex3	ΩN Ex4	ΩN Ex5	ΩN Ex6	ΩN Ex7	ΩN Ex8	ΩN Ex9	ΩN Ex10	ΩN Ex11
1	0.005549	0.005571	0.005574	0.005548	0.005623	0.005551	0.005550	0.005079	0.005547	0.005542	0.005542
2	0.009382	0.009413	0.009418	0.009386	0.009496	0.009373	0.009390	0.008974	0.009376	0.009369	0.009369
3	0.025137	0.025189	0.025194	0.025134	0.025294	0.025144	0.025139	0.024857	0.025132	0.025118	0.025120
4	0.030335	0.030516	0.030547	0.030350	0.031039	0.030299	0.030372	0.029472	0.030310	0.030287	0.030299
5	0.067405	0.067452	0.067452	0.067393	0.067503	0.067434	0.067395	0.066422	0.067402	0.067394	0.067366
6	0.176863	0.176730	0.176704	0.176843	0.176338	0.176909	0.176825	0.174840	0.176874	0.176846	0.176849
7	0.161570	0.161605	0.161600	0.161549	0.161584	0.161615	0.161549	0.161606	0.161566	0.161576	0.161547
8	0.129194	0.128981	0.128955	0.129196	0.128497	0.129192	0.129174	0.128482	0.129208	0.129211	0.129183
9	0.184231	0.184038	0.184007	0.184216	0.183548	0.184268	0.184192	0.184969	0.184244	0.184273	0.184278
10	0.099172	0.099004	0.098989	0.099185	0.098656	0.099143	0.099170	0.098848	0.099179	0.099190	0.099199
11	0.055246	0.055519	0.055561	0.055261	0.056236	0.055208	0.055293	0.059249	0.055243	0.055264	0.055312
12	0.029521	0.029592	0.029606	0.029531	0.029769	0.029497	0.029542	0.030853	0.029530	0.029541	0.029545
13	0.019916	0.019872	0.019871	0.019925	0.019793	0.019897	0.019922	0.019652	0.019917	0.019920	0.019919
14	0.005141	0.005172	0.005177	0.005144	0.005260	0.005135	0.005148	0.005256	0.005143	0.005141	0.005143
15	0.001337	0.001345	0.001346	0.001338	0.001364	0.001336	0.001339	0.001440	0.001328	0.001328	0.001328
Sums =	1	1	1	1	1	1	1	1	1	1	1

Table C.3: Normalized evaluated group PFNS ratios for Examples 1 through 11.

Grp #	ΩN2/ΩN1	ΩN3/ΩN1	ΩN4/ΩN1	ΩN5/ΩN1	ΩN6/ΩN1	ΩN7/ΩN1	ΩN8/ΩN1	ΩN9/ΩN1	ΩN10/ΩN1	ΩN11/ΩN1
1	1.00395	1.00440	0.99983	1.01339	1.00025	1.00019	0.91531	0.99955	0.99875	0.99864
2	1.00323	1.00383	1.00041	1.01218	0.99904	1.00085	0.95653	0.99936	0.99861	0.99863
3	1.00208	1.00227	0.99987	1.00624	1.00027	1.00007	0.98885	0.99982	0.99927	0.99931
4	1.00598	1.00699	1.00049	1.02321	0.99881	1.00124	0.97157	0.99918	0.99844	0.99882
5	1.00070	1.00070	0.99981	1.00144	1.00042	0.99985	0.98541	0.99995	0.99983	0.99942
6	0.99925	0.99910	0.99989	0.99703	1.00026	0.99979	0.98856	1.00007	0.99991	0.99992
7	1.00022	1.00019	0.99988	1.00009	1.00028	0.99987	1.00023	0.99998	1.00004	0.99986
8	0.99835	0.99815	1.00002	0.99460	0.99998	0.99984	0.99449	1.00011	1.00013	0.99991
9	0.99895	0.99879	0.99992	0.99629	1.00020	0.99979	1.00401	1.00007	1.00023	1.00026
10	0.99831	0.99816	1.00013	0.99479	0.99971	0.99998	0.99673	1.00007	1.00018	1.00027
11	1.00495	1.00570	1.00027	1.01791	0.99931	1.00085	1.07245	0.99995	1.00032	1.00120
12	1.00241	1.00286	1.00034	1.00839	0.99919	1.00069	1.04512	1.00029	1.00066	1.00082
13	0.99779	0.99769	1.00043	0.99380	0.99903	1.00029	0.98670	1.00001	1.00020	1.00012
14	1.00595	1.00697	1.00049	1.02319	0.99880	1.00123	1.02236	1.00042	0.99996	1.00040
15	1.00545	1.00625	1.00045	1.02027	0.99882	1.00109	1.07699	0.99301	0.99292	0.99267

Table C.4: Normalized evaluated group PFNS uncertainties for Examples 1 through 11.

Grp #	fN1	fN2	fN3	fN4	fN5	fN6	fN7	fN8	fN9	fN10	fN11
1	7.36%	7.48%	7.49%	7.37%	7.77%	7.35%	7.38%	16.97%	7.33%	7.35%	7.36%
2	6.45%	6.52%	6.54%	6.46%	6.74%	6.43%	6.47%	14.99%	6.43%	6.46%	6.46%
3	4.36%	4.38%	4.38%	4.36%	4.43%	4.36%	4.36%	6.59%	4.36%	4.36%	4.36%
4	5.12%	5.21%	5.23%	5.13%	5.47%	5.10%	5.14%	68.75%	5.09%	5.80%	5.73%
5	2.58%	2.58%	2.58%	2.58%	2.58%	2.58%	2.58%	3.95%	2.58%	5.23%	5.23%
6	1.99%	1.99%	1.99%	1.99%	1.98%	1.99%	1.99%	3.21%	1.99%	1.86%	1.85%
7	2.03%	2.02%	2.02%	2.03%	2.01%	2.03%	2.03%	3.23%	2.03%	1.76%	1.76%
8	2.21%	2.20%	2.20%	2.21%	2.18%	2.21%	2.21%	3.30%	2.21%	2.21%	2.20%
9	2.14%	2.12%	2.12%	2.14%	2.10%	2.14%	2.13%	3.19%	2.14%	2.14%	2.14%
10	3.19%	3.18%	3.17%	3.18%	3.15%	3.19%	3.18%	4.23%	3.19%	3.18%	3.18%
11	6.06%	6.12%	6.13%	6.05%	6.28%	6.07%	6.06%	9.79%	6.04%	6.06%	6.01%
12	6.18%	6.16%	6.16%	6.19%	6.12%	6.17%	6.19%	8.17%	6.17%	6.17%	6.16%
13	7.58%	7.57%	7.57%	7.58%	7.57%	7.58%	7.57%	9.61%	7.58%	7.58%	7.57%
14	16.07%	16.37%	16.42%	16.10%	17.22%	16.01%	16.14%	74.40%	15.68%	15.74%	15.73%
15	15.77%	15.93%	15.96%	15.75%	16.37%	15.79%	15.76%	24.53%	15.56%	15.58%	15.58%

Table C.5: Normalized evaluated group PFNS uncertainty ratios for Examples 1 through 11.

Grp #	fN2/fN1	fN3/fN1	fN4/fN1	fN5/fN1	fN6/fN1	fN7/fN1	fN8/fN1	fN9/fN1	fN10/fN1	fN11/fN1
1	1.017	1.018	1.001	1.056	0.999	1.003	2.306	0.997	0.999	1.000
2	1.011	1.013	1.002	1.045	0.996	1.003	2.324	0.997	1.001	1.001
3	1.004	1.005	1.000	1.015	0.999	1.001	1.512	1.000	1.000	1.000
4	1.018	1.021	1.002	1.070	0.996	1.004	13.435	0.995	1.134	1.119
5	1.000	1.000	1.000	1.002	0.999	1.000	1.532	1.000	2.027	2.025
6	0.997	0.997	1.000	0.992	1.000	1.000	1.609	1.000	0.932	0.927
7	0.997	0.996	1.000	0.991	1.000	1.000	1.594	1.000	0.870	0.867
8	0.995	0.994	1.000	0.985	1.000	0.999	1.496	1.000	0.999	0.996
9	0.993	0.993	1.000	0.981	1.001	0.999	1.491	1.001	1.003	1.001
10	0.997	0.996	0.999	0.990	1.001	0.999	1.329	1.000	0.998	0.998
11	1.011	1.013	0.999	1.038	1.002	1.000	1.617	0.997	1.000	0.993
12	0.995	0.995	1.001	0.990	0.997	1.001	1.321	0.998	0.997	0.997
13	1.000	0.999	1.000	0.999	1.001	1.000	1.268	1.000	1.000	0.999
14	1.018	1.021	1.002	1.071	0.996	1.004	4.628	0.976	0.979	0.979
15	1.010	1.012	0.998	1.038	1.001	0.999	1.555	0.987	0.988	0.988

Table C.6: Evaluated PFNS average energies and their uncertainties for Examples 1 through 11.

	Ex1 ε	Ex2 ε	Ex3 ε	Ex4 ε	Ex5 ε	Ex6 ε	Ex7 ε	Ex8 ε	Ex9 ε	Ex10 ε	Ex11 ε
ε	2.0189	2.0192	2.0193	2.0191	2.0204	2.0185	2.0192	2.0419	2.0189	2.0192	2.0194
% Unc ε	0.848%	0.855%	0.854%	0.849%	0.869%	0.848%	0.849%	2.517%	0.844%	0.845%	0.843%

Nuclear Data Section
International Atomic Energy Agency
Vienna International Centre, P.O. box 100
A-1400 Vienna, Austria

E-mail: nds.contact-point@iaea.org
Fax: (43-1) 26007
Telephone: (43-1) 2600 21725
Web: http://www-nds.iaea.org